

A MODEL PREDICTIVE CONTROL STRATEGY
FOR A BRIDGE DECK HEATED BY A
GEOTHERMAL HEAT PUMP SYSTEM

By

STEPHEN CHRISTOPHER JENKS

Bachelor of Science

University of Missouri – Rolla

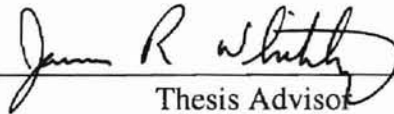
Rolla, Missouri

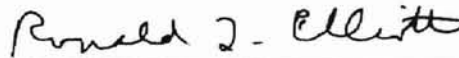
1999

Submitted to the Faculty of the
Graduate College of the
Oklahoma State University
in partial fulfillment of
the requirements for
the Degree of
MASTER OF SCIENCE
December, 2001

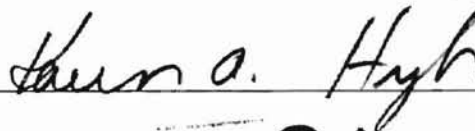
A MODEL PREDICTIVE CONTROL STRATEGY
FOR A BRIDGE DECK HEATED BY A
GEOTHERMAL HEAT PUMP SYSTEM

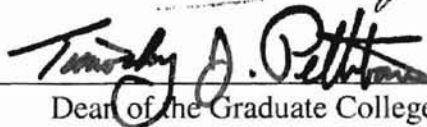
Thesis Approved:


Thesis Advisor








Dean of the Graduate College

ACKNOWLEDGEMENTS

I would like to thank Dr. James (Rob) Whiteley for his advice and expertise while developing the control system. Dr. Whiteley has also spent a lot of time reading (and rereading) this thesis, which has been greatly appreciated.

All of the programming required for this project was done in Visual Basic. I would like to thank Mr. Paul Priba and Mr. Will Adams at Conoco Inc. for spending many hours of their valuable time giving me a crash course in Visual Basic during the summer of 2000.

Many people are working on the OSU Smart Bridge project and several of them have given me a great deal of assistance. I would like to thank Dr. Kala Pandit and Mr. Derek (Deke) Arndt for gathering all of the archived weather data I requested. I would also like to thank Mr. Xiaobing Liu for the bridge deck model technical support he offered.

Last, but not least I would like to thank my wife, Crissie, for her constant encouragement and patience over the course of this project.

TABLE OF CONTENTS

| Chapter | Page |
|---|------|
| I. Introduction | |
| 1.1 Problem Description..... | 1 |
| 1.2 OSU Geothermal Smart Bridge Project..... | 2 |
| 1.3 Control Group Deliverables..... | 5 |
| 1.4 Thesis Organization..... | 7 |
| II. Background | |
| 2.1 Introduction..... | 9 |
| 2.2 Road Weather Information Systems (RWIS)..... | 10 |
| 2.3 Heated Bridge Applications In The U.S..... | 11 |
| 2.3.1 Tenth Street Pedestrian Viaduct – Lincoln, Nebraska..... | 11 |
| 2.3.2 Silver Creek – Salem, Oregon..... | 12 |
| 2.3.3 Highland Interchange – Portland, Oregon..... | 13 |
| 2.3.4 Second Street Overcrossing – Hood River, Oregon..... | 14 |
| 2.3.5 U.S. 287 – Amarillo, Texas..... | 15 |
| 2.3.6 Route 60 Bridge –Amherst County, Virginia..... | 16 |
| 2.4 Summary..... | 17 |
| III. Smart Bridge Control Solution | |
| 3.1 Introduction..... | 20 |
| 3.2 MPC Approach..... | 21 |
| 3.3 Smart Bridge MPC Approach | 26 |
| 3.4 Summary..... | 32 |
| IV. Smart Bridge Control System Implementation | |
| 4.1 Introduction..... | 33 |
| 4.2 First Principles Bridge Deck Model..... | 34 |
| 4.2.1 Bridge Deck Model Parameters, Inputs, and Outputs..... | 34 |
| 4.2.2 Predicted Bridge Response to Forecasted Weather Conditions..... | 37 |
| 4.3 Setting the Reference Trajectory..... | 38 |
| 4.3.1 Identifying Preferential Icing Potential..... | 39 |
| 4.3.2 Reference Trajectory Strategy..... | 41 |
| 4.4 Calculating Control Decisions..... | 43 |
| 4.4.1 The Dynamic Matrix..... | 45 |
| 4.4.2 Projected and Residual Error Vectors..... | 47 |
| 4.4.3 Output Error Weighting Matrix..... | 48 |
| 4.4.4 Input Weighting Matrix..... | 49 |

| Chapter | Page |
|---|------|
| 4.4.5 Input Move Constraints..... | 50 |
| 4.5 Optimization Technique..... | 51 |
| 4.5.1 Multiple Variable Search Method..... | 52 |
| 4.5.2 Single Variable Search Method..... | 54 |
| 4.6 Programming Notes..... | 58 |
| 4.7 Summary..... | 60 |
| I. Weather Inputs | |
| 5.1 Introduction..... | 62 |
| 5.2 Oklahoma Mesonet..... | 63 |
| 5.3 NEXRAD..... | 64 |
| 5.3.1 Hourly Digital Precipitation Array..... | 66 |
| 5.3.2 Calculation of Precipitation Rate From DPA Data | 68 |
| 5.4 Rapid Update Cycle Forecast Model..... | 72 |
| 5.5 Constructing Forecasts for the Smart Bridge..... | 75 |
| 5.6 Solar Radiation Forecast..... | 77 |
| 5.7 Infrastructure Requirements for Accessing Weather Inputs..... | 80 |
| 5.8 Summary..... | 81 |
| II. Case Studies | |
| 6.1 Introduction..... | 82 |
| 6.2 Bridge Deck Parameters..... | 83 |
| 6.3 Case 1 – December 23-26,2000..... | 85 |
| 6.3.1 Case 1 – Weather Conditions..... | 85 |
| 6.3.2 Case 1 – Performance for 2°C Dew Point Depression Rule..... | 88 |
| 6.4 Case 2 – December 12-17, 2000..... | 89 |
| 6.4.1 Case 2 – Weather Conditions..... | 92 |
| 6.4.2 Case 2A – Performance Results for 4°C Dew Point Point Depression Rule..... | 95 |
| 6.4.3 Case 2B – Performance Results for 2°C Dew Point Point Depression Rule..... | 100 |
| 6.5 Summary..... | 103 |
| III. Conclusions and Recommendations | |
| 7.1 Contribution of Reported Work..... | 105 |
| 7.2 Satisfaction of Project Deliverables..... | 105 |
| 7.3 Conclusions..... | 107 |
| 7.4 Recommendations for Future Work..... | 108 |
| Bibliography..... | 109 |

LIST OF TABLES

| Table | Page |
|---|------|
| 2-1 Danish Meteorological Institute Measured RWIS Variables..... | 11 |
| 2-2 Summary of conditions required to automatically turn bridge deck heating systems on and off..... | 18 |
| 4-1 Bridge deck parameters used in the first principles bridge deck model..... | 36 |
| 4-2 Input variables to the first principles bridge deck model..... | 36 |
| 4-3 Output variables from the first principles bridge deck model..... | 37 |
| 4-4 Icing potential rules used in the current version of the Smart Bridge control system..... | 40 |
| 4-5 Cyclic search stopping criteria..... | 53 |
| 4-6 Parameters in the current version of the Smart Bridge control system that might be used in the adaption module..... | 59 |
| 5-1 Oklahoma Mesonet measurements..... | 64 |
| 5-2 RUC forecast variables used in Smart Bridge control system..... | 73 |
| 6-1 Bridge deck parameters for the Smart Bridge at OSU Stillwater..... | 83 |
| 6-2 Weather conditions used to produce step response mdoel..... | 84 |

LIST OF FIGURES

| Figure | Page |
|--------|--|
| 1-1 | A road sign warning motorists of ice on an approaching bridge..... 1 |
| 1-2 | The major components used in a geothermal Smart Bridge..... 3 |
| 3-1 | Adjust the gas pedal position to maintain the speed of a bus at 65 mph..... 22 |
| 3-2 | Bus speed and gas pedal position under the influence of the automatic cruise control..... 23 |
| 3-3 | Bus speed and gas pedal position when the bus driver manipulates the gas pedal position..... 24 |
| 3-4 | MPC analog of operator thought process..... 26 |
| 3-5 | Selecting the desired CV trajectory..... 30 |
| 3-6 | Steps performed by the Smart Bridge MPC algorithm at each sample time..... 31 |
| 4-1 | The first principles bridge deck model is used to calculate \hat{y} 38 |
| 4-2 | Example of how the Smart Bridge control system sets r 42 |
| 4-3 | When first indication of preferential icing occurs at present time the entire reference trajectory is set at the setpoint value..... 43 |
| 4-4 | Example step response model used by the Smart Bridge control system..... 46 |
| 4-5 | Case where the controller can be detuned after the threat of preferential icing has passed..... 49 |
| 4-6 | One iteration of a cyclic search consists of a move in each coordinate direction..... 53 |
| 4-7 | Flow diagram of cyclic search method for minimizing a multiple variable objective function..... 54 |
| 4-8 | The two-point equal interval line search reduces the search region by one third after each iteration..... 55 |
| 4-9 | A large penalty is added to the objective function to prevent violated constraints..... 56 |
| 4-10 | Flow diagram of the two-point equal interval algorithm used to conduct line searches..... 56 |
| 4-11 | Selected screen captures from the Smart Bridge control software..... 59 |
| 4-12 | Summary flow diagram for Smart Bridge control algorithm..... 61 |

| Figure | | Page |
|--------|--|------|
| 5-1 | Location of WSR-88D radar stations..... | 65 |
| 5-2 | Elevations, height, and range scanned by NEXRAD in the course of one 360° volume scan..... | 66 |
| 5-3 | Partial binary hexadecimal DPA message..... | 67 |
| 5-4 | A sample DPA image from the Twin Lakes, OK radar station. DPA outputs an array of 131 rows and 131 columns..... | 68 |
| 5-5 | Precipitation rate is estimated using the current DPA reading and past values of precipitation rate..... | 69 |
| 5-6 | Distance (km) from the nearest point of precipitation to Stillwater, OK..... | 71 |
| 5-7 | Calculated precipitation rate using Equation 5-1 and 5-2..... | 71 |
| 5-8 | RUC outputs a 12-hour forecast at the top of every third hour starting at 00:00 GMT. A 3-hr forecast is generated at the top of all other hours..... | 74 |
| 5-9 | Sample 12-hour forecast for Stillwater, Ok..... | 74 |
| 5-10 | A RUC forecast for air temperature issued at 03:00 GMT..... | 76 |
| 5-11 | Example of how the twelve-hour forecast is updated when a three-hour forecast is provided..... | 77 |
| 5-12 | The solar angle of incidence, θ , partially determines the amount of solar radiation absorbed by the bridge deck pavement..... | 78 |
| 5-13 | Solar radiation forecast issued at 03:00 local time..... | 79 |
| 5-14 | During daylight hours the solar radiation forecast is a sine wave that passes through the current solar radiation measurement..... | 79 |
| 5-15 | Proposed infrastructure for transmitting real time weather data to Smart Bridge control systems..... | 80 |
| 6-1 | Step response model used in all simulations presented in Chapter VI..... | 84 |
| 6-2 | Case 1 air temperature and sky temperature..... | 86 |
| 6-3 | Case 1 solar radiation..... | 87 |
| 6-4 | Case 1 precipitation rate..... | 87 |
| 6-5 | Case 1 dew point depression..... | 88 |
| 6-6 | Case 1 average bridge surface temperature..... | 90 |
| 6-7 | Case 1 bridge loop supply temperature..... | 90 |
| 6-8 | Case 1 bridge loop flowrate..... | 91 |
| 6-9 | Case 1 heat input to bridge..... | 91 |
| 6-10 | Case 2 air temperature and sky temperature..... | 92 |
| 6-11 | Case 2 solar radiation..... | 93 |
| 6-12 | Case 2 dew point depression..... | 93 |
| 6-13 | Case 2 precipitation rate..... | 94 |
| 6-14 | Case 2A average surface temperature..... | 96 |
| 6-15 | Case 2A bridge loop supply temperature..... | 96 |
| 6-16 | Case 2A bridge loop flowrate..... | 97 |

| Figure | Page |
|---|------|
| 6-17 Case 2A heat input to bridge..... | 9 |
| 6-18 Comparison of RUC dew point depression forecasts to observed values..... | 99 |
| 6-19 Comparison of RUC precipitation forecast to observed values..... | 99 |
| 6-20 Case 2B average surface temperature..... | 101 |
| 6-21 Case 2B bridge loop supply temperature..... | 102 |
| 6-22 Case 2B bridge loop flowrate..... | 102 |
| 6-23 Case 2B heat input to bridge..... | 103 |

NOMENCLATURE

| | |
|--------------|---|
| OSU | Oklahoma State University |
| RWIS | Road Weather Information Systems |
| MPC | Model Predictive Control |
| CV | Controlled Variable |
| DV | Disturbance Variable |
| MV | Manipulated Variable |
| \hat{y} | Predicted average bridge deck surface temperature response with no future control action |
| r | Reference trajectory |
| A | Dynamic Matrix |
| a | Step response model |
| n | Length of step response model |
| p | Prediction horizon |
| m | Control horizon |
| Δu | Vector of MV adjustments |
| \hat{e} | Projected error vector |
| Δu^* | Optimal sequence of MV adjustments vector |
| e_r | Residual error vector |
| u_{\min} | Minimum MV constraint vector |
| u_{\min} | Minimum MV constraint |
| u_{\max} | Maximum MV constraint vector |
| u_{\max} | Maximum MV constraint |
| u | Vector of MV moves in absolute variables |
| L | Lower triangular matrix for converting deviation MVs to absolute MVs |
| u_0 | Vector with all elements set to previous MV value (absolute) |
| x_t | Test vector |
| k | Coordinate direction index |
| i | Iteration count in line search |
| j | Coordinate direction in which line search is conducted |
| <Penalty> | Bracket operator used with line search |
| GUI | Graphical user interface |
| RUC | Rapid Update Cycle |
| WSR-88D | Weather Surveillance Radar – 1988 Doplar |
| DPA | Digital Precipitation Array |
| NCEP | National Centers for Environmental Prediction |

| | |
|--------------------|--|
| θ | Solar angle of incidence |
| Φ | Objective function |
| Γ | Output error weighting matrix |
| γ | Vector of output error weights |
| Λ | Input weighting matrix |
| ρ | Scalar for adjusting line search step size |
| γ | Used to calculate precipitation rate, represents precipitation accumulation during the last hour excluding time since the previous DPA message |
| β | Used to calculate precipitation rate, represents precipitation accumulation since the previous DPA message |
| R_{t_{k-1}, t_k} | Precipitation rate from last DPA message until current DPA message |

CHAPTER I

INTRODUCTION

1.1 Problem Description

Motorists commonly see signs like the one below as they approach bridges in the United States. These signs have been put in place to warn drivers of preferential icing on the bridge. Preferential icing is defined as the formation of ice on a bridge deck before ice appears on approaching sections of road. Most frequently, two phenomena contribute to this condition. First, because the top and bottom surfaces of a bridge are exposed to the elements, bridge decks are capable of losing heat much faster than roads built on grade. The second factor is that bridges often span a body of water. This water provides water vapor to condense and freeze on the cold bridge deck [1].



Figure 1- 1: A road sign warning motorists of ice on an approaching bridge.

Preferential icing makes bridges very hazardous even when warning signs are posted. Drivers have a false sense of security about the condition of the pavement on an approaching bridge. They automatically make the assumption that the condition of the bridge is the same as the condition of the approaching road. However, this assumption is not necessarily true because, as described above, bridges cool faster than the adjacent roadway.

In most instances ice is prevented or removed from our nation's roads using salt or one of a number of deicing chemicals. A major problem associated with applying salt and other deicing chemicals to bridge decks is that these materials cause corrosion of concrete and steel in the bridge. By using corrosion-free deicing methods the potential exists to double the life of a bridge deck [2].

In summary, preferential icing on bridge decks poses two significant problems. First and foremost, preferential icing on bridges represents a safety hazard for drivers. Secondly, traditional means of removing ice and snow from bridge decks cause structural damage to bridges. This damage is costly because of the reduced lifecycle of the bridge. Therefore, there is a strong incentive from safety and economic standpoints to effectively eliminate preferential icing from bridge decks in a manner that is not corrosive to the structure of the bridge.

1.2 OSU Geothermal Smart Bridge Project

The Oklahoma State University (OSU) Geothermal Smart Bridge Project was initiated in response to the problems described in Section 1.1. Funding for the OSU Geothermal Smart Bridge Project is provided by grants from the U.S. Department of Transportation's Federal Highway Administration and the State of Oklahoma. The mission of this project is to "research, design, and demonstrate technically feasible, economically acceptable, and environmentally compatible Smart Bridge systems to enhance the nation's highway system safety and to reduce its life cycle cost [1]."

The Smart Bridge system is a bridge deck equipped with a heating system for prevention of preferential icing. Although there are many ways to heat a bridge deck, the approach taken by the OSU project uses a hydronically-heated deck with geothermal energy as the heat source. Figure 1-2 shows the major components of the Smart Bridge system. These components consist of: a ground loop heat exchanger, ground loop circulating pump, heat pump, bridge loop circulating pump, a hydronically-heated bridge deck, and a controller.

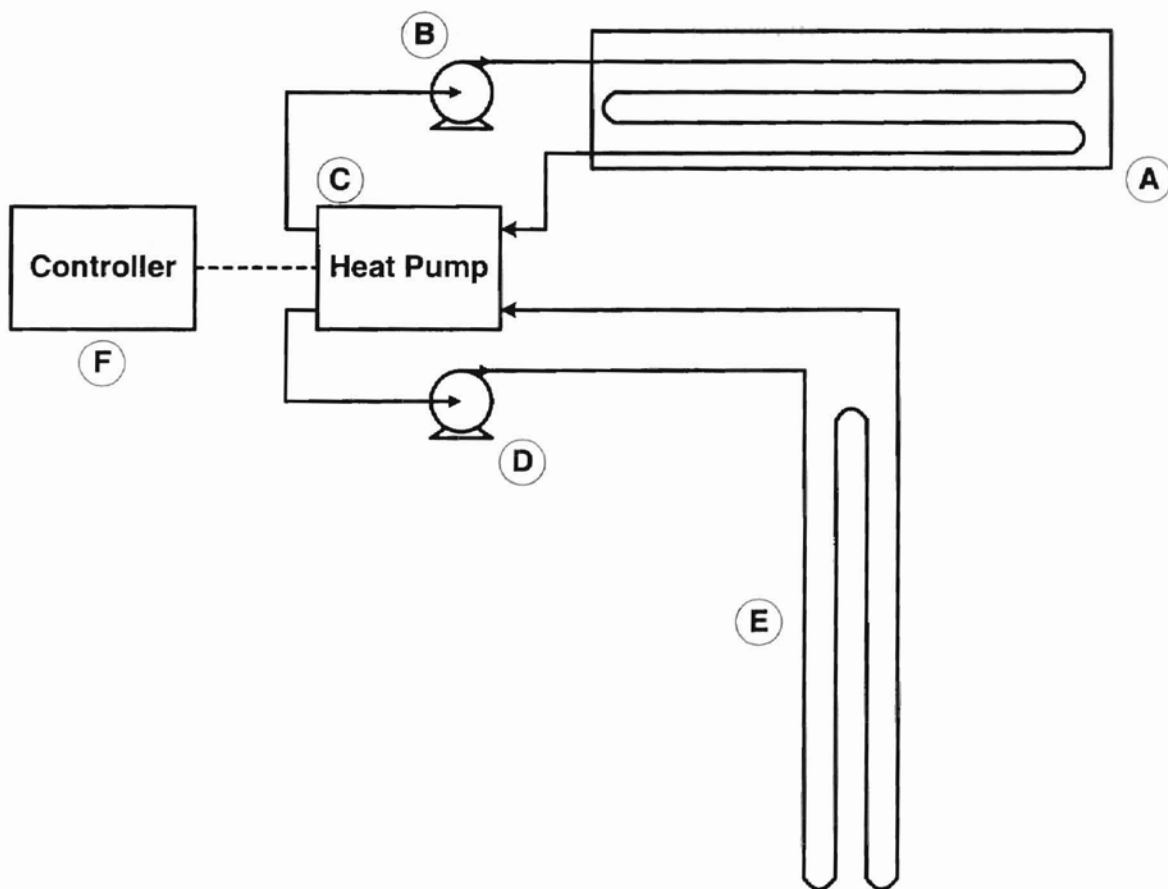


Figure 1- 2: The major components used in a geothermal Smart Bridge.

**A) Hydronically-heated bridge deck B) Bridge loop circulating pump
C) Heat pump D) Ground loop circulating pump E) Ground loop
heat exchanger, F) Controller**

A hydronically-heated bridge deck has tubes buried in the pavement. Heat is transferred to the bridge deck when a warm fluid is pumped through the tubes. A ground source heat pump, which recovers energy stored in the earth, is used to heat the fluid circulated through the bridge deck. Energy is supplied to the heat pump from the ground loop heat exchanger. A ground loop heat exchanger consists of several underground tubes. When a cool fluid is pumped through the ground loop heat exchanger heat is transferred from the earth to the fluid.

The bridge deck heating system operates automatically. Decisions to initiate, continue, or stop heating the bridge deck are based on measurements at the bridge site, information from available intelligent transportation systems, and local weather forecasts. The automatic nature of the control has given rise to the informal name “Smart Bridge” [1].

The following deliverables have been established for the OSU Geothermal Smart Bridge project [1]:

- *Manuals and seminars will be developed to provide guidance for designers of smart bridges. The seminars and manuals will cover design practices, optimal design, optimal operation, control strategies, and cost/benefit analysis.*
- *Design software will be developed to provide guidance for designers of smart bridges. The design software will allow state departments of transportation designers as well as private industry designers to determine required ground loop heat exchanger size and configuration, heat pump sizing, circulating pump sizing, the effects of various control and operating strategies, energy*

consumption, electricity costs, approximate first costs, life cycle costs, anticipated bridge deck life extension, and projected cost/benefit ratios.

- *Advanced modeling software will be developed for additional research and “what if?” design studies.*
- *Recommended weather sampling, forecasting, control strategies, and operating strategies will be made available.*
- *Verification of reduced corrosion rates for internal reinforcing steel elements in the heated bridge deck, an assessment of bridge lifetime extension, and an economic analysis of smart bridge systems will be completed.*
- *Technology transfer to professionals, including bridge designers and construction managers, of the above deliverables listed above will be maximized.*

1.3 Control Group Deliverables

Several OSU faculty members with varying backgrounds are involved in the Smart Bridge project. Detailed tasks have been assigned to each investigator so that the project deliverables might be completed as efficiently as possible. The work covered in this thesis specifically addresses Task 4.3.1.1: Integrated Control Strategies. Concepts presented in this thesis represent the second-generation control strategy. Details of the first-generation control strategy are found in [3].

Completion of Task 4.3.1.1 requires development of user-friendly control system software with commercially available components. In addition, the control system must

be modular to ensure flexibility, reliability, ease of maintenance, and to maximize technology transfer. All software developed to run the control system presented in this thesis is written in Visual Basic, an inherently modular programming language.

The control system must meet certain performance requirements. First, the control system should guarantee that preferential icing is prevented. Second, the control system should minimize operating costs by only engaging the bridge deck heating system at times required to prevent preferential icing. By meeting these performance objectives, the control system also contributes to reducing the capital costs associated with the bridge deck by minimizing the size and cost of the heating system. That is, an efficient control system reduces the need to over-design the heating system.

While the control concepts and techniques required for this task are well established, integrating these ideas into the Smart Bridge project requires innovation. The control system presented in this work is a novel application of advanced control concepts. Also novel is the integration of real-time National Weather Service (NWS) forecast and radar data. Advanced control techniques in conjunction with forecast and radar data facilitates proactive prevention of bridge deck icing to an extent not seen in existing heated bridge deck systems. Future efforts beyond the scope of this work will incorporate adaptive techniques into the final control system to allow the controller to learn with time, further improving its performance.

1.4 Thesis Organization

This thesis is organized as follows. Chapter II begins with a discussion of Road Weather Information Systems (RWIS). RWIS, which are used in Europe and the United States, represent a logical precursor to the Smart Bridge project. Chapter II also gives a background of heated bridge decks that have been implemented in the U.S. A brief description of the heating technique, energy source, and control system for each bridge is given. Performance results for each bridge are also discussed.

Chapter III presents a qualitative discussion of the Smart Bridge control strategy. An analogy between controlling the temperature of a bridge deck and the speed of a bus is made. Chapter III sets the stage for the detailed work reported in Chapters IV and V.

Chapter IV provided details of the current Smart Bridge control strategy. The first-principles bridge deck model (developed as part of Task 4.1.1 of the Smart Bridge project) plays an important role in the Smart Bridge control system. Chapter IV begins with a description of the first-principles bridge deck model and how it applies to the Smart Bridge control system. Details regarding the application of model predictive control (MPC) to a geothermal Smart Bridge are discussed in the remaining sections of Chapter IV.

Chapter V describes the weather inputs required for the Smart Bridge control strategy. With the help of the Oklahoma Climatological Survey at the University of Oklahoma, the Smart Bridge project is able to integrate the most recent weather technologies into the control system. Specifically, the control system takes advantage of NEXRAD Doppler radar data and the Rapid Update Cycle weather forecasting model. Chapter V describes these information sources and explains how they are used by the

Smart Bridge control system. Chapter V also explains how these weather inputs are made available to the control system.

Chapter VI shows how the controller performs under various weather conditions. Results for simulated case studies are discussed.

Chapter VII provides concluding remarks and recommendations for future developers of the Smart Bridge control software.

CHAPTER II

BACKGROUND

2.1 Introduction

Road weather information systems (RWIS) provide information about driving and road conditions. RWIS technology is used in several U.S. states and some countries in Europe. Section 2.2 discusses RWIS, a logical precursor to the OSU Geothermal Smart Bridge project.

Section 2.3 provides background information on existing applications of heated bridge technology (HBT). Because the work covered in this thesis focuses on the design of a Smart Bridge control system, the control rules and instrumentation of existing heated bridges are emphasized. Some of the heated bridge decks described in this chapter use a heat source other than geothermal energy. However, the fundamental variables considered by the Smart Bridge control system (bridge deck temperature and rate of heat input to the bridge deck) are identical to those of existing applications of HBT. Therefore it is worthwhile to consider techniques and performance of existing HBT when designing the Smart Bridge control system.

Funding for HBT research was provided between 1992 and 1997 as part of the Applied Research and Technology program (section 6005) of the Intermodal Surface Transportation Efficiency Act [4]. A total of eight heated bridge decks were constructed in five states (Oregon, Virginia, West Virginia, Nebraska, and Texas) as a result of this program. In July 1999 the Office of Bridge Technology, part of the Federal Highway Administration, published a report on the results of the HBT work. The HBT report

gives the scope, operating controls, construction details, costs, and operating experience for each bridge. This chapter draws heavily from the results of the report [4].

2.2 Road Weather Information Systems (RWIS)

A RWIS is a network of remote weather stations that reports various weather and road conditions. Over the past 10 years, RWIS have been installed by most states where roadway icing is a concern [5]. Road maintenance crews responsible for clearing ice and snow use RWIS data to efficiently allocate their time and resources to locations where snow or ice is most threatening. By utilizing RWIS data, state transportation agencies have reduced labor and material costs as well as increased road safety. In Massachusetts, for example, the state Highway Department estimates that the statewide system of weather stations could save up to \$200,000 per year in the maintenance budget [6].

European countries, particularly Denmark and the United Kingdom, have active RWIS [7]. The Danish Meteorological Institute runs one of the most sophisticated RWIS systems. Over 200 remote road weather stations spread throughout the country comprise the Danish RWIS. A list of monitored variables in the Danish system is shown in Table 2-1. RWIS information is used in weather and pavement models to predict hazardous conditions.

The Smart Bridge project represents a logical extension to RWIS programs. RWIS data is used to initiate a manual response to hazardous conditions (i.e. maintenance crews must be sent to clear roads and prevent ice). The Smart Bridge control system takes this concept a step further by using weather data and other inputs to initiate an

automatic response to preferential icing conditions. In the next section, existing heated bridge deck control strategies are discussed. All of the bridges discussed are equipped with instrumentation that is part of a state RWIS (or monitors similar variables). Furthermore, the Smart Bridge control system requires an RWIS station or similar instrumentation at the bridge site.

Table 2- 1: Danish Meteorological Institute Measured RWIS Variables

| | |
|-------------------------------------|-----------------------------------|
| Temperature at 2-meter height | Fractional cloud cover |
| Specific humidity at 2-meter height | Cloud height |
| Surface Pressure | Road surface temperature |
| Wind Speed at 10-meter height | Road service water level |
| Precipitation intensity | Road surface ice accumulation |
| Dewpoint at 2-meter height | Vertical road temperature profile |

2.3 Heated Bridge Applications In The U.S.

2.3.1 Tenth Street Pedestrian Viaduct – Lincoln, Nebraska

Lincoln, Nebraska is home to a 1204 foot long by 12 foot wide heated pedestrian viaduct. This system is similar to a Smart Bridge design in the sense that it is hydronic. Heat is transferred to the bridge deck by pumping a 35% propylene glycol-water solution through tubes embedded in the pavement. While the Smart Bridge uses geothermal energy, the Tenth Street viaduct uses a natural-gas-fired boiler to heat the propylene glycol-water solution.

A number of sensors are utilized by the Tenth Street viaduct's automatic control system. Temperature sensors set in the bridge deck monitor the pavement temperature.

Two heated precipitation sensors are located on the bridge deck to detect when moisture is present. Instrumentation is also provided to monitor the propylene glycol-water temperature and flowrate.

An on/off controller is used to engage and disengage the heating system. The heating system is turned on when the bridge deck temperature drops below 4°C, the ambient temperature is below 2°C, and moisture is detected. The heating system is automatically turned off when the bridge deck temperature reaches 13°C (an adjustable setpoint).

The Tenth Street viaduct heating system experienced three precipitation events in the winter of 1994. During one event the heating system had to be operated manually due to inaccurate moisture sensing. Because the moisture sensors are heated, they eventually melted all of the snow within a small radius. This caused the sensor to give a “no moisture” reading and prevented the heating system from turning on. Snow continued to accumulate on the bridge deck until a “snow igloo” completely covered the moisture sensor.

2.3.2 Silver Creek – Salem, Oregon

In the foothills of the Cascade Mountains southeast of Salem, Oregon on state highway 214 is a two lane heated bridge deck. The 900 foot long bridge spans the North Fork of Silver Creek. Much like a Smart Bridge, it is hydronic and uses geothermal energy as a heat source. Like the heated pedestrian viaduct in Nebraska, the Silver Creek bridge has a 35% propylene glycol-water solution in the bridge loop heat exchanger.

In addition to the heating system, this bridge is also equipped with a bridge deck flooding system. Several nozzles mounted on the upslope side of the bridge spray well water onto the deck to remove accumulated ice and snow.

Two controllers are used to implement on/off control of the bridge deck heating system. One of the controllers is a Tekmar 661 snowmelt controller, which uses proprietary logic. A Delta-Therm SMC-120A snow sensing system serves as the other heating system controller. Rules for the Delta-Therm controller are similar to those used by the controller at the pedestrian viaduct in Nebraska. Heating begins when the ambient air temperature falls below a specified temperature and moisture is sensed on the bridge. Operation continues for a required minimum amount of time and then until the ambient temperature or the bridge deck temperature rise above predetermined levels.

The Silver Creek bridge automatic heating system successfully cleared all snow and ice from the bridge deck. This result is markedly different than what was seen at the pedestrian viaduct in Nebraska, which had to be controlled manually after moisture sensors failed.

2.3.3 Highland Interchange – Portland, Oregon

The Highland Interchange is a two-lane electrically heated bridge deck over U.S. 26 near the Oregon Zoo in Portland, OR. Thirty-six heating cables, each 500 feet long, are embedded in the pavement. Instrumentation for measuring air temperature, wind speed, wind direction, humidity, and precipitation are present. Sensors to detect pavement temperature, moisture, and ice are also located on the bridge deck.

Initially, the control strategy for Highland Interchange was similar to those of the Silver Creek bridge and Tenth Street pedestrian viaduct. Heating was initiated when moisture was detected on the bridge deck and the temperature fell below a specified level. Ice and snow was successfully cleared during a 1996 ice storm. However, the following winter ice was not melted due to malfunctioning moisture sensors. The controller was reprogrammed to activate the heating system when the dew point is above 0°F and the air temperature falls between 20°F and 33°F.

2.3.4 Second Street Overcrossing – Hood River, Oregon

Two heated bridges lay end-to-end at the Second Street Overcrossing bridge in Hood River, Oregon. The south bridge spans a set of railroad tracks while an interstate highway lies beneath the north bridge. A Delta-Therm electric system using mineral-insulated cables is used to heat the south bridge. The north bridge is divided into three panels. A heat pump is used to heat the west panel, a boiler system for the east panel, and the center panel is electrically heated.

Instrumentation for the Second Street Overcrossing is similar to the bridges that have been previously discussed. Devices for measuring air temperature, humidity, wind speed, wind direction, pavement temperature, and pavement moisture are present. Unlike any of the bridges discussed above, the bridges at this site are equipped with a frost detector. The frost detector compares the signal from a heated moisture sensor to that of a moisture sensor with a disabled heating circuit. Frost is assumed to be on the bridge

when the heated sensor reports the presence of moisture and the unheated sensor does not report moisture.

The bridge panels are highly instrumented and employ a very simple control rule. Heating is initiated when the ambient temperature drops below 35°F and the humidity is greater than 95%. Heating continues for a minimum run time of 30 minutes and continues until the pavement temperature reaches 36°F. Performance results were not reported.

2.3.5 U.S. 287 – Amarillo, Texas

Like the Second Street overcrossing in Oregon, the U.S. 287 site is comprised of two bridges, one for northbound traffic and the other for southbound traffic. This pair of two lane bridges passes over N. 15th Avenue in Amarillo, Texas. Both decks are heated hydronically and use geothermal energy as a heat source. The northbound bridge is equipped with a heat pump. A heat pump was not installed on the southbound bridge to evaluate if the ground-loop-only system is capable of supplying enough energy to prevent ice and snow accumulation.

Instrumentation for measuring air and pavement temperature is provided. Sensors for detecting moisture and ice are also installed on the bridge. Heating is automatically initiated when the deck temperature falls below 35°F and there is precipitation in the forecast. The source of precipitation forecasts used by the control system is unknown. Acceptable performance was achieved by both heating systems, suggesting that the heat pump on the northbound lane is unnecessary.

2.3.6 Route 60 Bridge – Amherst County, Virginia

Amherst County, Virginia is home to a 117-foot long two lane heated bridge deck. A propane-fired boiler is used to heat a 50% propylene glycol-water solution. The heated propylene glycol-water solution is then pumped through an ammonia evaporator. Ammonia vapor rises out of the evaporator and is distributed by several manifolds to 241 steel heat pipes embedded in the bridge deck. Heat is transferred to the bridge deck when the ammonia vapor condenses on the inside surface of the heat pipes. The heat pipes, which are oriented transversely, have been placed in the bridge deck at an angle, such that the end of each heat pipe (furthest away from the distribution manifolds) is slightly higher. The sloped in the heat pipes allows the condensed ammonia to trickle back to the evaporator section of the heating system.

Instrumentation for measuring air temperature, wind speed, pavement temperature, and relative humidity is installed at the site. Other instrumentation includes a solar radiation sensor, an ice detector, an infrared video camera for observing temperature distribution on the pavement surface, and a heated precipitation meter. The heating system is automatically engaged under any of the following three conditions: snow or ice is detected on the surface of the bridge deck, the precipitation sensor indicates precipitation when the pavement temperature is below 35°F, or moisture is detected on the deck when the pavement temperature is below 35°F. A clear surface reading for more than ten minutes or a pavement temperature above 49°F will cause the heating system to turn off. At times, the controller's performance was compromised when moisture sensors failed to register when moisture was present on the bridge deck.

Also, the controller engaged the heating system unnecessarily due to false reports of ice by the ice sensor.

2.4 Summary

Although the heated bridges discussed in this chapter are different in many ways (heat source, heating capacity, climate conditions), they all use similar instrumentation and control strategies. All use on/off control. That is to say the controller will turn the heating system on if a certain set of conditions occur and off otherwise. The most common rule used is that if moisture is present on the bridge surface and the air temperature is below a certain value, then the heating system is activated. Close relatives of this moisture-temperature rule utilize humidity-temperature, dew point-temperature, and precipitation-temperature combinations. The criteria for turning off the heating system are commonly one or more of the following: a minimum runtime must be observed, the bridge deck temperature must exceed a minimum allowable value, the air temperature must exceed a minimum allowable value, and no moisture is detected on the bridge deck. Table 2-1 summarizes the control rules for each bridge.

Although all of the previously discussed control strategies are capable of removing preferential icing, they cannot guarantee the prevention of preferential icing. The control strategies discussed in this chapter do not engage the bridge deck heating system until after icing conditions have been detected. Further more, once the heating

Table 2- 2 Summary of conditions required to automatically turn bridge deck heating systems on and off.

| Bridge | Conditions Required to Turn Heating System On | Conditions Required to Turn Heating System Off |
|---|--|---|
| Tenth Street Pedestrian Viaduct – Lincoln, Nebraska | Pavement T < 39°F AND Air T < 36°F AND Moisture on Bridge Deck | Pavement Temperature > 55°F |
| Silver Creek – Salem, Oregon (control rules partially proprietary) | Air T < Specified Value AND Moisture on Bridge Deck | Air T > 35-37°F OR Pavement T > Specified Value |
| Highland Interchange – Portland, Oregon | 20°F < Air T < 33°F AND Dew Point > 0°F | Unknown |
| Second Street Overcrossing – Hood River, Oregon | Air T < 35°F AND Relative Humidity > 95% | 30-minute minimum runtime AND Pavement T > 36°F |
| U.S. 287 – Amarillo, Texas | Pavement T < 35°F AND Precipitation Forecast | Unknown |
| Route 60 Bridge – Amherst County, Virginia | Snow or Ice on Pavement OR Precipitation Present AND Air T < 35°F OR Moisture on Bridge Deck AND Pavement T < 35°F | No Moisture on Pavement for 10 minutes OR Pavement T > 40°F |

system has been turned on, it may take several hours before the bridge is warm enough to deice.

To prevent preferential icing the control system should begin heating the bridge before icing conditions set in. By accessing real-time weather forecasts, the Smart Bridge control system knows the timing and severity of icing conditions. The control system also accounts for the time required to raise the temperature of a bridge deck. This way heating is initiated several hours in advance of icing conditions to ensure that the bridge deck is warm enough to prevent ice formation. Although simply put, this is the basic control strategy. A qualitative discussion of the control concepts used by the Smart Bridge control system is presented in the following chapter. A detailed presentation of the Smart Bridge control algorithm is given in Chapter IV.

CHAPTER III

SMART BRIDGE CONTROL SOLUTION

3.1 Introduction

The previous chapter presented control strategies for existing heated bridge decks. A common aspect of these control strategies is that they only use current weather and pavement conditions to control the bridge deck heating system. This type of reactive-only control strategy is referred to as feedback control. Feedback control means that the bridge heating system will not be activated until after ice, moisture, precipitation, or high humidity has been detected. Because heating a bridge is a slow process (requires hours), snow or ice could accumulate on the bridge while the pavement heats.

Only one of the bridges mentioned in Chapter II, U.S. 287 in Amarillo, Texas, uses forecasted conditions (precipitation forecast) in addition to feedback control. By accessing precipitation forecasts, the Amarillo bridge control system is capable of taking proactive measures to prevent ice and snow. When the Amarillo bridge control system recognizes that precipitation coinciding with cold air temperature is in the forecast, the heating system is turned on. By heating the bridge before the potential for preferential icing exists, the probability of preferential icing or snow accumulation is significantly reduced. Our Smart Bridge control solution takes the proactive strategy employed by the Amarillo bridge control system to a new level.

Using information about the present as well as predicted information about the future to make control decisions is a key aspect of a control technique called model predictive control (MPC). The Smart Bridge control system is based on the principles of

MPC, a departure from the feedback control strategies discussed in Chapter II. This chapter is intended to convey fundamental ideas about the MPC technique, and qualitatively convey how MPC is applied in the Smart Bridge control system. This chapter sets the stage for Chapter IV, a quantitative discussion of MPC as it applies to the Smart Bridge control system.

3.2 MPC Approach

MPC is an algorithm for calculating control action. The basic MPC calculation mimics the actions of a smart operator [8]. In this section a comparison is made between the actions of a smart operator and a feedback controller. The intent is to demonstrate the concepts of MPC and also show the advantages MPC has over feedback control. An everyday example, controlling the speed of a bus, is used to make these points.

Consider a charter bus, a vehicle with relatively poor acceleration, traveling on a level section of interstate highway. Initially the bus has a speed of 65 mph and the gas pedal is depressed 25%. A quarter of a mile ahead of the bus's current position is a long, uphill section of highway. The control problem at hand is to manipulate the position of the gas pedal (0-100% depressed) such that bus's speed is kept as close as possible to 65 mph (i.e. maintain constant speed). Figure 3-1 illustrates this hypothetical control problem.

First, assume that the driver has engaged the automatic cruise control. Automatic cruise control is an example of pure feedback control. As described earlier, a feedback



Figure 3- 1: Adjust the position of the gas pedal to maintain the speed of the bus at 65mph.

controller makes adjustments only when there is a discrepancy between the measured and desired values of the controlled variable. Therefore, at the outset of the hypothetical control problem the cruise control maintains a gas pedal position of 25% depressed. However, upon reaching the hill gravity begins to slow the bus down. The cruise control reacts to the discrepancy between the bus's measured speed of 62 mph and the desired speed of 65 mph by depressing the gas pedal to 30%. This process continues until the bus is eventually back at the desired speed. Figure 3-2 shows the bus's speed and how the cruise control responded during the hypothetical experiment. Although the cruise control was able to get back to setpoint, this only happened after a -10 mph deviation took place. This example shows that a feedback controller is capable of controlling a given process. However, the reactive nature of this type of control strategy dictates that disturbances (the hill in this example) may cause significant upsets to the controlled variable (speed of the bus).

Now consider the case where the bus driver manipulates the gas pedal position rather than the automatic cruise control. Like the cruise control case, initially the bus is

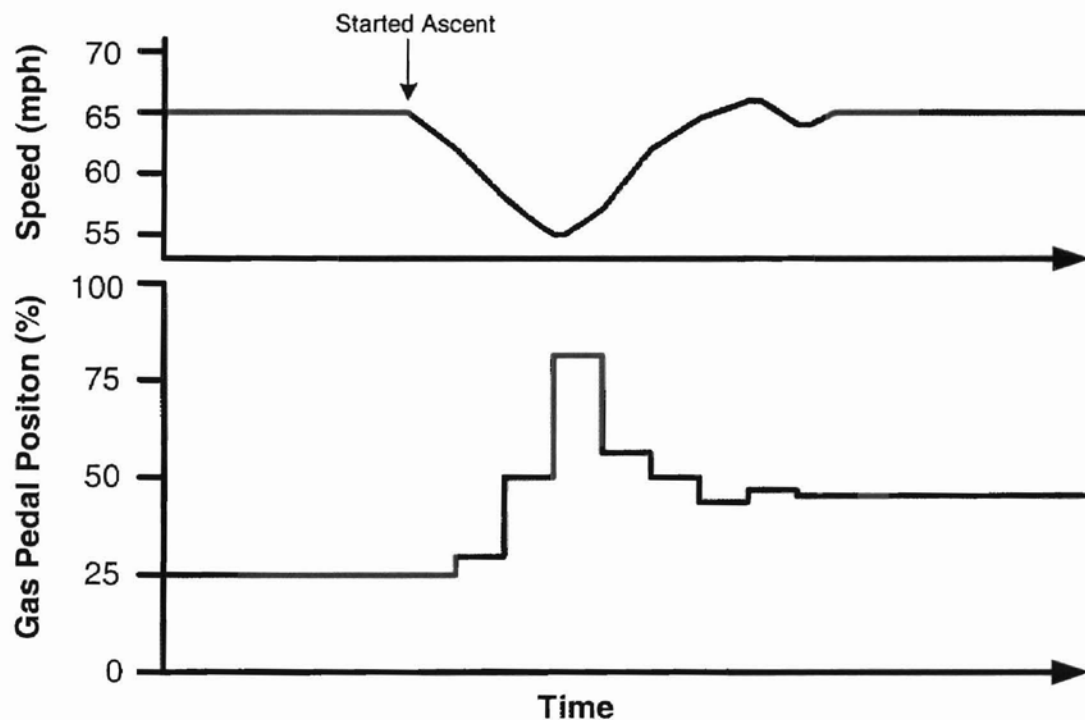


Figure 3- 2: Bus speed and gas pedal position under the influence of the automatic cruise control.

traveling on a flat section of interstate at 65 mph with the gas pedal depressed 25% of its total range. When the bus is an eighth of a mile away from the base of the hill the bus driver has the following thought, “if the bus doesn’t start gaining momentum now, it will slow down a lot when we start going up that hill.” After considering this situation, the bus driver moves the gas pedal to 35%. An increase of the position of the gas pedal by 10% is based on the driver’s knowledge of how the bus responds to changes in the gas pedal position. A couple of seconds later the bus driver looks at the speedometer, which reads 67 mph, repeats his thought process, and subsequently moves the gas pedal to 50%. This process continues until eventually the bus is once again traveling at a speed of 65 mph while going up the hill. Figure 3-3 shows how the speed of the bus and the gas

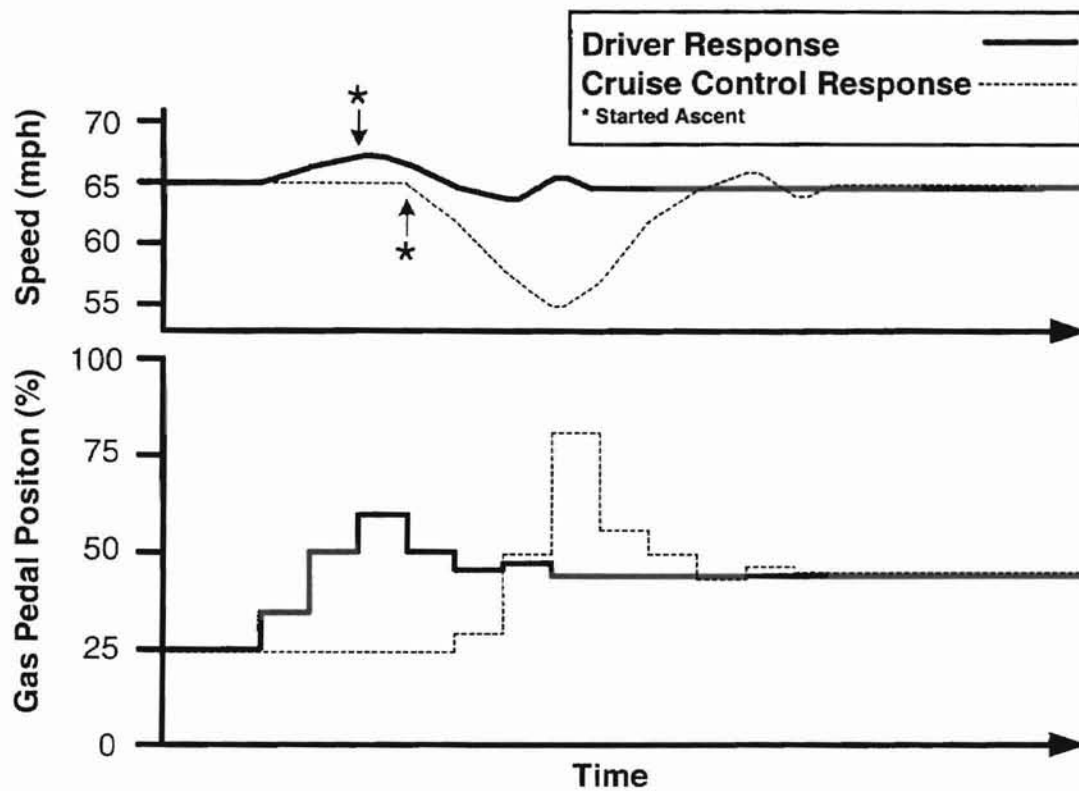


Figure 3- 3: Bus speed and gas pedal position when the bus driver manipulates the gas pedal position. The dashed profiles show the results for the cruise control case.

pedal position varied over the course of this hypothetical experiment. The bus speed and pedal position for the cruise control case have been superimposed onto Figure 3-3 for comparison. Figure 3-3 shows that increasing the speed of the bus before it reached the hill resulted in a +2.5 mph deviation from the 65 mph setpoint as opposed to the -10 mph deviation exhibited by the automatic cruise control. Therefore, in the context of minimizing the deviation from setpoint, the bus driver did a better job of rejecting the effect of the hill (a disturbance) on the speed of the bus.

Ultimately, the bus driver is able to outperform the automatic cruise control because his control algorithm (i.e. thought process) is more sophisticated than that of the

cruise control. The bus driver has three distinct advantages over the automatic cruise control. First, the bus driver is able to recognize disturbances in the near future. Second, the bus driver can predict the influence these disturbances will have on the speed of the bus. Third, the bus driver is able to determine the best course of action to counteract the influence of disturbances.

As mentioned earlier, MPC is designed to mimic this thought process. Figure 3-4 shows the MPC analog of the bus driver's thought process. First, the bus driver measures the current speed (controlled variable, CV) of the bus (Fig. 3-4 A). When he sees a hill (disturbance variable, DV) ahead, he predicts the effect it will have on the speed of the bus if he leaves the gas pedal (manipulated variable, MV) at 25% in the future (Fig. 3-4 curve B). Based on the prediction and an understanding of how the speed of the bus responds to changes in the gas pedal position, the driver estimates a course of action (Fig. 3-4 D) that will allow him to best meet his objective (Fig. 3-4 curve C) of maintaining a constant speed of 65 mph. Profile E in Figure 3-4 shows what the driver expects to happen if he uses the course of action shown in profile D. Therefore, the best thing the driver can do at the current time is implement the first step in his planned course of action (denoted by curve F in Fig. 3-4). This process is then repeated on a periodic basis.

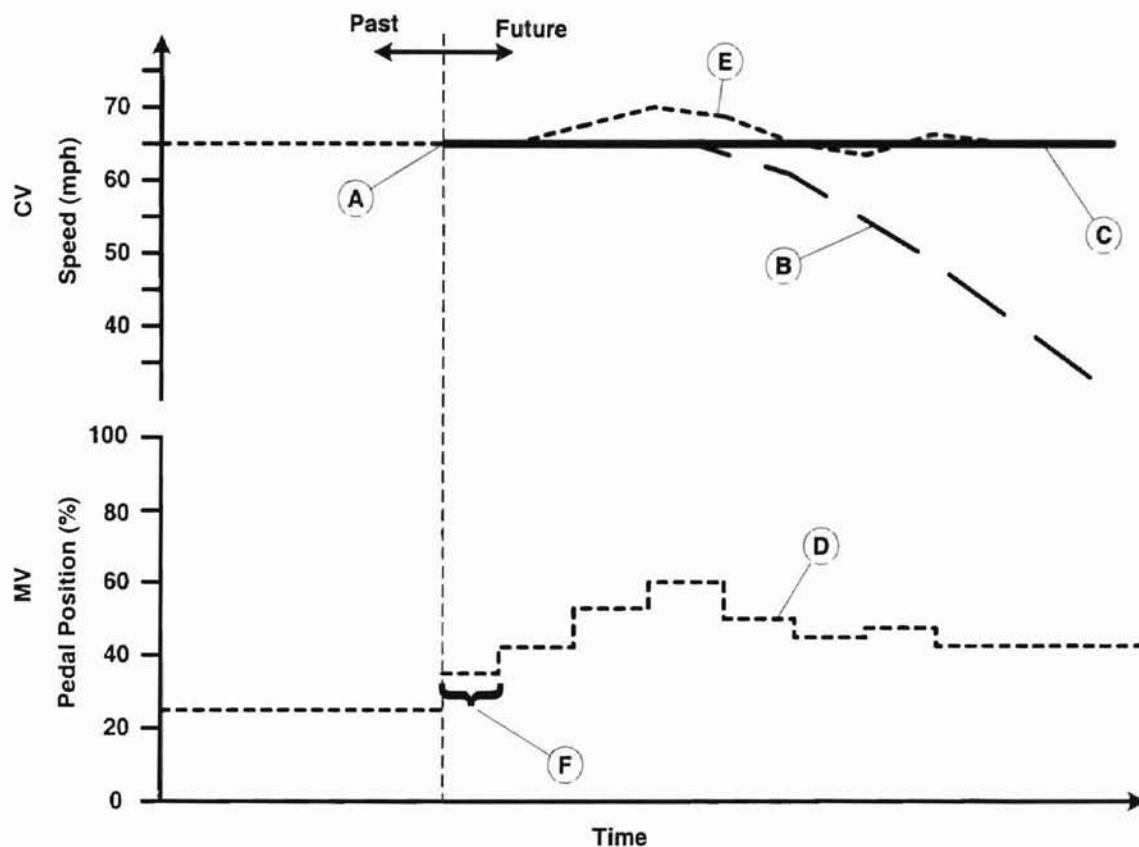


Figure 3- 4: MPC analog of operator thought process. A) Current CV measurement B) Predicted CV response with no future MV moves C) Desired CV response D) Optimal set of future MV moves E) Predicted CV response after optimal set of MV moves F) Best control move to make at the current time.

3.3 Smart Bridge MPC Approach

The previous section outlined how a bus driver uses an MPC approach to control the speed of a bus. In this section the MPC control strategy is described as it applies to the Smart Bridge. As in the previous section, Section 3.3 is a conceptual presentation of the Smart Bridge MPC strategy. Details concerning implementation of these concepts are covered in Chapter IV, Model Predictive Control Implementation.

The primary Smart Bridge control objective is to prevent preferential icing and snow accumulation on the surface of a heated bridge deck. To meet this objective, the Smart Bridge control system uses MPC to control the average bridge deck surface temperature (CV for this problem) by manipulating the temperature of the fluid circulated through the bridge deck (MV's for this problem).

In Section 3.2, the first step in the bus driver's control algorithm was to measure the current value of the CV. Likewise, the first step in the Smart Bridge control strategy is to measure the present value of the average bridge deck temperature. The average bridge deck temperature is the average temperature measurement from numerous thermocouples located in the bridge deck. Thermocouples located on the one-quarter scale OSU test bridge are embedded one eighth inch below the pavement surface.

Assessment of the magnitude and timing of future disturbances is the second step of the MPC control strategy. Just as the driver in Section 3.2 was able to see that the bus was approaching a hill, the Smart Bridge control system has access to forecasted weather conditions. At any given time, the Smart Bridge control system has a 12-hour forecast for the following weather variables: air temperature, precipitation rate, relative humidity, wind speed, wind direction, and solar radiation. The forecasted conditions are the output of a complex weather model operated by the National Weather Service. This model and other weather inputs are discussed in Chapter V, Weather Inputs.

The next phase of the Smart Bridge MPC algorithm is to predict the affect predicted weather conditions will have on the average bridge deck surface temperature if the bridge loop heating fluid temperature and flowrate are held constant. As mentioned above, forecasted weather conditions are available for the next 12-hour period. These

forecasted conditions serve as inputs to a first-principles heat transfer model of the bridge deck, which is used to calculate how the average pavement temperature will respond over the next 12 hours. Section 4.2 covers specific details of the first-principles bridge deck model. The point here is that weather forecasts are used in conjunction with the bridge deck model to calculate the equivalent of profile B in Figure 3-4. Furthermore, this predicted bridge response is a key factor in the ability of the Smart Bridge control system to take proactive measures to prevent preferential icing.

Before the controller can calculate a future course of action it must be provided with the desired CV trajectory. For the example given in Section 3.2, the desired CV trajectory was a constant speed of 65 mph. For the Smart Bridge the control objective is prevention of preferential icing and snow accumulation on the bridge deck. To meet this objective the average bridge deck temperature must be above 0°C at times when preferential icing or frozen precipitation is likely. Unlike a constant desired bus speed from the previous section, a constant bridge deck temperature is not desirable. This is because there will be times when preferential icing or snow is not a risk, and therefore it is acceptable if the average bridge deck temperature is below 0°C . Furthermore, it is economically inefficient to heat the bridge deck when preferential icing or snow accumulation is not imminent. All of these points are considered by the Smart Bridge control system when determining the future desired average bridge deck temperature trajectory.

Three pieces of information are necessary to calculate the desired CV trajectory. First, a set of “icing potential” rules is needed to establish weather conditions that indicate when preferential icing or freezing precipitation is likely to occur. The second

requirement is the 12-hour weather forecast mentioned above. The Smart Bridge control system uses the weather forecast in conjunction with the icing potential rules to determine time periods in the future when the bridge deck temperature should be greater than 0°C . Finally, a reasonable bridge deck heating rate in $^{\circ}\text{C/hr}$ is required so as not to request a desired bridge deck temperature trajectory that is unfeasible.

Figure 3-5 represents a hypothetical situation when the bridge deck heating system must be engaged to prevent preferential icing. By applying the icing potential rules to the 12-hour weather forecast, the controller determines that the risk of preferential icing is high between +5 and +8.5 hours into the future. For this case, the Smart Bridge control system sets the desired average bridge deck temperature to 1°C from +4 hours until +12 hours into the future. A desired value of 1°C is specified between +4 and +5 hours as safety factor. From the +0 hours until +4 hours into the future the desired CV trajectory is set to a temperature ramp with a user-specified slope.

The final step of the MPC algorithm is to calculate a set of future control moves that compensates for the difference between the predicted CV response without future control moves, and the desired CV trajectory. In the example of Section 3.2, the bus driver was able to carry out this step using his intuition about the effect of pushing the gas pedal on the speed of the bus. With MPC, the controller uses a mathematical model (see Section 4.4.1 on step response models) to calculate the best

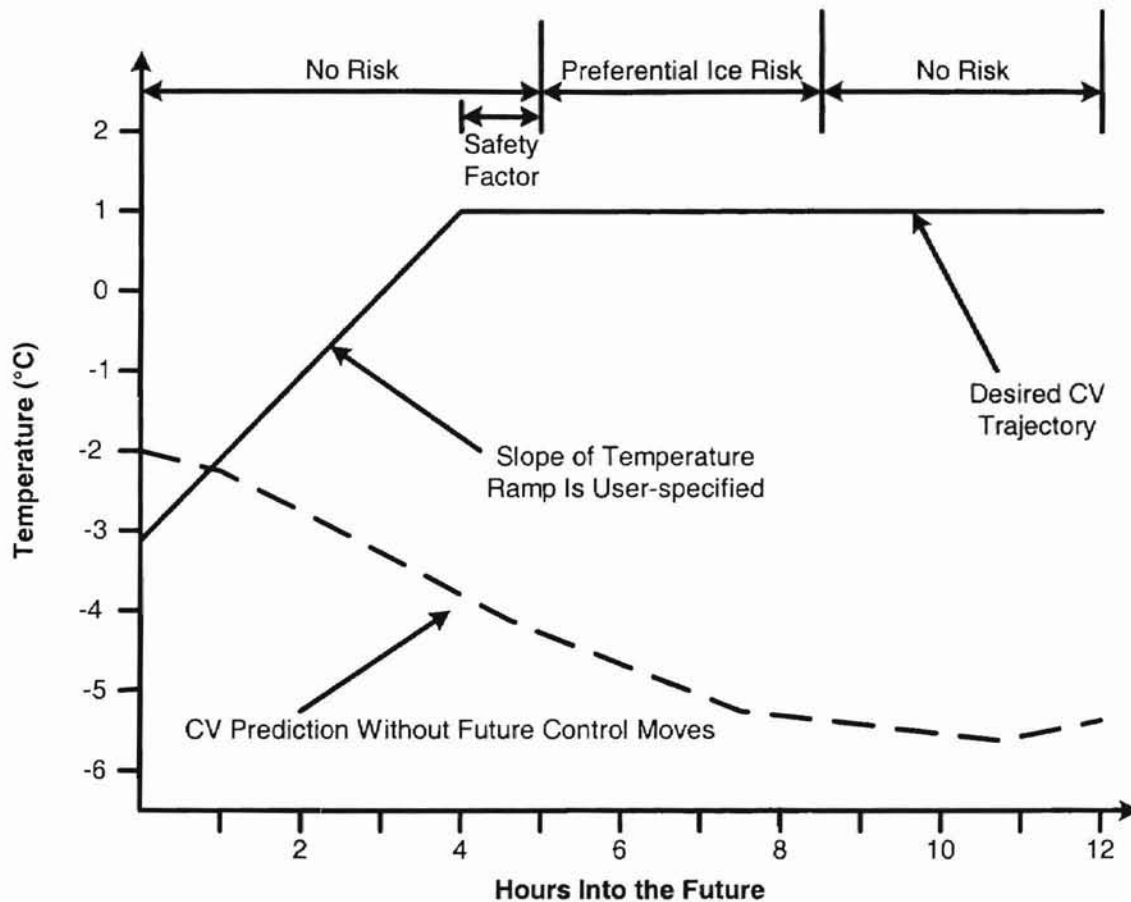


Figure 3- 5: Selecting the desired CV trajectory. The weather forecast, icing potential rules, maximum bridge deck heating rate, and CV prediction without future control moves are considered.

way to change the manipulated variable in the future. After calculating the best set of future control moves, the controller implements the first control move in this sequence.

An MPC strategy repeats the steps discussed above at a specified frequency, defined by the sample period. The current version of the Smart Bridge control system uses a sample period of 15 minutes. Figure 3-6 is a flow diagram that shows the major steps taken by the Smart Bridge control system every 15 minutes.

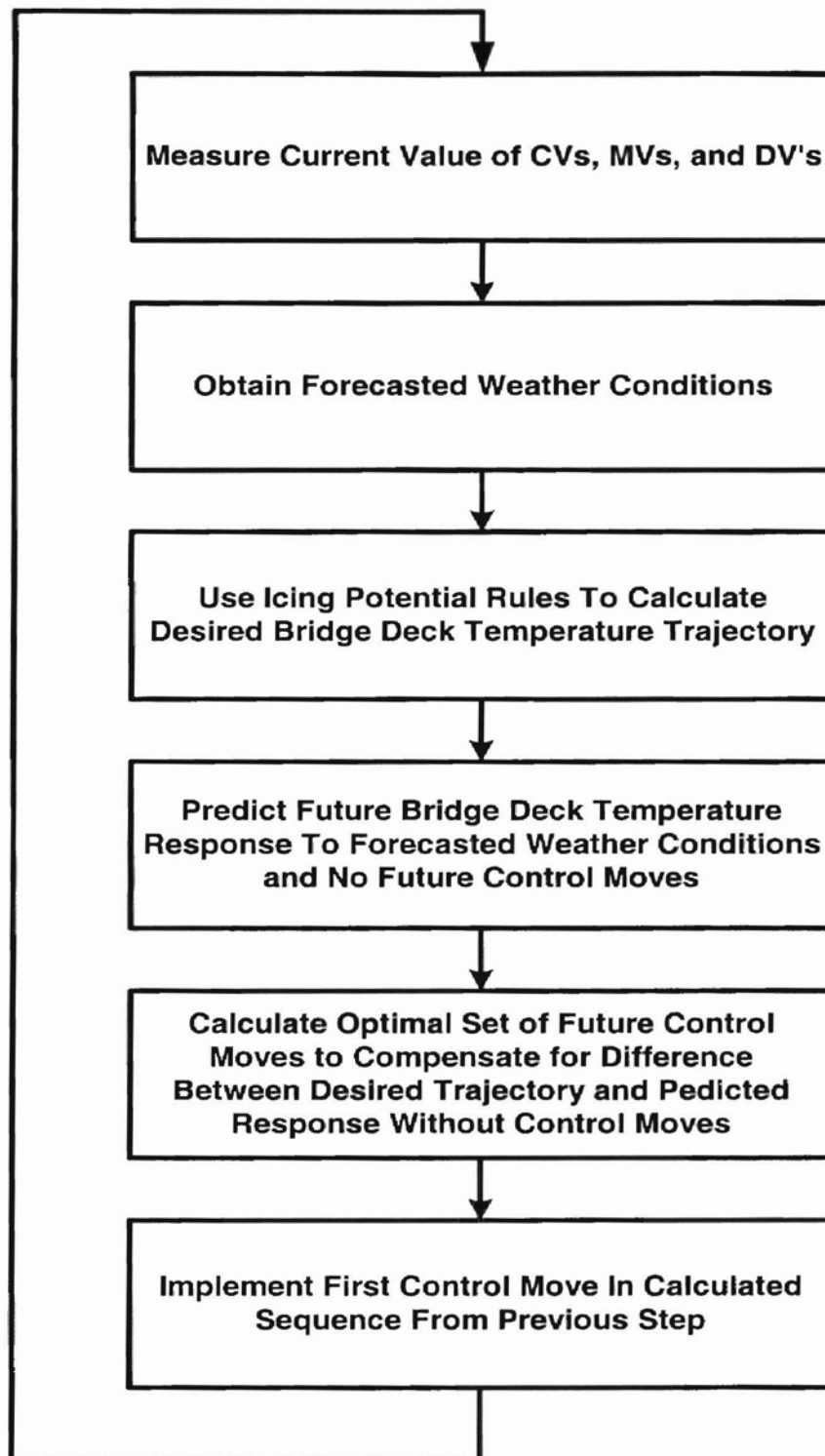


Figure 3- 6: Steps performed by the Smart Bridge MPC algorithm at each sample time.

3.4 Summary

Fundamental concepts of MPC have been presented qualitatively in this chapter. Section 3.2 described a hypothetical control problem, controlling the speed of a bus with a disturbance in the near future. The response the bus's automatic cruise control was compared to the response under the control of the bus driver. This example is intended to show that in general, the proactive nature of MPC is capable of much better disturbance rejection than pure feedback control. This statement is particularly true of slow processes like heating a bridge deck.

The Smart Bridge control system uses an MPC strategy. Section 3.3 describes how MPC is applied to the Smart Bridge control problem. Weather forecasts play an important role in the Smart Bridge control system, facilitating predictions of future bridge deck temperature profile and determination of desired deck temperature trajectory. The predictive nature of MPC gives the Smart Bridge control system the ability not only of anticipating when preferential icing will occur, but also of preventing preferential icing by heating the bridge deck before ice can form. This proactive strategy sets the Smart Bridge control system apart from the control strategies of Chapter II, which all use reactive (i.e. feedback) control algorithms.

CHAPTER IV

SMART BRIDGE CONTROL SYSTEM IMPLEMENTATION

4.1 Introduction

The Smart Bridge control system uses an MPC strategy to make control decisions. MPC refers to a class of algorithms that compute a sequence of manipulated variable adjustments in order to optimize the future behavior of a plant [9]. This implies that control decisions made using an MPC strategy result from the solution of an optimization problem. Chapter IV formulates the optimization problem used by the Smart Bridge control system.

Section 4.2 discusses the first-principles bridge deck model and the role it plays in the Smart Bridge optimization problem. Topics include model parameters, inputs, outputs, and calculating the bridge deck response to forecasted weather conditions. Section 4.3 discusses how the Smart Bridge control system sets the desired average bridge deck surface temperature trajectory. Section 4.4 presents the optimization problem used to calculate control decisions. Topics covered in Section 4.4 include process models, tuning parameters, and operating constraints. Section 4.5 discusses the numerical technique employed by the Smart Bridge control system to solve the optimization problem presented in Section 4.4. Topics included in Section 4.5 include multiple variable search method, line search method, and convergence criteria. Section 4.6 identifies parameters in the optimization problem that future researchers might use in developing the adaptive portion of the Smart Bridge control system.

4.2 First-principles Bridge Deck Model

Investigators from the OSU Mechanical and Aerospace Engineering department have developed a first-principles bridge deck model as part of Task 4.1.1: Develop and Validate Advanced Modeling Software. Complete descriptions of the bridge deck model are available in [10] and [11]. The bridge deck model uses a system of partial differential equations to describe the energy balance around a hydronically heated bridge deck. A two-dimensional finite difference approach is used to numerically solve this system of equations. The bridge deck model considers heat transfer due to solar radiation, thermal radiation, convection at the pavement surfaces, rain and snow evaporation (sensitive and latent heat effects), conduction through the bridge deck and tube walls, and heat transfer from the bridge loop fluid [10].

Section 4.2 describes the inputs and parameters required by the model as well as the steps taken by the Smart Bridge control system to calculate the predicted bridge deck response.

4.2.1 Bridge Deck Model Parameters, Inputs, and Outputs

The first-principles bridge deck model is general in the sense that the properties of the simulated bridge deck are user-specified. These parameters are passed to the first-principles bridge model as arguments and must be specified before the Smart Bridge control system is activated. The Smart Bridge control system user interface has been designed in such a manner that the bridge deck parameters are easily configured.

Table 4-1 lists the bridge deck parameters (and units) required by the first-principles bridge deck model.

In addition to the bridge deck parameters, a set of input variables is passed to the bridge deck model. Ambient weather conditions, bridge loop flowrate, and bridge loop supply temperature are included in the set of bridge deck model inputs. Table 4-2 lists the input variables (with units). The current Smart Bridge control system is designed to acquire ambient conditions (except rainfall and snowfall) from Oklahoma Mesonet data. Typically instrumentation at the bridge site or a nearby RWIS station would provide local weather conditions to the control system. The Smart Bridge control system calculates snowfall and rainfall rates from NWS radar data. Bridge loop supply temperature is the MV, and is set automatically by the Smart Bridge control system.

Given a set of bridge deck parameters, the first-principles bridge deck model calculates the thermal effects of the input variables on the bridge deck. These effects are reflected in the model outputs. Bridge deck model outputs (with units) are given in Table 4-3.

Table 4-1: Bridge deck parameters used in the first-principles bridge deck model.

| | |
|---|--|
| Pavement Length (m) | Absorptivity Coefficient (dimensionless) |
| Pavement Width (m) | $C_{p, \text{Layer 1}}$ ($\text{J/m}^3 \text{ } ^\circ\text{C}$) |
| Slab Orientation ($^\circ$ from North) | $C_{p, \text{Layer 2}}$ ($\text{J/m}^3 \text{ } ^\circ\text{C}$) |
| Pavement Thickness (m) | k_{Pipe} ($\text{W/m } ^\circ\text{C}$) |
| Pipe Spacing (m) | Wall Thickness of Pipe (m) |
| Pipe Diameter (m) | Fluid Type (2 for GS-4) |
| Pipe Depth Below Surface (m) | Weight % GS-4 (%) |
| Depth to Interface 1 (m) | Number of Flow Circuits |
| $k_{\text{Layer 1}}$ ($\text{W/m } ^\circ\text{C}$) | Length of Pipe Per Circuit (m) |
| $k_{\text{Layer 2}}$ ($\text{W/m } ^\circ\text{C}$) | Transient Time Step (sec) |
| Emmissivity Coefficient (0.9) | Bottom Boundary Condition |
| Minimum Flow Condition (kg/sec) | |

Table 4-2: Input variables to the first-principles bridge deck model.

| | |
|---------------------------------------|---|
| Air Temperature ($^\circ\text{C}$) | Solar Radiation ($\text{W/ m}^2 \text{ } ^\circ\text{C}$) |
| Humidity Ratio (kg water/kg dry air) | Solar Angle of Incidence (radians) |
| Sky Temperature ($^\circ\text{C}$) | Snowfall Rate (mm/hr water equivalent) |
| Wind Speed (m/sec) | Rainfall Rate (mm/hr water equivalent) |
| Wind Direction ($^\circ$ from North) | Bridge loop supply temperature ($^\circ\text{C}$) |
| | Bridge loop flowrate (kg/sec) |

Table 4-3: Output variables from the first-principles bridge deck model.

| |
|--|
| Average Bridge Deck Surface Temperature (°C) |
| Bridge Loop Return Temperature (°C) |
| Heat Transfer Rate From Bridge Loop (kJ/sec) |

4.2.2 Predicted Bridge Response to Forecasted Weather Conditions

The Smart Bridge control system uses the first-principles bridge deck model to calculate the average bridge deck surface temperature response to forecasted weather conditions (refer to Chapter V, Weather Inputs) in the absence of future control moves. This predicted response is represented in Figure 4-1 by the vector \hat{y} .

At each sample time the Smart Bridge control system first updates the weather forecast. A 12-hour prediction horizon is used in the current control system. The length of the prediction horizon was intentionally set to match that of the NWS forecast product used by the control system (see Chapter V).

To calculate \hat{y} , the Smart Bridge control system steps forward through time in 15-minute increments until the end of the prediction horizon is reached. Each time step is equal to one sample period. At each time step the Smart Bridge control system calls the first-principles bridge deck model, using the forecasted weather conditions and the current MV value as inputs to the bridge deck model. The average bridge deck surface temperature computed at each time step comprises the elements of \hat{y} .

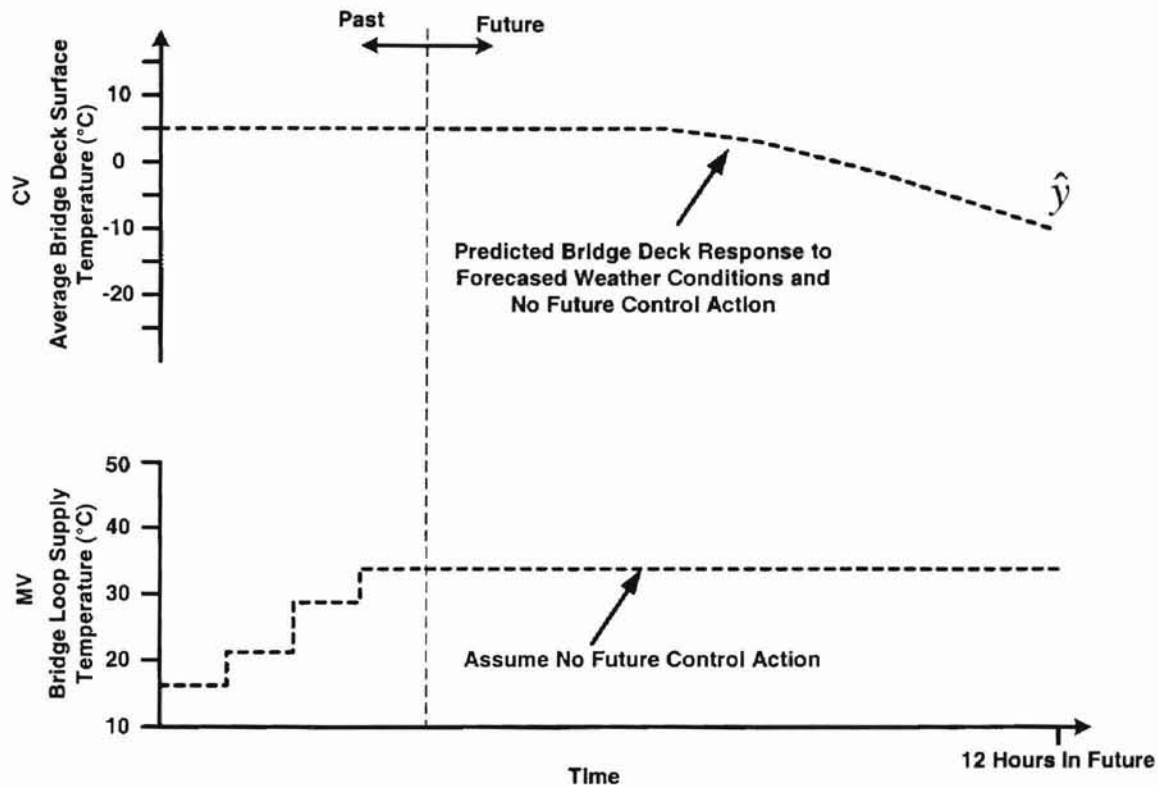


Figure 4- 1: The first-principles bridge deck model is used to calculate \hat{y} .

4.3 Setting the Reference Trajectory

This section outlines the procedure for setting the reference trajectory, \mathbf{r} . Vector \mathbf{r} represents the desired future response of the CV. In the case of the Smart Bridge control system, \mathbf{r} is the desired future path of the average bridge deck surface temperature. To prevent preferential icing, \mathbf{r} should be set such that the desired average bridge deck temperature is above freezing at all times when the potential for preferential icing exists. Section 4.3.1 describes how the Smart Bridge control system analyzes the weather forecast for preferential icing potential. Section 4.3.2 explains how the Smart Bridge control system sets \mathbf{r} based on forecasted preferential icing potential.

4.3.1 Identifying Preferential Icing Potential

The Smart Bridge control system uses a rule-based approach to identify when the potential for preferential icing exists. Two “icing potential” rules are built into the current version of the Smart Bridge control system. These icing potential rules have been recommended by investigators working on Task 4.3.1.1: Weather Inputs.

The first rule is based on dew point depression, defined in Equation 4-1. This rule says that a potential for preferential icing exists any time the dew point depression falls below a specified threshold. This rule guarantees that the average bridge deck surface temperature is above 0°C any time the air has a high moisture content. The second icing potential rule states that a potential for preferential icing exists any time there is precipitation. This rule guarantees that the control system will attempt to drive the average bridge deck surface temperature to the setpoint temperature at times when moisture is on the pavement. For cases when the average bridge surface temperature is far above the setpoint value, the control system will attempt to cool the bridge deck by setting the bridge loop supply temperature at the lower constraint. Logic has been built into the control system that turns the heating system off when the MV is set at the lower constraint. Effectively, this logic means that the control system will not perceive a summer rain as a preferential icing threat. Table 4-4 lists the icing potential rules used in the Smart Bridge control system.

$$\text{Dew Point Depression} = \text{Air Temperature} - \text{Dew Point Temperature} \quad (\text{Eq. 4-1})$$

Table 4- 4: Icing potential rules built into the current version of the Smart Bridge control system

| <u>Icing Potential Rules</u> |
|---|
| 1. A potential for preferential icing exists any time the dew point depression falls below a specified threshold. |
| 2. A potential for preferential icing exists any time there is precipitation. |

In accordance with project deliverables, the Smart Bridge control system software has been written in a modular fashion. The icing potential rules discussed above are contained in a module. The modular format of the Smart Bridge control software makes adding, removing, or modifying more sophisticated icing potential rules straightforward.

Along these lines, simulation results suggest that the dew point depression rule should be modified. Because a hard threshold is used, sometimes the forecasted dew point depression will oscillate around the threshold. This means that if the dew point depression is very close to the threshold, small changes in dew point depression can mean the difference between a perceived preferential icing threat and no perceived threat. This problem is illustrated in one of the case studies presented in Chapter VI. A fuzzy threshold, rather than the hard threshold currently implemented is one way to handle this issue.

4.3.2 Reference Trajectory Strategy

The reference trajectory is used to maintain the average bridge deck surface temperature above 0°C at times when the potential for preferential icing exists. Therefore, the first step in setting r is to identify times in the future when preferential icing is likely. To carry out this step, the Smart Bridge control system evaluates the icing potential rules listed above using the currently available weather forecast.

From the first indication of preferential icing in the forecast to the end of the forecast, the reference trajectory is set to a nominal setpoint above 0°C . The current version of the Smart Bridge control system uses a nominal setpoint of 1°C . The nominal setpoint is a user-adjustable parameter. To provide a margin of safety, the control system assumes that preferential icing will occur one hour before the first indication in the forecast.

Prior to the one-hour safety margin, r is set to a temperature ramp. A temperature ramp is used as the path the controller should use to raise the current bridge deck temperature to the setpoint temperature. The slope of the temperature ramp is a user-specified parameter. Selecting a ramp slope that is too steep will result in an unfeasible reference trajectory in the sense that the bridge deck heating system will not be able to supply enough heat. Selecting a ramp slope that is too flat will result in inefficient performance in the sense that the bridge deck heating system will operate longer than necessary. A 2°C/hr slope is used for the temperature ramp in the current version of the Smart Bridge control system.

Figure 4-2 shows a situation where the icing potential rules predict that the first indication of preferential icing is four hours into the future. Figure 4-2 demonstrates how

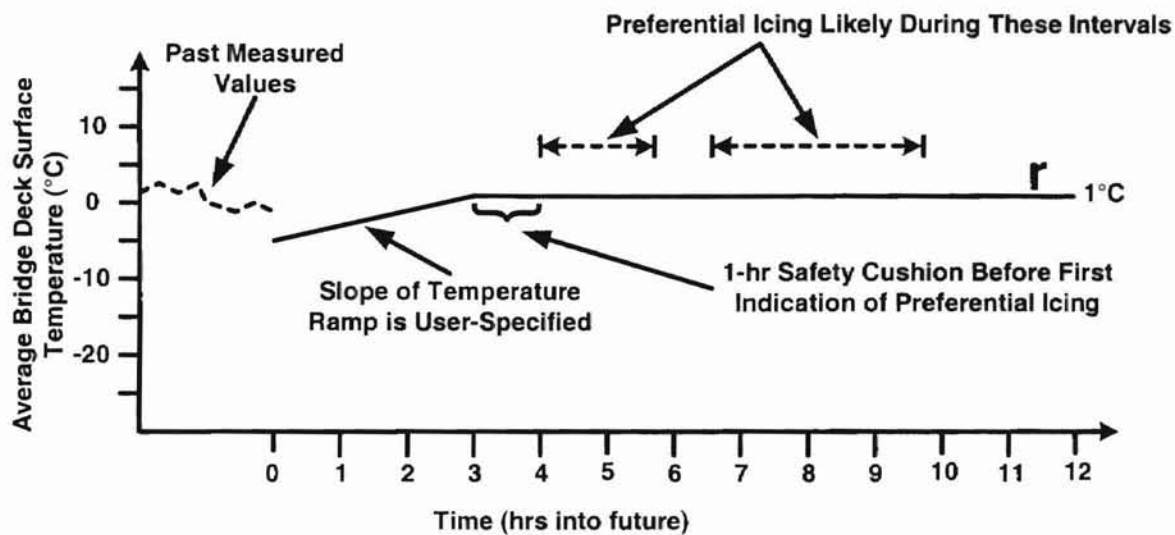


Figure 4- 2: Example of how the Smart Bridge control system sets r .

the Smart Bridge control system would set the reference trajectory for this hypothetical situation according to the strategy presented above. Note that the temperature ramp is independent of the current average bridge deck surface temperature, insuring that the bridge deck heating system does not operate longer than it needs to.

Figure 4-3 shows that when preferential icing is forecasted for the present time, the entire reference trajectory is set at the setpoint value, as opposed to using a temperature ramp. In this case a temperature ramp is not used because the bridge should be warm enough to prevent preferential icing at the current time.

In Figures 4-2 and 4-3, the reference trajectory is set to the setpoint value at times when preferential icing is no longer predicted to occur (10-12 hrs in Figure 4-2 and 2-12 hrs in Figure 4-3). This has been done strictly for programming purposes. In reality, because there is no risk of preferential icing, the heating system should not be used during these times. This issue is handled in Section 4.4.3.

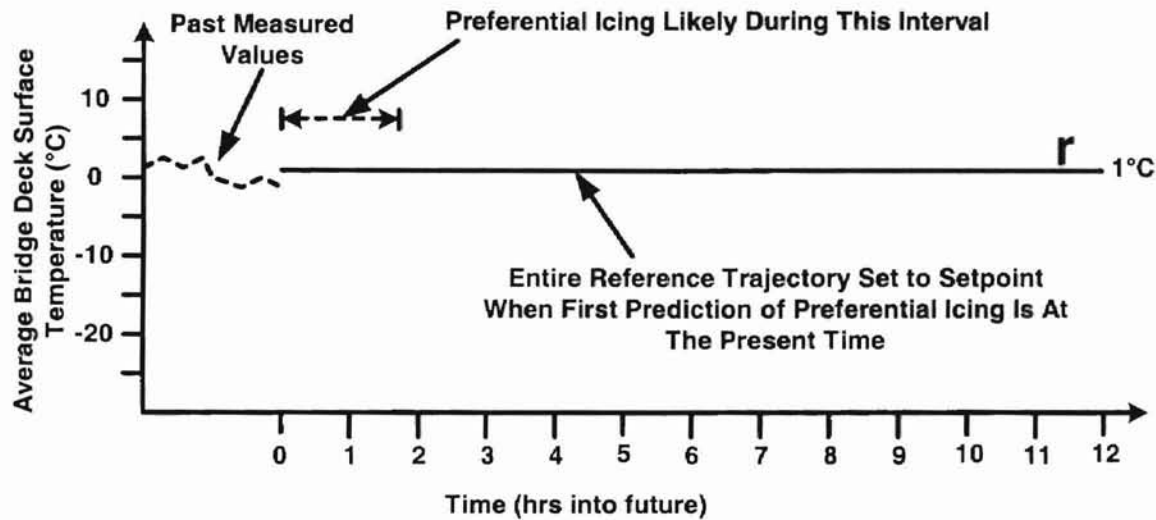


Figure 4- 3: When first indication of preferential icing occurs at present time the entire reference trajectory is set at the setpoint value.

4.4 Calculating Control Decisions

At each sample period the Smart Bridge control system calculates a sequence of future bridge loop supply temperature (MV) adjustments. After the sequence of future MV adjustments is calculated, the first adjustment in the sequence is selected as the current control action. By only implementing the first move in the sequence of MV adjustments, the assumption is made that over time the control performance will be optimized with minimal affects from any modeling errors.

The sequence of future MV moves is the solution to an optimization problem. Equations 4-2 and 4-3, respectively, define the objective function and constraints that apply to the Smart Bridge control problem. Equations 4-2 and 4-3 represent the standard formulation used for model predictive control. The first term on the right-hand side of

Equation 4-2 is called the error penalty term. The purpose of the error penalty term is to penalize the objective function for large discrepancies between the predicted response without control action (\hat{y}) and the desired response (r). The second term in Equation 4-2 is called the move suppression term. The purpose of the move suppression term is to penalize the objective function for large moves in the manipulated variable. Equation 4-3 defines the constraints imposed on the MV. For example, the bridge loop supply temperature is constrained between 10°C and 50°C by the operating limits of the bridge deck heating system. Qualitatively, the optimization problem given in Equations 4-2 and 4-3 says to pick the sequence of MV adjustments that causes \hat{y} to follow r but not at the expense of making unacceptably large MV adjustments. Also, the sequence of MV adjustments must not violate constraints established for the MV.

$$\min_{\Delta u} \Phi = (\hat{e} - A \Delta u)^T \Gamma (\hat{e} - A \Delta u) + \Delta u^T \Lambda^T \Lambda \Delta u \quad (\text{Eq. 4-2})$$

$$\text{s.t.} \quad u_{\min} \leq u \leq u_{\max} \quad (\text{Eq. 4-3})$$

where: Φ = objective function

\hat{e} = projected error vector

A = dynamic matrix

Δu = sequence of future MV adjustments

Γ = output error weighting matrix

Λ = input error weighting matrix

Details concerning the variables used in Equations 4-2 and 4-3 are presented in the following sections.

4.4.1 The Dynamic Matrix

In Equation 4-2, \mathbf{A} is called the dynamic matrix. The dynamic matrix is constructed using step response models relating manipulated (cause) and controlled (effect) variables. A step response model shows the response of a process output to a unit step change in a particular process input when all other process inputs are held constant. Because the Smart Bridge control system has one MV and one CV, only one step response model is required to construct the dynamic matrix. The step response model used in the Smart Bridge control system reflects the response of the average bridge deck surface temperature to a $+1^\circ\text{C}$ step change in the bridge loop supply temperature. The Smart Bridge control system is designed so that the required step response model is constructed automatically when the user configures the bridge deck parameters. The technical supplement [12] accompanying this thesis gives more details about generating the step response model. Figure 4-4 shows the approximate shape and magnitude of this step response model.

The vector, \mathbf{a} , is used to represent the MV-CV step response model. Components of the vector \mathbf{a} are shown in Figure 4-4, and are recorded at the user-specified sample rate for the control system. Vector \mathbf{a} must contain at least n components, the number of sample periods required for the CV response to stabilize. Note that the components of \mathbf{a} are given in deviation variables, defined as the departure from the original steady state conditions.

Equation 4-4 defines the dynamic matrix, \mathbf{A} , in terms of the step response vector, \mathbf{a} . Matrix \mathbf{A} has p rows and m columns. p is called the prediction horizon. A 15-minute sample rate and 12-hour prediction horizon ($p = 48$) is used in the current version of the

Smart Bridge control system. A 12-hour prediction horizon was selected because the weather forecasting products incorporated into the control system provide a 12-hour forecast. m is called the control horizon, and equals the length of the sequence of MV adjustments vector, Δu . A 6-hour control horizon ($m = 24$) is used in the current version of the Smart Bridge control system, which is based on the dynamics of the process. Typical values for p range from 20 to 50. The control horizon, m , should be shorter than p . Typically, m is one fourth to one third of p [13]. The Smart Bridge control system uses an m to p ratio of one half

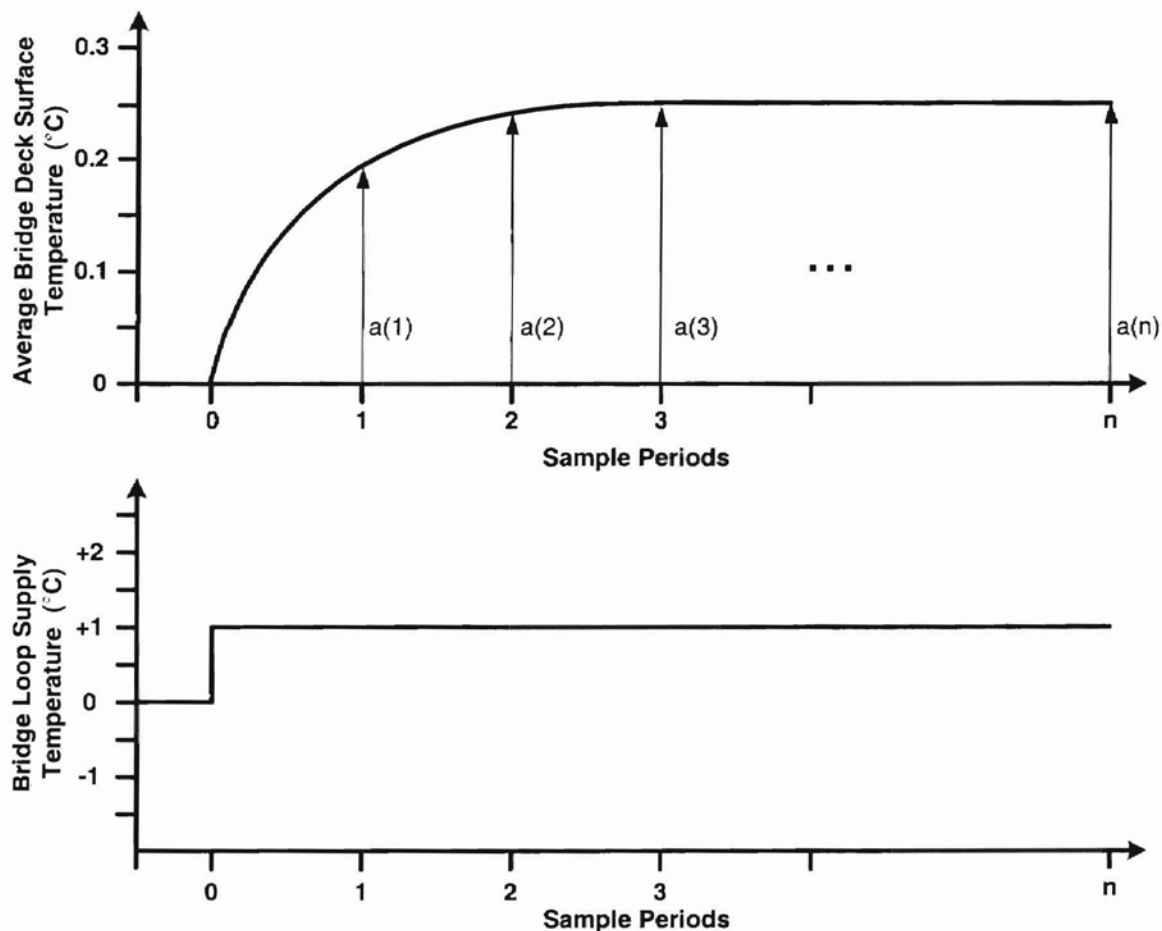


Figure 4- 4: Example step response model used by the Smart Bridge control system.

$$\mathbf{A} = \begin{bmatrix} a(1) & 0 & 0 & \dots & 0 \\ a(2) & a(1) & 0 & \dots & 0 \\ a(3) & a(2) & a(1) & \dots & 0 \\ \dots & \dots & \dots & \dots & \dots \\ a(m) & a(m-1) & a(m-2) & \dots & a(1) \\ a(m+1) & a(m) & a(m-1) & \dots & a(2) \\ a(p) & a(p-1) & a(p-2) & \dots & a(p-m+1) \end{bmatrix} \quad (\text{Eq. 4-4})$$

4.4.2 Projected and Residual Error Vectors

In Equation 4-2, $\hat{\mathbf{e}}$ is the projected error vector. The projected error vector, defined in Equation 4-5, is the difference between the reference trajectory, \mathbf{r} , and the predicted bridge response, $\hat{\mathbf{y}}$.

$$\hat{\mathbf{e}} = \mathbf{r} - \hat{\mathbf{y}} \quad (\text{Eq. 4-5})$$

The effect of a given sequence of MV adjustments on a CV can be approximated by the term $\mathbf{A} \Delta \mathbf{u}$. The residual error vector, \mathbf{e}_r , defined in Equation 4-6 is the difference between the projected error vector and the influence of the sequence of MV adjustments. By selecting a sequence of MV adjustments that causes $\mathbf{A} \Delta \mathbf{u}$ to better compensate for $\hat{\mathbf{e}}$, the magnitude of \mathbf{e}_r will diminish. Furthermore, the error penalty term in Equation 4-2 represents the sum of the weighted squared residual error. The influence of the error penalty term on the objective function is diminished as the selected $\Delta \mathbf{u}$ reduces \mathbf{e}_r .

$$\mathbf{e}_r = \hat{\mathbf{e}} - \mathbf{A} \Delta \mathbf{u} \quad (\text{Eq. 4-6})$$

4.4.3 Output Error Weighting Matrix

The output error weighting matrix, Γ , is a diagonal ($p \times p$) matrix that serves as a tuning parameter for the Smart Bridge control system. Γ is defined in Equation 4-7. A tuning parameter is used to manipulate the control performance by putting more emphasis on certain terms in the objective function.

Γ is a tuning parameter that appears in the error penalty term of the objective function. Elements on the diagonal of Γ are part of the vector γ . Elements of the vector γ penalize corresponding elements of the residual error vector. The current version of the Smart Bridge control system is designed so that components of \mathbf{e}_r in the near future are penalized more than components of \mathbf{e}_r in the distant future. This configuration forces the control system to respond more aggressively to residual error in the near future rather than the distant future. The control system uses $\gamma(1) - \gamma(16) = 2.5$, $\gamma(16) - \gamma(32) = 1.0$, and $\gamma(33) - \gamma(48) = 0.7$.

$$\Gamma = \begin{bmatrix} \gamma(1) & 0 & \dots & 0 & 0 \\ 0 & \gamma(2) & \dots & 0 & 0 \\ \dots & \dots & \dots & \dots & \dots \\ 0 & 0 & \dots & \gamma(p-1) & 0 \\ 0 & 0 & \dots & 0 & \gamma(p) \end{bmatrix} \quad (\text{Eq. 4-7})$$

The Γ -matrix is also used to detune the Smart Bridge control system at times when a reference trajectory is not required. A situation when this rule applies is shown in Figure 4-5. Figure 4-5 shows that preferential icing is likely for the first six hours of the prediction horizon. Although the strategy given in Section 4.3 dictates that the reference trajectory is set to 1°C over the entire prediction horizon, residual errors at times after the

threat of preferential icing has passed are inconsequential. The Smart Bridge control system addresses this particular situation by setting components of γ corresponding to times after the threat of preferential icing has passed equal to zero. For the example shown in Figure 4-5, $\gamma(25)$ - $\gamma(48)$ are set to zero.

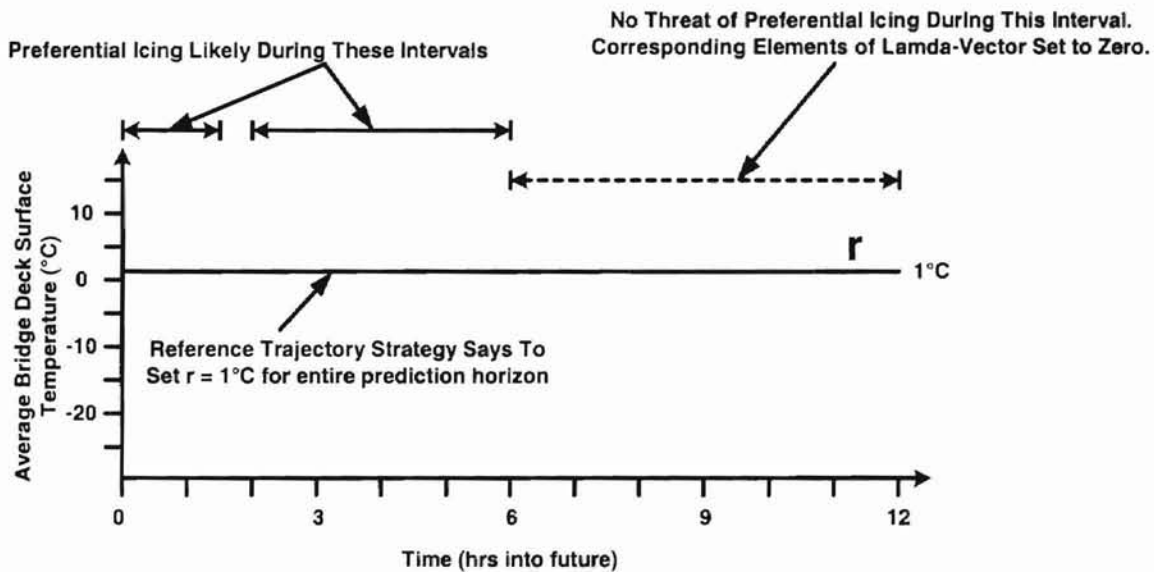


Figure 4- 5: Case where the controller can be detuned after the threat of preferential icing has passed.

4.4.4 Input Weighting Matrix

Another tuning parameter in the Smart Bridge control system is the input weighting matrix, Λ . Λ is an $(m \times m)$ diagonal matrix that appears in the move suppression term of Equation 4-2. Λ is defined in Equation 4-8. Elements of the vector λ make up the diagonal elements of Λ . Elements of λ weight corresponding elements of the sequence of MV adjustments, Δu . Selection of λ reflects the relative importance of

suppressing large MV moves compared to the relative importance of compensating for residual error. All elements of λ used in the Smart Bridge control system are set to a value of 1.

$$\Lambda = \begin{bmatrix} \lambda(1) & 0 & \dots & 0 & 0 \\ 0 & \lambda(2) & \dots & 0 & 0 \\ \dots & \dots & \dots & \dots & \dots \\ 0 & 0 & \dots & \lambda(m-1) & 0 \\ 0 & 0 & \dots & 0 & \lambda(m) \end{bmatrix} \quad (\text{Eq. 4-8})$$

4.4.5 Input Move Constraints

When controlling a process one must typically respect constraints on process inputs and outputs [8]. In our case, we only need to consider input constraints. In other words, it doesn't do any good to minimize the objective function given in Equation 4-2 by selecting a series of MV adjustments that is unachievable. The Smart Bridge control system is no different, as the bridge deck heating system has operating limits. These operating limits translate to constraints on the bridge loop supply temperature. The current version of the Smart Bridge control system assumes that the range of available bridge loop supply temperatures is 10-50°C.

Equation 4-3 defines the input constraints. \mathbf{u}_{\min} is a vector of length m with every element set to the lower constraint on the bridge loop supply temperature, 10°C.

Likewise, \mathbf{u}_{\max} is a vector of length m with every element set to the upper constraint on the bridge loop supply temperature, 50°C. \mathbf{u} is the vector of MV inputs that has been converted from the vector of MV adjustments, $\Delta\mathbf{u}$, using Equation 4-9. \mathbf{u}_0 is an m -

element vector with all elements set to the bridge loop supply temperature at the end of the previous sample period. \mathbf{L} is the $(m \times m)$ lower triangular matrix defined in Equation 4-10.

$$\mathbf{u} = \mathbf{L} \Delta \mathbf{u} + \mathbf{u}_0 \quad (\text{Eq. 4-9})$$

$$\mathbf{L} = \begin{bmatrix} 1 & 0 & \dots & 0 & 0 \\ 1 & 1 & \dots & 0 & 0 \\ \dots & \dots & \dots & \dots & \dots \\ 1 & 1 & \dots & 1 & 0 \\ 1 & 1 & \dots & 1 & 1 \end{bmatrix} \quad (\text{Eq. 4-10})$$

The constraints given in Equation 4-3 are violated if any of the elements of \mathbf{u} are less than the corresponding element of \mathbf{u}_{\min} . Similarly, the constraints given in Equation 4-3 are violated if any of the elements in \mathbf{u} are greater than the corresponding element of \mathbf{u}_{\max} .

4.5 Optimization Technique

The optimization problem given in Equation 4-2 and 4-3 is solved using an iterative search method. Section 4.5 outlines how the search for $\Delta \mathbf{u}^*$, the set of MV adjustments that minimizes Φ , is carried out. Because the solution to the control problem is a vector, a multiple variable search method is required. Section 4.5 describes the multiple variable search technique utilized in the Smart Bridge control system.

4.5.1 Multiple Variable Search Method

A cyclic method with line searching is used to solve the optimization problem presented in Equations 4-2 and 4-3. A cyclic search is an iterative technique used to minimize multiple variable objective functions [14] like the one given in Equation 4-2. Each iteration of a cyclic search is complete when the objective function has been minimized in each coordinate direction. After an iteration is complete the objective function is re-evaluated to test for convergence. If the convergence criteria are not satisfied the algorithm begins another iteration.

Figure 4-6 shows one iteration for a two-dimensional cyclic search. The first move is from the original guess, \mathbf{x}_0 , to $\mathbf{x}_{1,1}$. This move minimizes the objective function along a line that passes through \mathbf{x}_0 and in the direction of coordinate 1. The second move is from $\mathbf{x}_{1,1}$ to $\mathbf{x}_{1,2}$, which minimizes the objective function along a line through $\mathbf{x}_{1,1}$ and in the direction of coordinate 2. These two steps combine for the first iteration of a cyclic search to minimize the objective function shown in Figure 4-6. The second iteration starts from $\mathbf{x}_{1,2}$.

The cyclic search method used in the Smart Bridge control system minimizes Equation 4-2 by adjusting $\Delta \mathbf{u}$, a vector with 24 elements. This means that each iteration in the cyclic search consists of 24 individual coordinate searches. The algorithm stops iterating when any of the stopping criteria listed in Table 4-5 are satisfied. The stopping criteria in Table 4-5 are not currently user-adjustable parameters. However because of the modular structure of the control software it would not be difficult to add, remove, or adjust the criteria. Figure 4-7 is a flow diagram that summarizes the steps used in the cyclic search algorithm used in the Smart Bridge control system.

The multivariable search algorithm always uses an initial guess of $\Delta \mathbf{u} = \mathbf{0}$, which corresponds to no future control action. The zero vector is chosen as an initial guess to guarantee that the algorithm starts with a vector that does not violate the input constraints given in Equation 4-3.

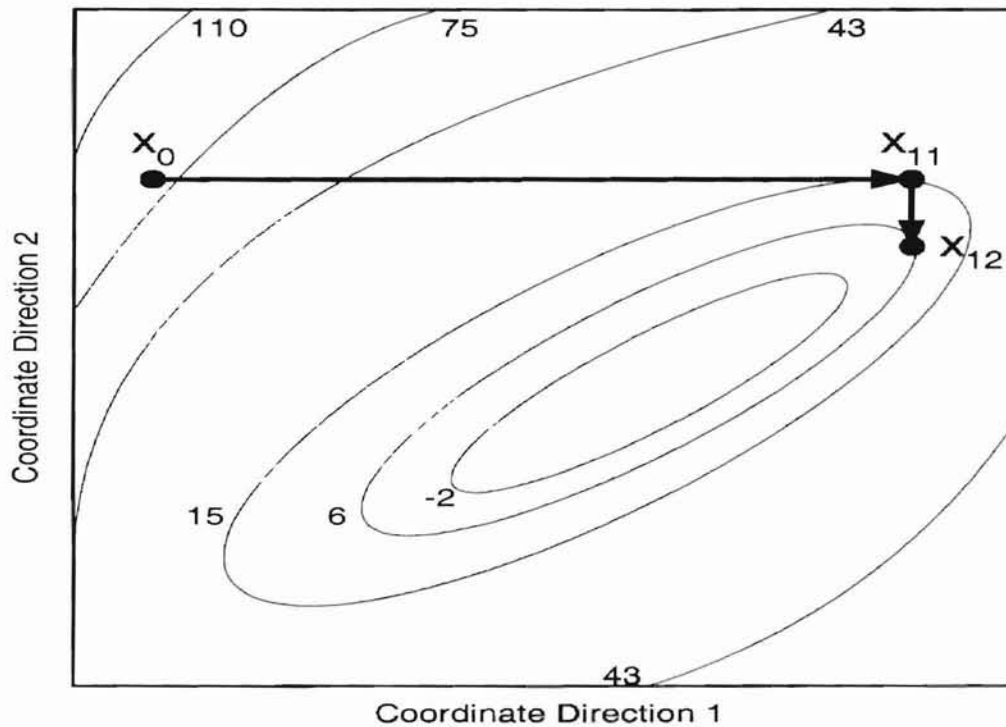


Figure 4- 6: One iteration of a cyclic search consists of a move in each coordinate direction.

Table 4- 5: Cyclic search stopping criteria.

- Stop iterating if the absolute value of the change in the objective function value after successive iterations is less than 1.
- Stop iterating if the iteration count is greater than 12.
- Stop iterating if all elements of the solution vector have changed less than 1°C after successive iterations (regardless of the change in the value of the objective function).

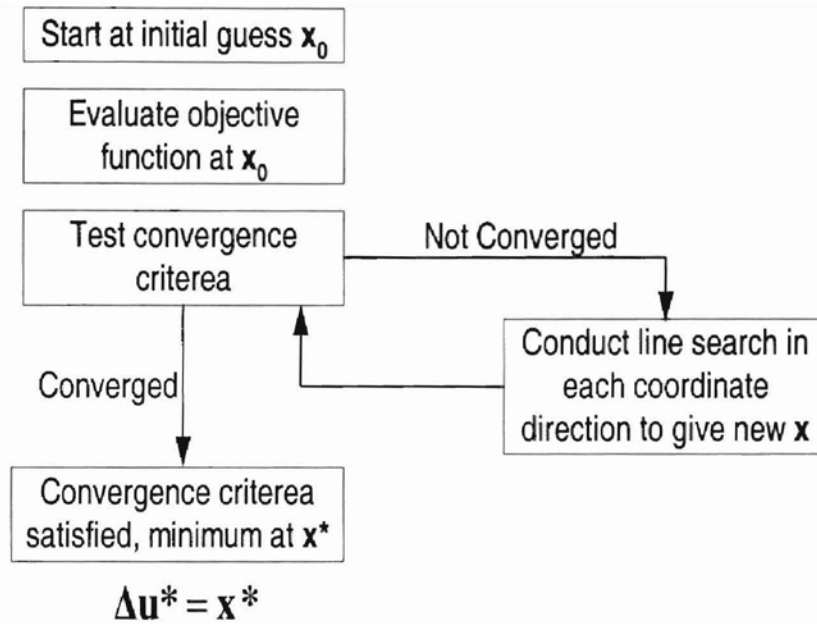


Figure 4- 7: Flow diagram of cyclic search method for minimizing a multiple variable objective function.

4.5.2 Line Search Method

The multiple dimension search method discussed above minimizes the objective function by taking steps in orthogonal coordinate directions. As mentioned in the previous section, the length of each orthogonal step minimizes the function in that particular coordinate direction. A two-point equal interval region elimination algorithm [14] is used to conduct a line search in each coordinate direction.

The region elimination method used to conduct line searches evaluates the objective function at four locations along the search line. The region where the value of the objective function is greatest is eliminated at the end of each line search iteration. Figure 4-8 shows two iterations of the line search method. Notice that after each iteration the search region is reduced by one third.

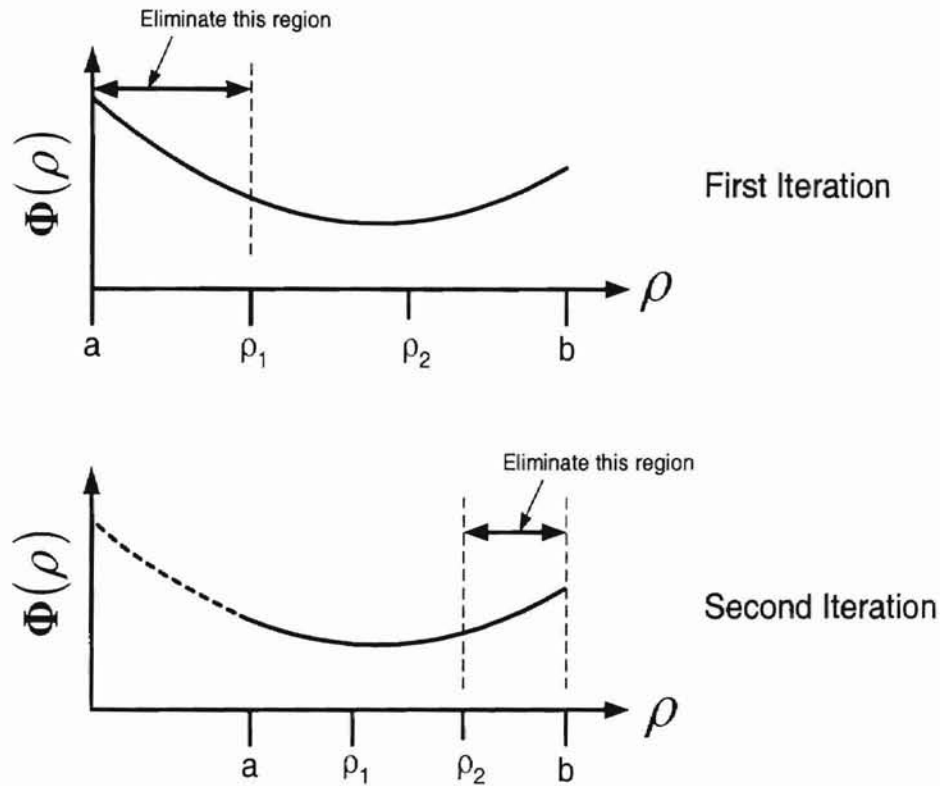


Figure 4- 8: The two-point equal interval line search reduces the search region by one third after each iteration.

The line search method also guarantees that the input constraints given in Equation 4-3 are not violated. Every time the objective function is evaluated, the input constraints in Equation 4-3 are checked. A large penalty is added to the objective function if the constraints are violated at the test location. The large penalty assures that areas where constraints are violated get eliminated from the search region. In Figure 4-9, regions where constraints are violated are represented by the cross hatched area. Because the bracket operator makes the value of the objective function very high in these regions, the line search method does not accept any moves into these regions.

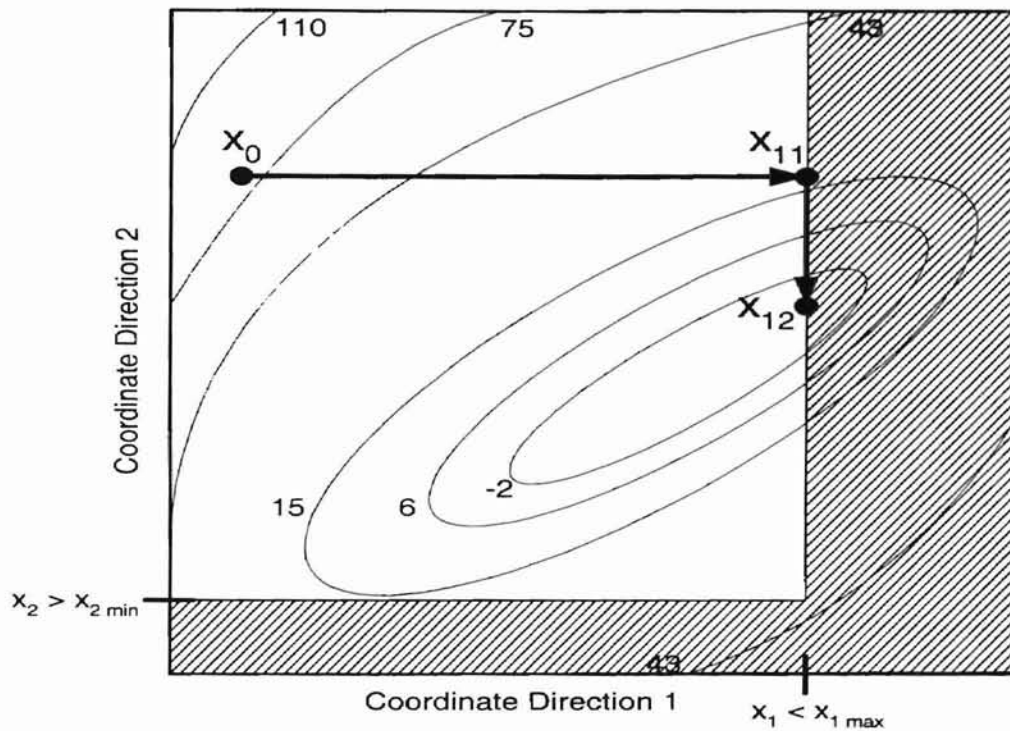


Figure 4-9: A large penalty is added to the objective function to prevent violated constraints.

A line search requires an initial search range and stopping criteria. The current version of the Smart Bridge control system uses an initial search region of -30°C to $+30^{\circ}\text{C}$ for all line searches. Also, a stopping criterion of 20 iterations is used for all line searches. This initial search range and stopping criteria reduces the size of the search range from 60°C to 0.2°C . Figure 4-10 is a flow diagram that summarizes the steps used in the two-point equal interval line search algorithm employed by the Smart Bridge control system.

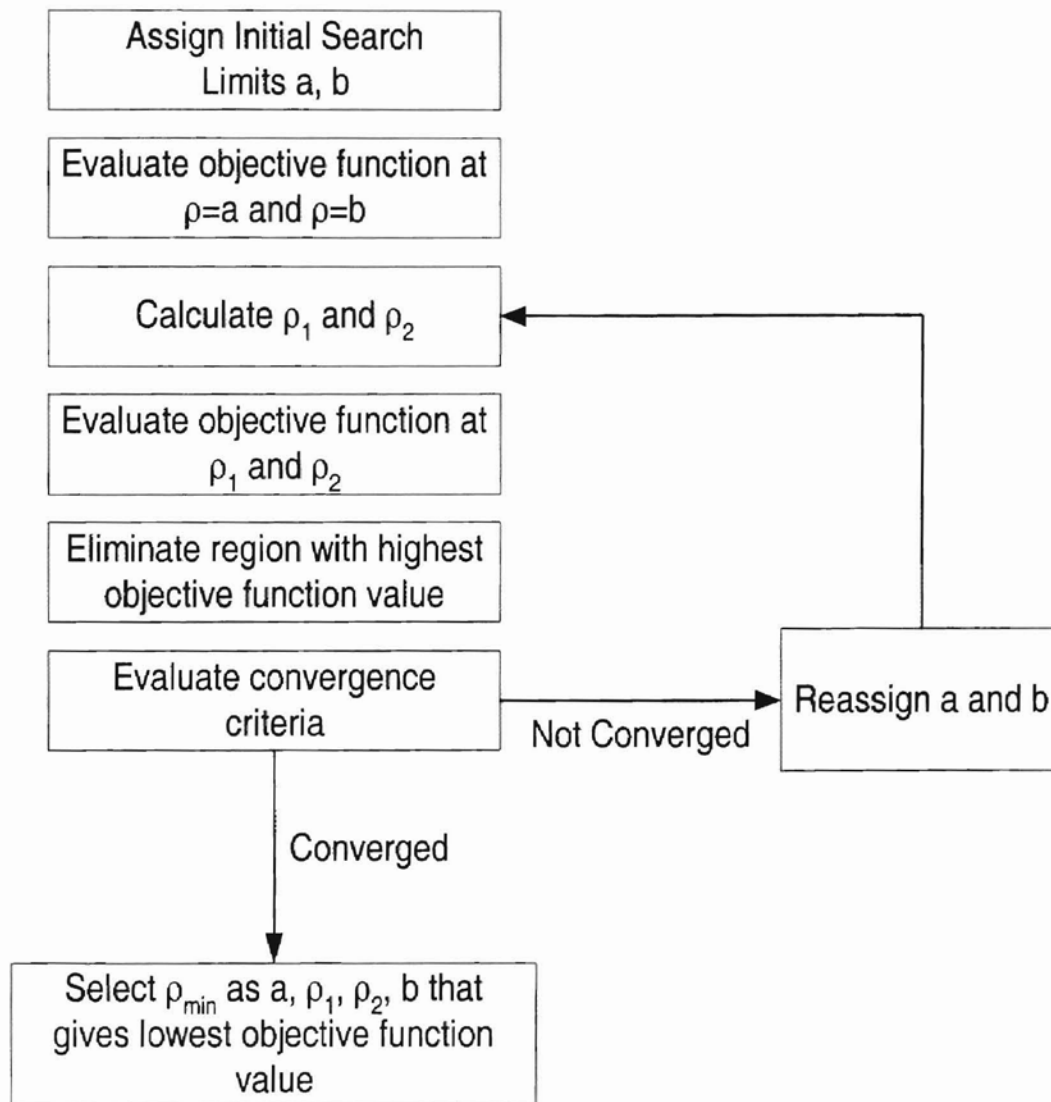


Figure 4- 10: Flow diagram of two-point equal interval algorithm used to conduct line searches.

4.6 Programming Notes

Section 1.3 outlined deliverables assigned to Task 4.3.1.1: Integrated Control Strategies. Among these deliverables are specifications regarding the design of the Smart Bridge control system software used to run the control algorithm presented in this chapter. Specifically, the control system software should be: user-friendly with commercially available components, and modular, to ensure flexibility, reliability, ease of maintenance, and to maximize technology transfer.

The Smart Bridge control system software has been programmed in Visual Basic 6.0. A user-friendly graphical user interface (GUI) has been constructed, making configuration and monitoring of the Smart Bridge control system straightforward. Figure 4-11 shows some selected screen captures from the Smart Bridge control system GUI.

Commercially available components from the National Instruments LABVIEW ComponentWorks suite have also been integrated into the Visual Basic code. These components, supplied as dll files, are used to enhance the GUI and facilitate matrix and vector operations required in the optimization problem discussed in Section 4.4.

The modular and object oriented nature of the Visual Basic language allows for reliability and easy maintenance of the Smart Bridge control system software. The modular format of the software also allows for great flexibility, which will be very important to future researchers that will integrate adaptive techniques into the Smart Bridge control system. Table 4-6 lists parameters in the current version of the Smart Bridge control system that might be in the adaption module. For more information regarding the modular structure of the Smart Bridge control system software, consult the technical documentation and source code accompanying this thesis [12].

Smart Bridge Control System GUI

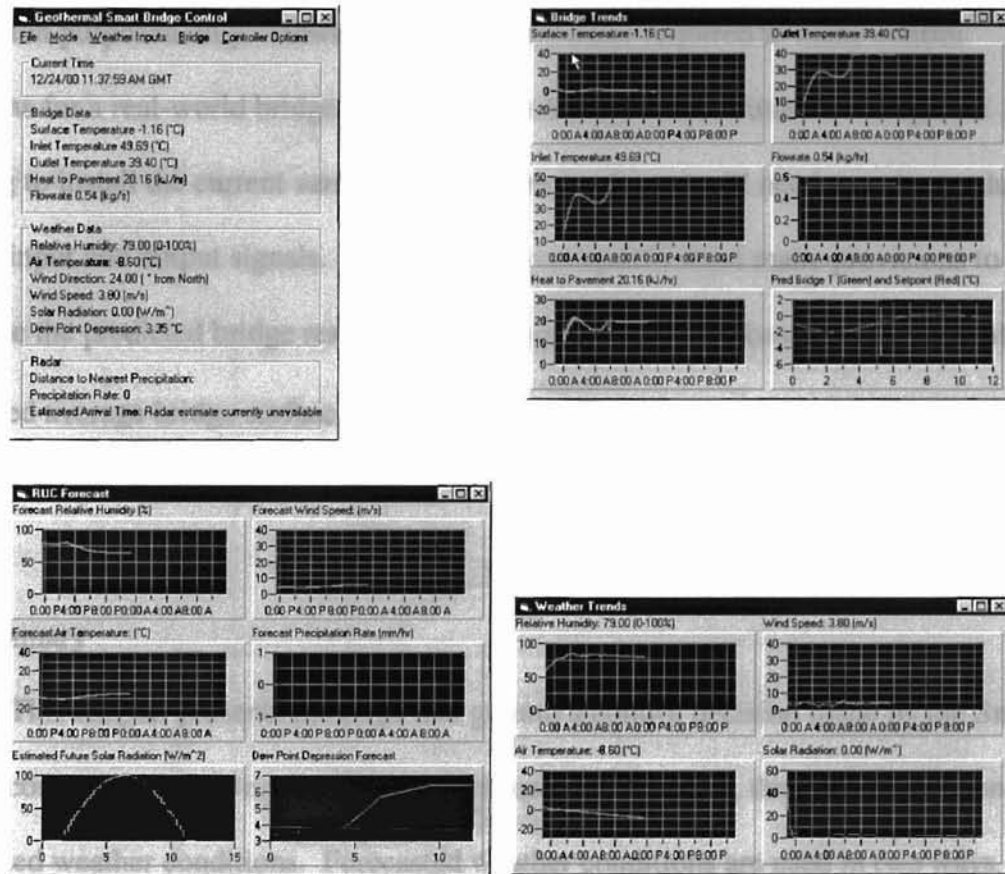


Figure 4- 11: Selected screen captures from the Smart Bridge control software.

Table 4- 6: Parameters in the current version of the Smart Bridge control system that might be used in the adaption module.

- First-principles bridge deck model parameters
- Icing potential rules
- Reference trajectory (slope of temperature ramp, length of safety cushion, and setpoint temperature)
- Objective function tuning parameters (p , m , Γ , Λ)

It should also be noted that the code written for this thesis is configured for simulation purposed only. However, all of the modules required to make control decisions for a real-world bridge are included in the software. Future investigators wishing to install the current version of the control software will need to write modules to handle input and output signals. Also, future investigators must make provisions to initialize the predicted bridge response, \hat{y} , shown in Figure 4-1 based on the current measured average bridge surface temperature.

4.7 Summary

This chapter presents the steps that go into a control decision made by the Smart Bridge control system. Because control decisions are proactive, they rely heavily on forecasted weather conditions. Forecasted weather conditions are used in two ways. First, the weather forecast is used in conjunction with a first-principles bridge deck model to predict how the average bridge deck surface temperature will respond to the weather forecast when no future control action is taken. Second, the weather forecast is used in conjunction with icing potential rules to determine when preferential icing will be a threat. This information is used to set the reference trajectory. The solution to the optimization problem given in Equations 4-2 and 4-3 represents a sequence of MV adjustments that balances following the reference trajectory with making acceptable sized control moves. Section 4.5 presented the optimization technique used to minimize the objective function in Eq. 4-2 while observing the constraints in Eq. 4-3. Section 4.6 mentioned the programming language used to construct the Smart Bridge control system

software. The language used is inherently modular which aligns with the deliverables of Task 4.3.1.1. A list of parameters that might be used by future researchers in the adaption module was also given. Figure 4-12 summarizes the steps that make up the Smart Bridge control algorithm.

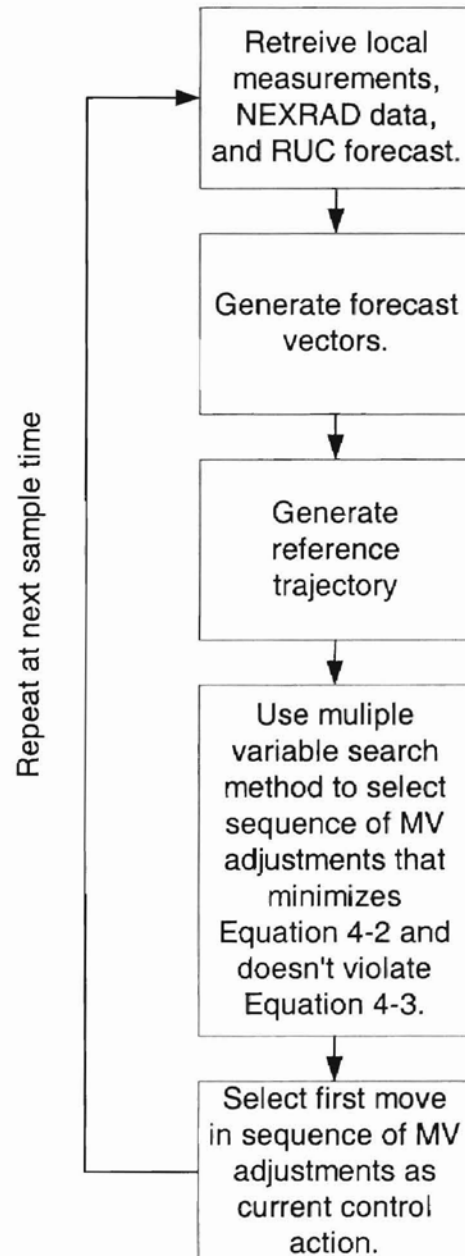


Figure 4- 12: Summary flow diagram for Smart Bridge control algorithm.

CHAPTER V

WEATHER INPUTS FOR THE SMART BRIDGE CONTROL STRATEGY

5.1 Introduction

Forecasted weather conditions form the basis for two important components of the Smart Bridge MPC software. First, the weather forecast is analyzed to determine if there are any times in the prediction horizon when preferential icing might occur. This analysis is used to construct the desired bridge deck temperature trajectory. Second, forecasted weather conditions (in conjunction with the first-principles bridge deck model) are used to predict how the bridge deck temperature will change over the course of the prediction horizon. Therefore, the performance of the Smart Bridge control system is heavily influenced by the accuracy and reliability of the weather forecasts it uses.

Sections 5.2, 5.3, and 5.4 describe the data sources used to generate the weather inputs. These data sources include the Oklahoma Mesonet, NEXRAD radar, and the National Weather Service Rapid Update Cycle (RUC) forecast model. All three data sources (or an equivalent source) are available throughout the United States, which insures maximize technology transfer of the Smart Bridge control software. Section 5.5 demonstrates how the information from the individual data sources is combined to construct the weather forecast used by the Smart Bridge control system. Section 5.6 explains how the Smart Bridge control software generates the solar radiation forecast (which is not available from RUC). Section 5.7 provides details about the infrastructure requirements that allow the Smart Bridge control system to gain access to the information described in the preceding sections. The second-generation control strategy presented in

this thesis has been designed under the assumption that the infrastructure described in Section 5.6 will be in place.

5.2 Oklahoma Mesonet

The Oklahoma Mesonet is a network of 114 remote weather stations distributed throughout the state of Oklahoma. The name "Mesonet" is derived from the meteorological term "mesoscale," which refers to weather features on a resolution of a few square kilometers to a few hundred square kilometers [15]. Tornadoes, thunderstorms, and squall lines are examples of mesoscale phenomenon.

Initially the Oklahoma Mesonet was intended to serve agricultural researchers. Today meteorologists, agriculturists, and planners throughout the state use weather data reported by the Oklahoma Mesonet [15]. Although instrumentation varies from station to station, Table 5.1 shows the weather conditions monitored at a typical Oklahoma Mesonet site.

Ideally, the second-generation control strategy would use weather data recorded by instruments located at the bridge site. However, weather monitoring instrumentation at the bridge site is not necessary if similar measurements are available from a nearby location. RWIS and the Oklahoma Mesonet represent possible alternatives to instrumentation at the bridge site. Remote instruments at RWIS or Mesonet stations might also serve as backup devices in the event that a bridge site instrument fails. Because a fully instrumented bridge was not in existence at the time this thesis was

written, the Smart Bridge control software has been programmed to use Oklahoma Mesonet data.

Table 5- 1: Oklahoma Mesonet measurements.

| | |
|-------------------------------------|--|
| •Relative Humidity at 1.5 m (%) | • Air Temperature at 1.5 m (°C) |
| •Average Wind Speed at 10 m (m/s) | • Vector Average Wind Speed (m/s) |
| •Wind Direction at 10 m (° from N) | • Standard Dev. of Wind Direction (° from N) |
| •Standard Dev. Of Wind Speed (m/s) | • Precipitation Since 00 GMT (mm) |
| •Maximum Wind Speed (m/s) | • Solar Radiation (W/m ²) |
| •Station Pressure (millibars) | • Average Wind Speed at 2 m (m/s) |
| •Air Temperature at 9 m (°C) | • Bare Soil Temperature at 10 cm (°C) |
| •Sod Soil Temperature at 10 cm (°C) | • Sod Soil Temperature at 5 cm (°C) |
| •Bare Soil Temperature at 5 cm (°C) | • Sod Soil Temperature at 30 cm (°C) |
| •Leaf Wetness | |

5.3 NEXRAD

The National Weather Service, Air Weather Service, and Federal Aviation Administration oversee the operation of a network of WSR-88D weather radars [16]. WSR-88D is an acronym for Weather Surveillance Radar, commissioned in 1988, and uses Doppler technology [17]. WSR-88D was developed to replace the outdated WSR-57S and WSR-74C radars [17]. NEXRAD, short for “next generation weather radar” is also used to reference the WSR-88D network. The NEXRAD network is comprised of approximately 160 sites throughout the United States and selected overseas locations.

Because NEXRAD offers complete coverage of the U.S., radar based components of the Smart Bridge control system can be used on every Smart Bridge. Figure 5-1 shows the location of radar stations that are part of the NEXRAD network [16]).

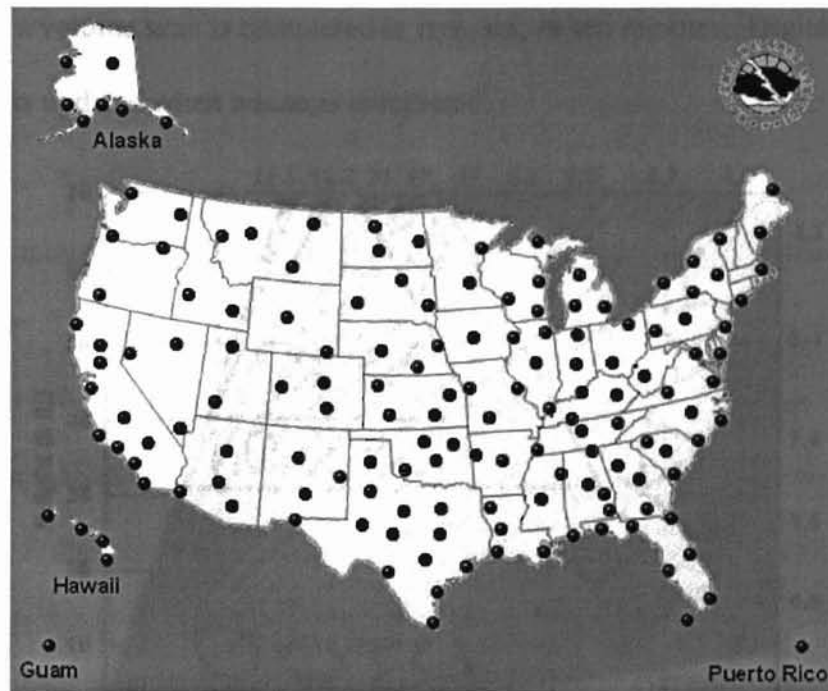


Figure 5- 1: Location of NEXRAD radar stations. The NEXRAD network provides coverage for the entire U.S., which allows for the radar components of the Smart Bridge control system to be utilized anywhere in the U.S.

NEXRAD radar emits energy pulses into the atmosphere. If the energy strikes an object (rain drop, bug, bird, etc), the energy is scattered in all directions. A small fraction of that scattered energy is directed back toward the radar. Computers analyze the strength and phase shift of the reflected energy signal to generate information about precipitation and wind [18].

A key difference between older radar technology and NEXRAD is the way the atmosphere is scanned. Older radars scanned the atmosphere at a single level whereas NEXRAD scans at multiple levels. By scanning the atmosphere at multiple levels,

meteorologists get a three-dimensional picture of the atmosphere that gives information about the vertical structure of a storm [17]. Figure 5-2 shows the elevation angles (top and right axes), range, and height of a NEXRAD volume scan. Depending on the mode of operation, a volume scan is completed in five, six, or ten minutes. Digital data from a radar station is updated when a scan is completed.

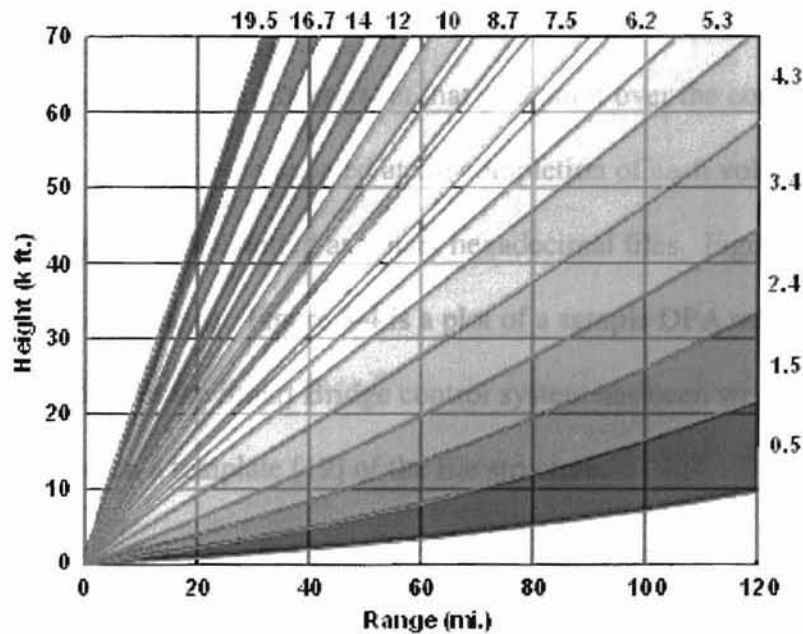


Figure 5- 2: Elevations, height, and range scanned by NEXRAD in the course of one 360° volume scan (elevation angles on top and right axes) [18].

5.3.1 Hourly Digital Precipitation Array

NEXRAD supports dozens of weather products that supply meteorologists with information about precipitation intensity and location, wind speed and direction, flash flood potential, and tornado activity. Sophisticated computer algorithms based on reflectivity data collected by the radar are used to generate these products. In the past, NEXRAD products were distributed to certain third party vendors only. However,

starting in December 2000 the National Weather Service made all NEXRAD products available to the public.

One product generated by NEXRAD is the One Hour Digital Precipitation Array (DPA). The DPA product is a 131x131 digital array, where each element corresponds to a grid location under the radar umbrella. Grid points are spaced 2.2 nautical miles (about 4 km) apart and cover the entire United States. Each element of the array represents the precipitation accumulation (in millimeters) at that grid point over the course of the previous hour. The entire array is updated at the completion of each volume scan.

DPA messages are transmitted as binary hexadecimal files. Figure 5-3 shows a portion of a raw DPA message. Figure 5-4 is a plot of a sample DPA output subsequent to decoding. A module in the Smart Bridge control system has been written to decode DPA messages based on a template [19] of the file structure.

| | | | | | | | |
|------|------|------|------|------|------|------|------|
| 0000 | 0000 | 0980 | 0000 | 0002 | 0000 | 04B8 | 0001 |
| 0060 | 1E9E | 04B0 | 1841 | 0001 | 0001 | 0480 | 14A2 |
| 1E9E | 1234 | 6530 | 0059 | 0001 | 0058 | 0001 | 0000 |
| FE89 | 03E8 | 00FA | 01CC | 0000 | 0001 | 4180 | 69E8 |
| 0064 | 0000 | 0000 | 0000 | 0015 | 0000 | 0000 | 0000 |
| 0000 | 0064 | 0000 | 0000 | 0000 | FFF4 | 0064 | 0000 |
| 0000 | 0000 | 0000 | 0000 | 0000 | 0000 | 0000 | 0000 |
| 0000 | 0000 | 0000 | 0000 | 0000 | 0000 | 0000 | 0000 |
| 005A | 5A00 | 0070 | 6D51 | 6455 | 6060 | 4F54 | 0040 |
| 5C3F | 4049 | 4900 | 4D42 | 4349 | 434E | 4B3D | 4430 |
| 4340 | 3F3D | 4644 | 4443 | 3A3D | 473F | 3A3A | 3D3D |
| 3C45 | 3A43 | 433C | 4E43 | 413C | 393F | 3F40 | 4038 |

Figure 5- 3: Partial binary hexadecimal DPA message.

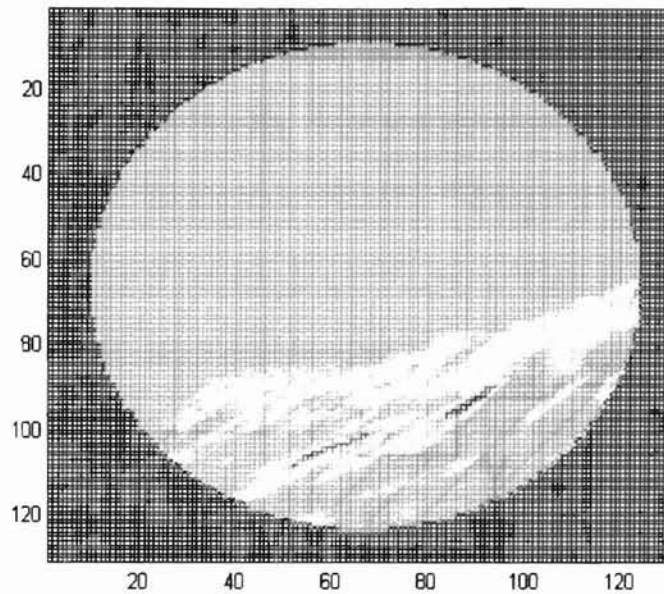


Figure 5- 4: A sample DPA image from the Twin Lakes, Ok radar station.

5.3.2 Calculation of Precipitation Rate From DPA Data

Precipitation has a strong influence on the bridge deck pavement temperature and is an input to the first-principles bridge deck model. It is possible to measure the precipitation rate using instrumentation, however, such devices can be unreliable when measuring freezing precipitation. Until a reliable device becomes available, precipitation rate calculated from DPA data is used instead. This subsection outlines how the precipitation rate can be estimated using DPA data.

As discussed above, the DPA reports how much precipitation has fallen over the course of the previous hour at grid locations in the area covered by the radar scan. The location of a particular bridge in the DPA is determined using the relative location of the bridge site to the NEXRAD station and the grid spacing. The problem is to calculate a

current precipitation rate from a sequence of readings that report total precipitation over the past hour. Figure 5-5 shows hypothetical data for precipitation rate up to the current time t_k .

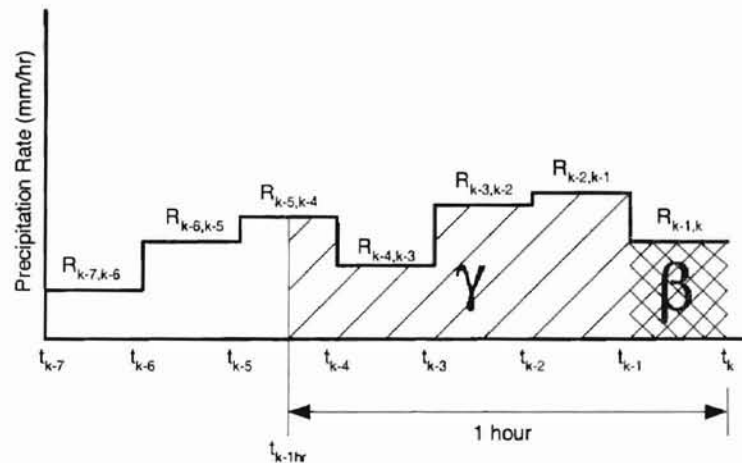


Figure 5- 5: Precipitation rate is estimated using the current DPA reading and past values of precipitation rate.

The single crosshatched area (γ) in figure 5-4 represents the precipitation (in mm) that has fallen over the course of the last hour excluding the time since the previous DPA update, $t_{k-1\text{hr}}$ to t_{k-1} . The double crosshatched (β) area in Figure 5-4 represents the precipitation (in mm) that has accumulated since the last DPA update, t_{k-1} to t_k . Equation 5-1 is used to calculate β , where DPA_k is the current DPA reading. Equation 5-2 is used to calculate the average precipitation rate from time t_{k-1} to t_k , R_{t_{k-1},t_k} (in mm/hr).

$$\beta = DPA_k - \gamma \quad (\text{Eq. 5-1})$$

$$R_{t_{k-1},t_k} = \frac{\beta}{t_k - t_{k-1}} \quad (\text{Eq. 5-2})$$

Due to the discrete nature of the DPA data and the assumption that the precipitation rate between consecutive time steps is constant, special consideration must be given to certain situations. When Eq. 5-2 is strictly followed, periods of negative precipitation rate can result. Examples of when Eq 5-2 might give a negative precipitation rate are periods of sudden (but brief) precipitation or periods when precipitation is tapering off. Eq. 5-2 gives a negative precipitation rate when γ is greater than DPA_k . Therefore, when implementing Equations 5-1 and 5-2, the stipulation that $R_{tk-1,tk}$ equals zero when $\beta < 0$ must be followed.

To illustrate this method of estimating precipitation rate, we consider data collected for May 3-4, 1999. NEXRAD DPA data from the Twin Lakes, Oklahoma radar station has been used to calculate the precipitation rate in Stillwater, Oklahoma during this period. Figure 5-6 is a plot of the distance from Stillwater to the nearest point of precipitation indicated by the Twin Lakes radar for this time period. Figure 5-7 shows the precipitation rate for the same time period as calculated by Equations 5-1 and 5-2.

Figure 5-6 shows two precipitation events (when the distance to nearest precipitation is zero). The first precipitation event occurred between approximately 10 and 13 hours after start. The second event occurred between 19 and 23 hours after start. A comparison of Figures 5-6 and 5-7 shows that the calculated precipitation rate is greater than zero at times when the radar indicated precipitation was falling at Stillwater.

It should be noted that the NEXRAD weather products containing information about precipitation rate and accumulation (including the DPA) could exhibit a large degree of error. Many studies comparing NEXRAD precipitation rate or accumulation to

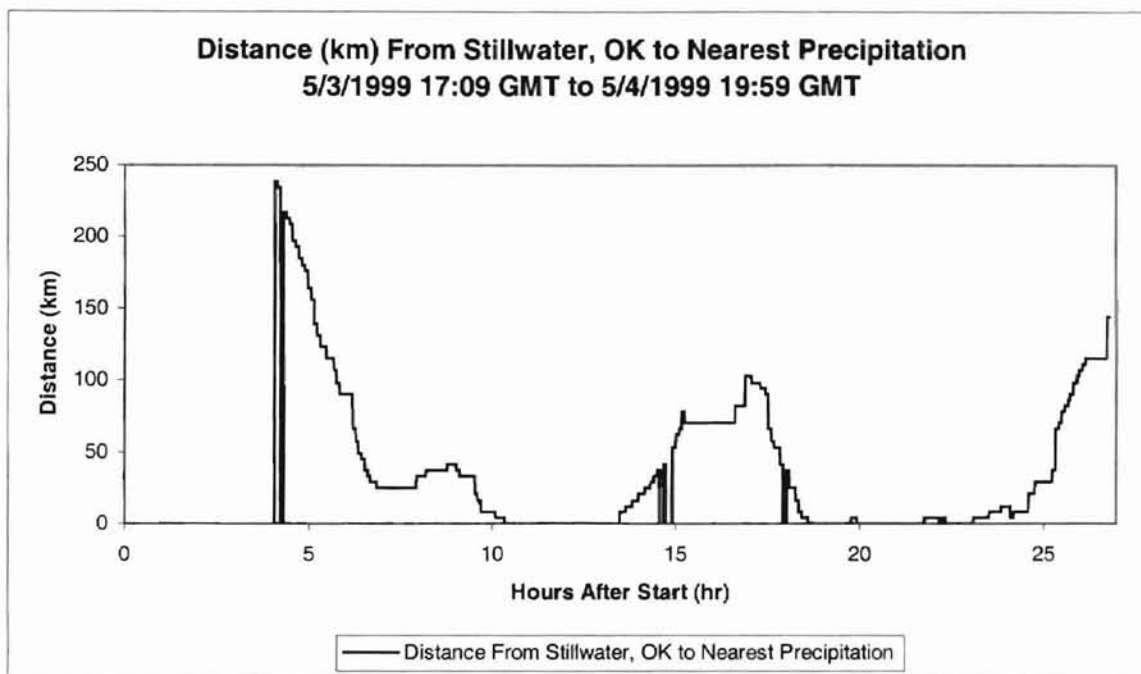


Figure 5- 6: Distance (km) from the nearest point of precipitation to Stillwater, Ok.

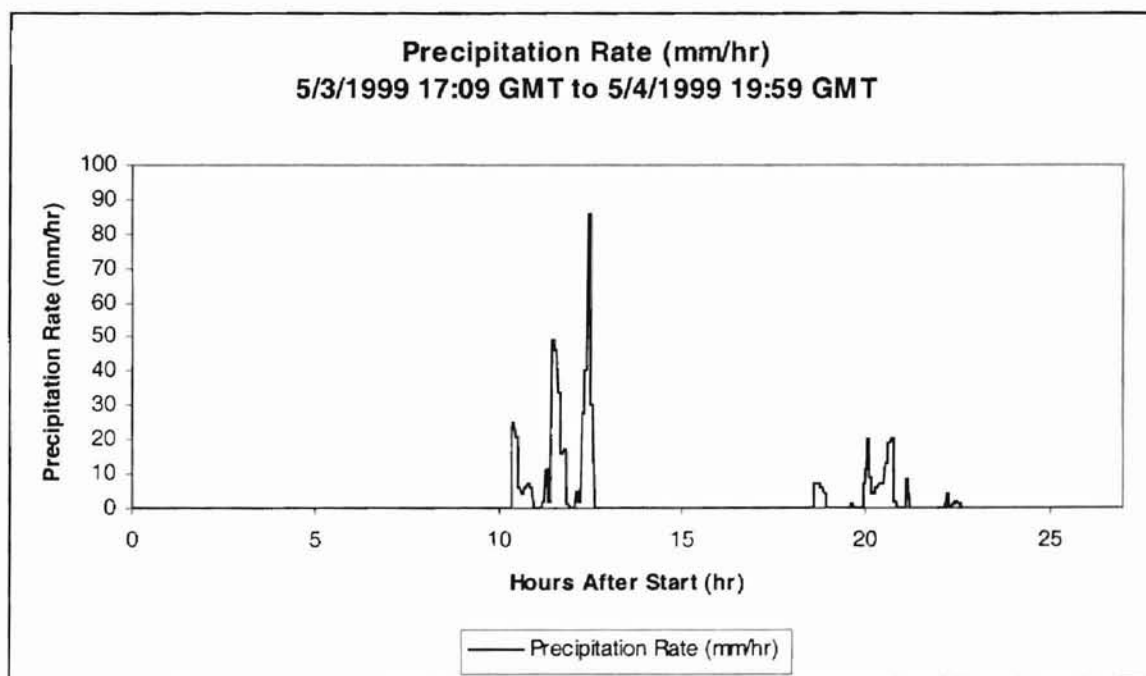


Figure 5- 7: Calculated precipitation rate using Equations 5-1 and 5-2.

rain gauge data confirm this result [20]. This is especially true for snow and freezing rain, due to the way radar signals reflect off these types of precipitation. However, NEXRAD does report the location of precipitation accurately. Therefore DPA data can be relied on for detecting precipitation at the bridge site more than precipitation intensity. Nevertheless, because conventional rain gauges (like those used in the Oklahoma Mesonet) generally fail to report frozen precipitation, a precipitation rate calculated from DPA data is the only alternative available at the current time.

5.4 Rapid Update Cycle Forecasting Model

The Rapid Update Cycle (RUC) is an atmospheric prediction system comprised primarily of a numerical forecast model [21]. RUC was designed to provide numerical forecast guidance for weather-sensitive users. RUC runs at the highest frequency of any forecast model at the National Centers for Environmental Prediction (NCEP), assimilating recent observations aloft and at the surface to provide very high frequency updates of current conditions and short-range forecasts using a sophisticated mesoscale model [22]. The original Rapid Update Cycle, RUC-1, was implemented in September 1994 at the National Centers for Environmental Prediction (NCEP). The newest version of RUC, called RUC-2, was implemented at NCEP in April 1998.

RUC provides forecasted weather conditions for every point in a grid spanning the continental U.S. Gridpoints are spaced 40km apart. The Smart Bridge control system uses forecast information from the grid point that is located nearest the bridge site. Because RUC offers complete coverage of the U.S., RUC-based components of the

Smart Bridge control software can be used on every Smart Bridge. Table 5-1 lists the RUC forecast variables used in the Smart Bridge control system.

Table 5- 2: RUC forecast variables used in the Smart Bridge control system.

| | |
|--|--|
| <ul style="list-style-type: none">• Temperature (°C)• Relative Humidity (%)• Wind Direction (° from North) | <ul style="list-style-type: none">• Wind Speed (m/s)• Rainfall (kg/m²) |
|--|--|

Every three hours, starting at 00:00 GMT, RUC generates a 0-hr, 3-hr, 6-hr, 9-hr, and 12-hr forecast. At the top of every hour (GMT) that isn't a multiple of three, RUC outputs a 0-hr and 3-hr forecast [23]. Figure 5-8 shows the type and timing of RUC forecasts provided. The raw RUC output contains forecast data for the entire grid spanning the U.S. Investigators from task 4.3.1.1: Weather Inputs have developed code to extract forecast information for the grid point nearest the bridge site from the raw RUC output. Figure 5-9 shows an example of a processed RUC message containing a 12-hour forecast for Stillwater, Ok. The Smart Bridge control system requires the processed RUC output to be formatted as shown in Figure 5-9.

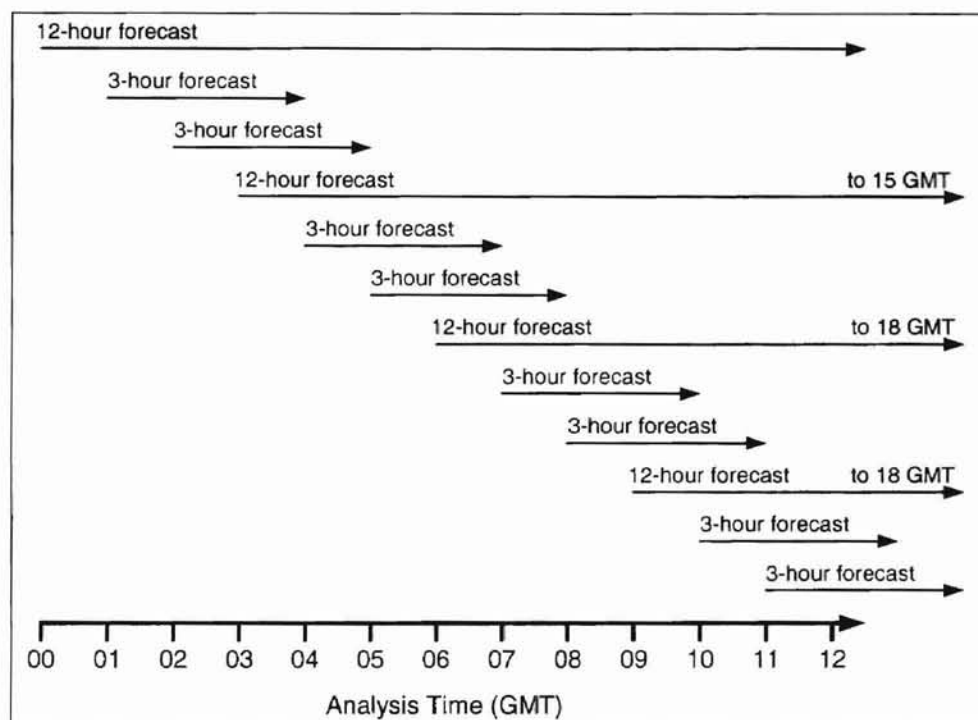


Figure 5- 8: RUC outputs a 12-hour forecast at the top of every third hour starting at 00:00 GMT. A 3-hr forecast is generated at the top of all other hours.

```

X-DIMENSION GRID SPACING (M): 81271
Y-DIMENSION GRID SPACING (M): 81271
GRID CORNER LATITUDE (DEG-N): 12.190
GRID CORNER LONGITUDE (DEG-E): -133.459
INPUT LATITUDE (DEG-N): 36.121
INPUT LONGITUDE (DEG-E): -97.095
INPUT X-COORDINATE (M): 4034067
INPUT Y-COORDINATE (M): -2078790
NEAREST GRID POINT: (50,26)
DISTANCE TO NEAREST G.P. (M): 45146
X-DISTANCE TO NEAREST G.P. (M): -29435
Y-DISTANCE TO NEAREST G.P. (M): 34231
MODEL OUTPUT FOLLOWS:
RECORD NUMBER, ISSUE TIME, VALID TIME, FORECAST LEAD TIME, TEMPERATURE
(C), RELATIVE HUMIDITY (PCT), WIND DIRECTION, WIND SPEED (M/S), RAINFALL
(KG/M2)
0, 200012121200, 200012121200, 0, -12.9, 59.0, 351.0, 1.9, -9999.00
1, 200012121200, 200012121500, 3, -14.9, 67.0, 6.6, 2.6, 0.00
2, 200012121200, 200012122100, 9, -11.0, 58.0, 98.1, 2.1, 0.00
3, 200012121200, 200012121800, 6, -12.0, 58.0, 72.8, 3.0, 0.00
4, 200012121200, 200012130000, 12, -12.0, 87.0, 106.2, 3.2, 1.20
  
```

Figure 5- 9: Sample 12-hour RUC forecast for Stillwater, Ok.

5.5 Constructing Weather Forecasts for the Smart Bridge

Chapters III and IV describe the important role weather forecasts play in the Smart Bridge control system. This section discusses the implementation issues associated with generating control system inputs from the weather data sources discussed in the previous sections of this chapter.

The first implementation issue deals with the disparity between the update frequency for RUC and the sample rate of the Smart Bridge control system. RUC generates forecasts at intervals of three hours into the future. The sample rate for the control system is less than that. The Smart Bridge control software addresses this issue in a straightforward manner by linearly interpolating between RUC forecast values.

The second implementation issue has to do with discrepancies between the RUC “zero hour” forecast and the actual weather measurements at the bridge site. These discrepancies are handled by replacing the RUC zero hour forecast with the values measured at the bridge site. By making the zero hour forecast agree with the current measurement at the bridge site, the bridge deck heating system will remain on at times when RUC might have indicated that the current conditions are not conducive to preferential icing. Figure 5-10 shows that the RUC zero hour forecast has been replaced by the bridge site temperature measurement. The Smart Bridge control software is programmed to use Oklahoma Mesonet readings and precipitation rates calculated from DPA as measured values.

At times when RUC only outputs a three-hour forecast the Smart Bridge control software replaces the first three hours of the old forecast vector. The remainder of the old forecast vector is retained and the last element of the previous forecast vector is held

constant. The forecast vector is extended to the end of the prediction horizon. Figure 5-11 shows the air temperature forecast vector generated at 04:00 GMT. This strategy frequently causes a discontinuity in the forecast vector (similar to 07:00 GMT in Figure 5-11). A more realistic forecast would use linear interpolation between the most recent forecasted values (i.e. between 07:00 and 09:00 GMT in Figure 5-11). Figure 5-11 also shows that the air temperature forecast for 15:00 GMT has been extended to 16:00 GMT.

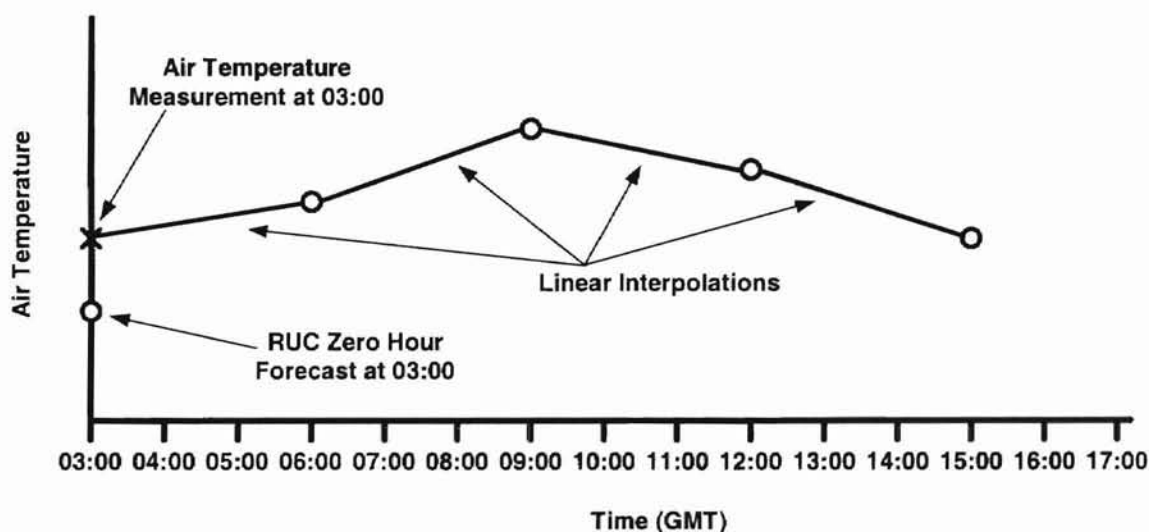


Figure 5- 10: A RUC forecast for air temperature issued at 03:00 GMT. Circles designate RUC output. Linear interpolation is used to generate forecast values between the RUC outputs. The current measurement is used in place of the RUC zero hour forecast.

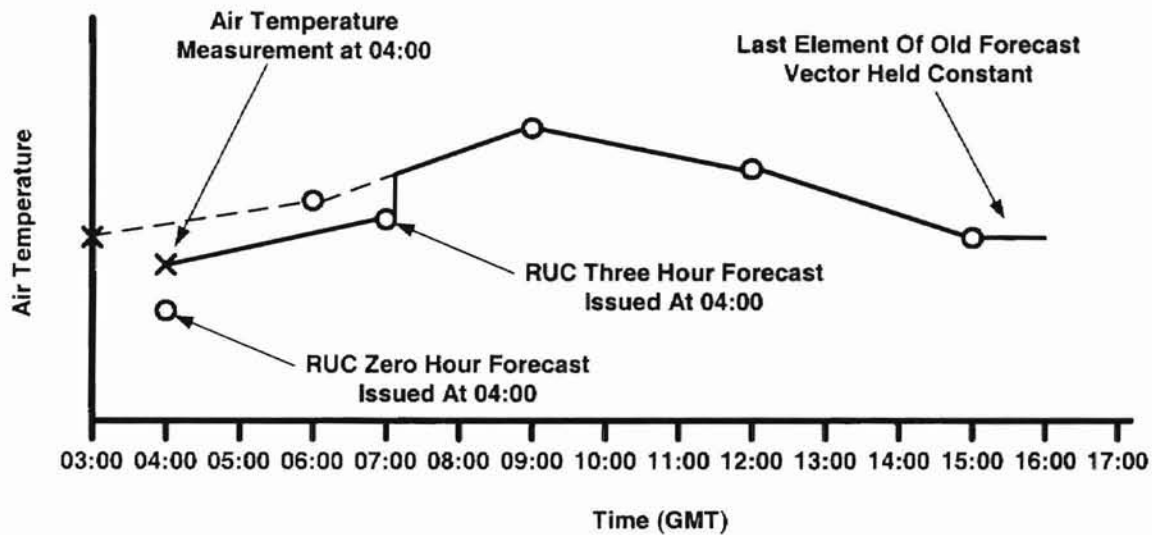


Figure 5- 11: Example of how the twelve-hour forecast is updated when a three-hour forecast is provided. At 04:00 GMT a new zero hour and three hour forecast is issued by RUC. The current measured value is used in place of the zero hour forecast. The forecast has been extended by holding the last element of the old forecast vector constant.

5.6 Solar Radiation Forecast

Solar radiation has a strong impact on the bridge deck pavement temperature. However, the RUC does not provide a solar radiation forecast. This section addresses how the Smart Bridge control software generates an estimated solar radiation forecast.

The solar angle of incidence, θ , at a given time, day, and latitude can be calculated. The solar angle of incidence is defined as the angle between a line pointing directly at the sun and a line perpendicular to the surface of the earth (see Figure 5-12). The amount of solar radiation absorbed by the bridge deck pavement is partially dependent on the solar angle of incidence.

When predicting future solar radiation the Smart Bridge control software considers two cases. The first case is when the current solar radiation measurement is 0

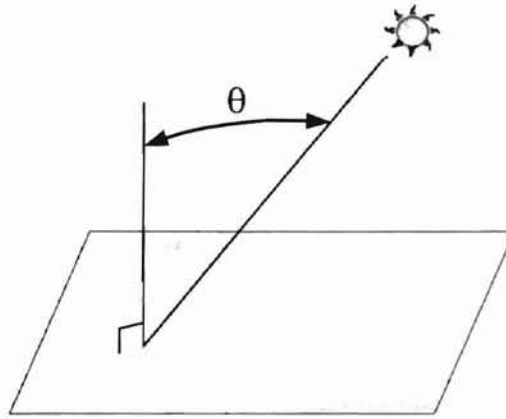


Figure 5- 12: The solar angle of incidence, θ , partially determines the amount of solar radiation absorbed by the bridge deck pavement.

W/m^2 , which indicates the sun is currently below the horizon. For this case the control software first calculates when the sun will rise and set. The solar radiation forecast vector is set to zero for all times before sunrise and after sunset. For times between sunrise and sunset, the solar radiation forecast is set to a sine wave with amplitude 100 W/m^2 and period of twice the number of daylight hours. An amplitude of 100 W/m^2 corresponds to a cloudy winter day and represents a conservative estimate. Like all other forecast inputs, the length of the solar radiation forecast equals the prediction horizon. Figure 5-13 shows the solar radiation forecast vector at 03:00 local time with a 12-hour prediction horizon.

The second case considered by the solar radiation forecast component of the Smart Bridge control software is when the sun is already up. For this case the sine wave of Figure 5-13 is scaled so that it passes through the current measurement. The implication of this rule is that the current degree of cloudiness is predicted for the rest of the day. Given the relatively strong influence solar radiation has on the bridge deck,

future investigators should refine the assumption that the current degree of cloudiness will persist for the rest of the day. Finally, all elements of the solar radiation forecast corresponding to times after sunset are set to 0 W/m^2 . Figure 5-14 shows the solar radiation forecast vector issued at 09:00 local time.

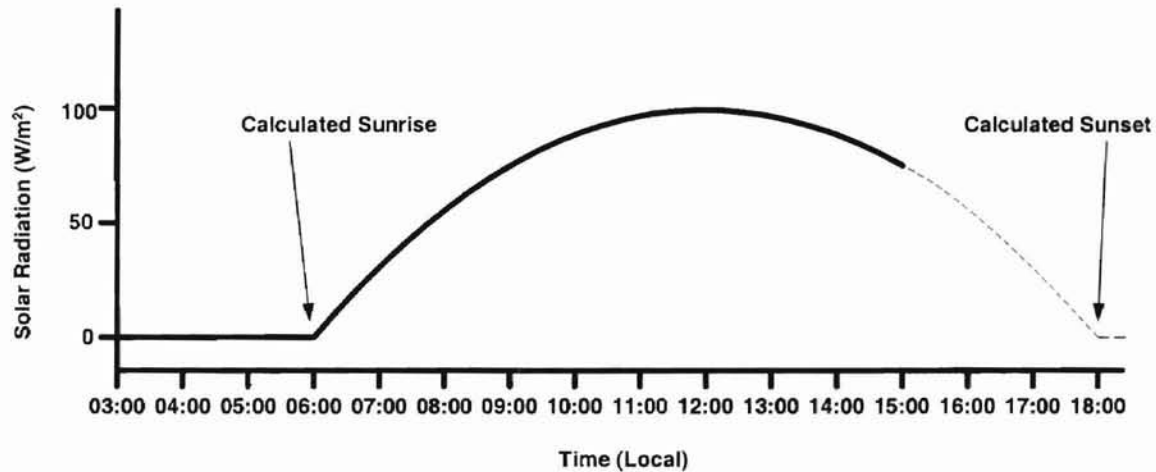


Figure 5- 13: Solar radiation forecast (solid line) issued at 03:00 local time. The forecast is zero before sunrise and a sine wave with amplitude 100 W/m^2 during daylight hours.

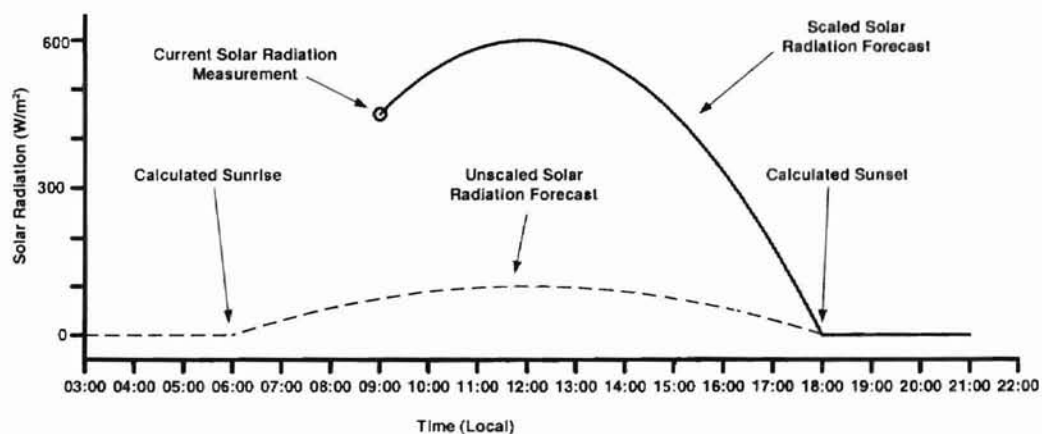


Figure 5-14: During daylight hours the solar radiation forecast is a sine wave that passes through the current measured solar radiation as well as the sunrise and sunset times.

5.7 Infrastructure Requirements

Before the Smart Bridge control software can be implemented, the required weather data must be accessible in real time. Investigators working on Task 4.3.1.1, Weather Inputs, have proposed a data transfer architecture for acquiring weather data in real time. The Smart Bridge MPC control strategy developed in this thesis has been designed under the assumption that the weather inputs described in sections 5.2, 5.3, and 5.4 will be available in real time via the data transfer architecture described in this section.

All federal forecast and observation data are ingested via satellite dish using the National Oceanic and Atmospheric Administration (NOAA)'s port data service. Raw data is then placed on a Linux Smart Bridge weather server via a local data manager (LDM). An LDM is a data routing tool that is used in the meteorological community. The Smart Bridge Weather server runs PERL scripts to extract pertinent information from the raw data files. Extracted weather data is sent via secure FTP connection to individual Smart Bridge control systems. Figure 5-15 is a diagram of the proposed data transfer architecture. State transportation agencies are responsible for providing LDM service.

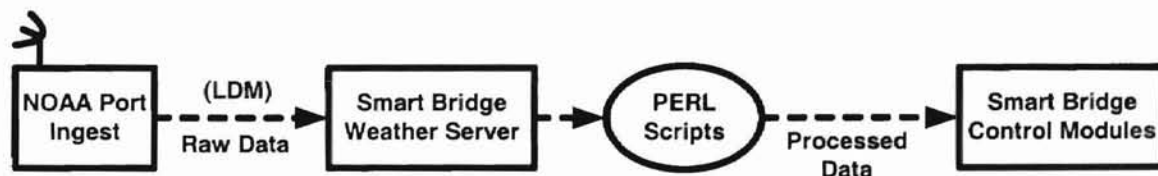


Figure 5- 15: Proposed infrastructure for transmitting real time weather data to Smart Bridge control systems.

5.8 Summary

The Smart Bridge MPC strategy is heavily dependent on forecasted weather conditions. Sections 5.2, 5.3, and 5.4 describe the data sources used by the Smart Bridge control software to generate weather forecasts. Section 5.5 discusses implementation issues associated with building weather forecasts and how the Smart Bridge control software addresses these issues. Section 5.6 illustrates how, in the absence of a forecast, the Smart Bridge control software constructs an approximate solar radiation forecast. Finally, Section 5.7 described the hardware and software required to give the Smart Bridge control system real time access to the weather inputs discussed earlier in the chapter. The Smart Bridge control software has been designed under the assumption that this infrastructure is in place.

CHAPTER VI

SIMULATION CASE STUDIES

6.1 Introduction

The main objective of Task 4.3.1.3, Integrated Control Strategies, of the OSU Geothermal Smart Bridge project is to develop a control system that prevents preferential icing on bridge decks. Furthermore, the control system should employ existing control techniques in conjunction with existing weather related data sources. Chapters III, IV, and V described the MPC technique and the weather inputs employed by the Smart Bridge control system. This chapter presents Smart Bridge control system performance results for three simulated case studies.

Case studies are presented for two time periods: December 23-26, 2000; and December 12-18, 2000. Archived Mesonet data from the Stillwater, OK Mesonet station were used in all case study simulations presented in this chapter. Simulations were carried out using the bridge deck parameters of the OSU test bridge. The OSU test bridge is described in Section 6.2.

Sections 6.3 and 6.4 present case study results for the time periods mentioned above. Each case study begins with a discussion of the weather conditions used for the simulation. The weather conditions determine when the dew point depression and precipitation rules discussed in Chapter IV will cause the control system to take action to prevent preferential icing. Control performance results are presented and discussed for each case.

6.2 Bridge Deck Parameters

All simulations for the case studies use the bridge deck parameters for the one-quarter scale geothermal Smart Bridge located on the OSU Stillwater campus. Table 6-1 gives these bridge deck parameters. As described in Chapter IV, the control system generates a step response model for use in the optimization algorithm. Table 6-2 lists the weather conditions that were specified to produce the step response model. Figure 6-1 shows the step response model used in all simulation cases presented in this chapter.

The Smart Bridge control system controls the average pavement temperature by manipulating the bridge loop supply temperature. Full-scale Smart Bridges will be equipped with a network of heat pumps for extracting heat from the ground. The number

Table 6-1: Bridge deck parameters for the Smart Bridge at OSU Stillwater.

| | |
|--|--|
| Pavement Length (9.144 m) | Absorptivity Coefficient (0.6) |
| Pavement Width (6.096 m) | $C_{p, \text{Layer 1}}$ ($2.2 \times 10^6 \text{ J/m}^3 \text{ }^\circ\text{C}$) |
| Slab Orientation (6° from North) | $C_{p, \text{Layer 2}}$ ($0 \text{ J/m}^3 \text{ }^\circ\text{C}$) |
| Pavement Thickness (0.1524 m) | k_{Pipe} ($0.439 \text{ W/m }^\circ\text{C}$) |
| Pipe Spacing (0.3048 m) | Wall Thickness of Pipe ($1.5875 \times 10^{-3} \text{ m}$) |
| Pipe Diameter (0.01905 m) | Fluid Type (2 = propylene glycol water solution) |
| Pipe Depth Below Surface (0.0889 m) | Weight % GS-4 (42%) |
| Depth to Interface 1 (15 m) | Number of Flow Circuits (10) |
| $k_{\text{Layer 1}}$ ($1.618041 \text{ W/m }^\circ\text{C}$) | Length of Pipe Per Circuit (19.811 m) |
| $k_{\text{Layer 2}}$ ($0 \text{ W/m }^\circ\text{C}$) | Transient Time Step (20 sec) |
| Emmissivity Coefficient (0.9) | Bottom Boundary Condition (1 = convection type) |
| Minimum Flow Condition (0 kg/sec) | |

Table 6- 2: Weather conditions used to produce step response model.

- Ambient Air Temperature = -13°C
- Relative Humidity = 18%
- Wind Speed = 0 m/s
- Wind Direction = 0° from North
- Solar Radiation = 0 W/m^2
- Solar Angle of Incidence = 0.785 radians
- Snowfall Rate = 6.35 mm/hr
- Rainfall Rate = 6.35 mm/hr
- Bridge Loop Supply Temperature = 30°C

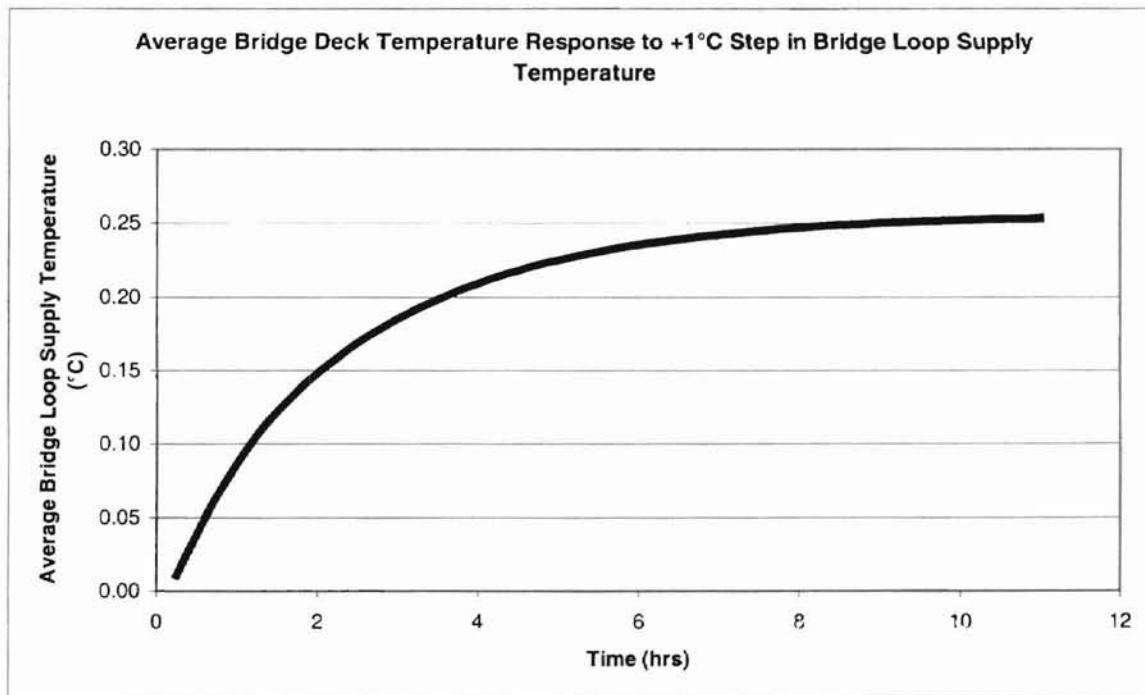


Figure 6- 1: Step response model used in all simulations presented in Chapter VI.

of heat pumps in the network that are turned on determines the bridge loop supply temperature. Because the test bridge on the OSU campus is equipped with a single heat pump, the bridge loop supply temperature cannot be manipulated without pulse moderation. However, for the simulations performed in the following sections the assumption has been made that the bridge loop supply temperature could be set anywhere between 10-50 °C. A bridge loop flowrate of zero indicates the heating system is off. A nominal flowrate (independent of the number of heat pumps turned on) is used when the heating system is on. The nominal flowrate for the OSU one-quarter scale bridge is 0.563 kg/sec.

6.3 Case 1 - December 23-26, 2000

This section presents the results of a simulated case study of the Smart Bridge control strategy. Conditions recorded at the Stillwater, Ok. Mesonet station from December 23, 2000, 07:00 GMT to December 26, 2000, 08:00 GMT were used as weather inputs. Section 6.3.1 describes the weather conditions for this time period. Section 6.3.2 presents the Smart Bridge control system performance results using a 2°C dew point depression rule.

6.3.1 Case 1 - Weather Conditions

Ambient conditions for Case 1, December 23-26 2000, are shown in Figures 6-2 through 6-5. Figure 6-2 indicates that the air temperature was below 0 °C for

approximately 75% of the 72-hour case study period. The lowest air temperature occurred December 24, where the temperature dipped to -9.8°C . Figure 6-3 is a plot of the solar radiation for Case 1. December 23 and 24 were sunny days, with a peak solar radiation of about 530 W/m^2 . December 25 was a cloudy day, with solar radiation readings peaking at 50 W/m^2 .

Figure 6-4 shows the precipitation rate for Case 1 as calculated from NEXRAD DPA data. Precipitation was detected throughout December 25. Figure 6-5 shows the actual dew point depression for Case 1. Figure 6-5 indicates that for the first 52 hours the dew point depression varied from 2.4°C to 11.8°C . After the initial 52 hours the dew point depression dropped sharply to approximately 1.6°C for the final 16 hours of the simulation.

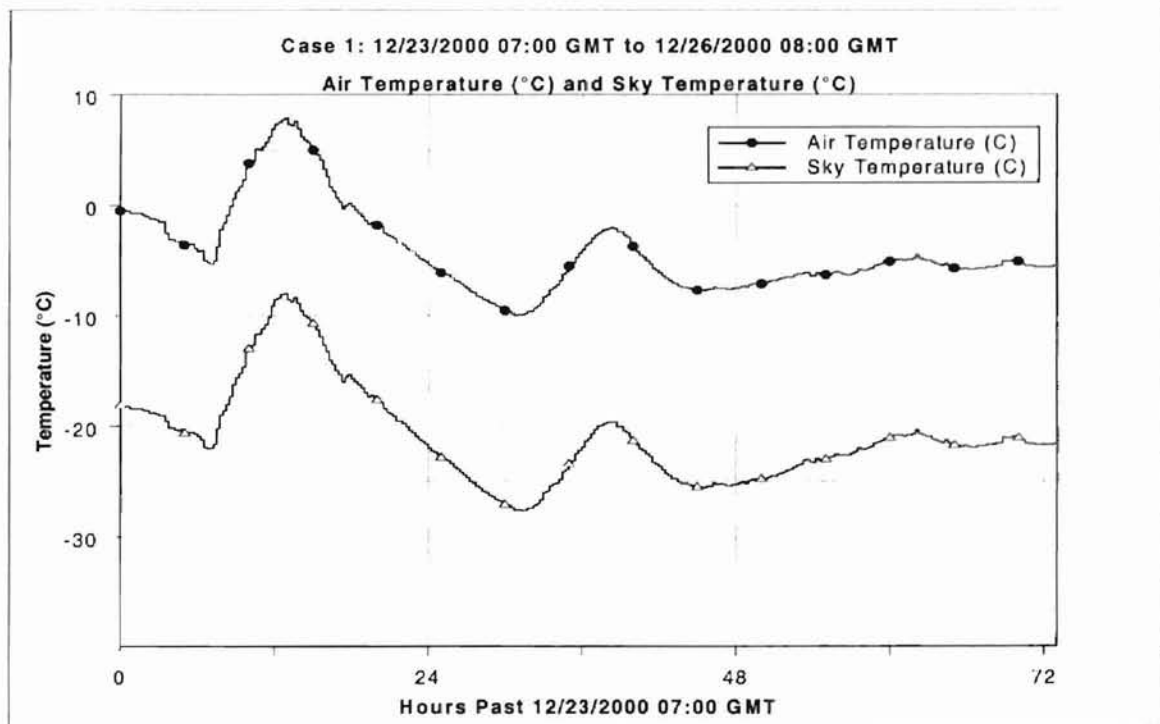


Figure 6- 2: Case 1 air temperature and sky temperature.

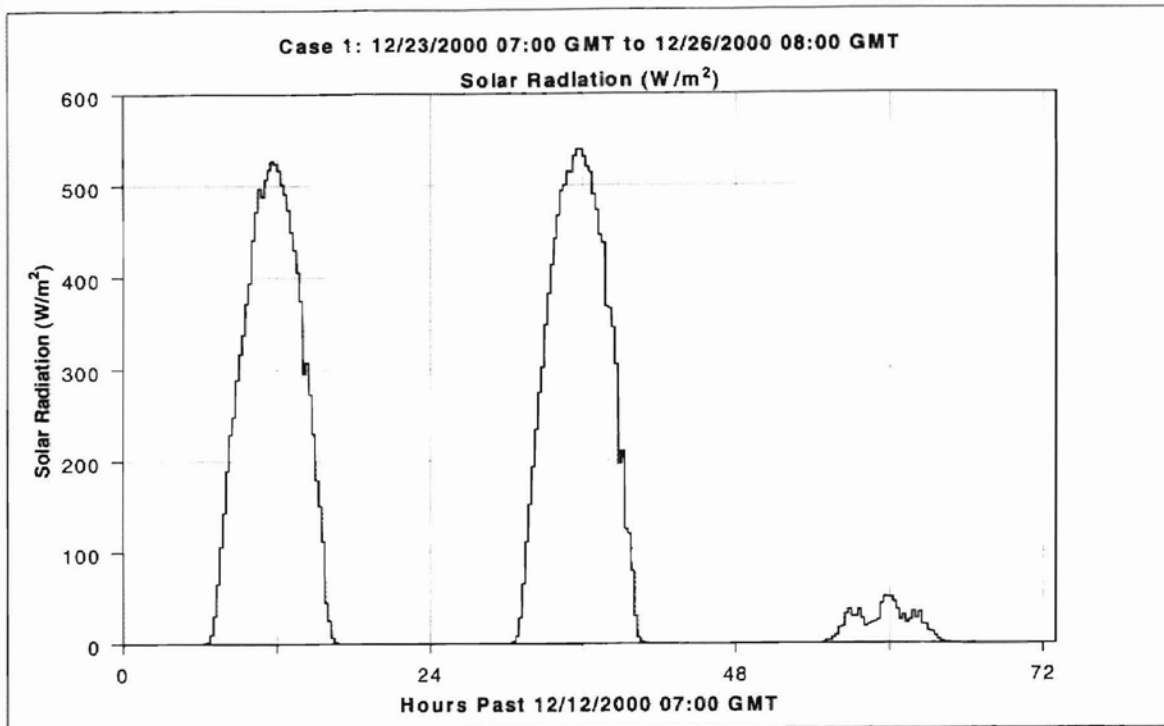


Figure 6- 3: Case 1 solar radiation.

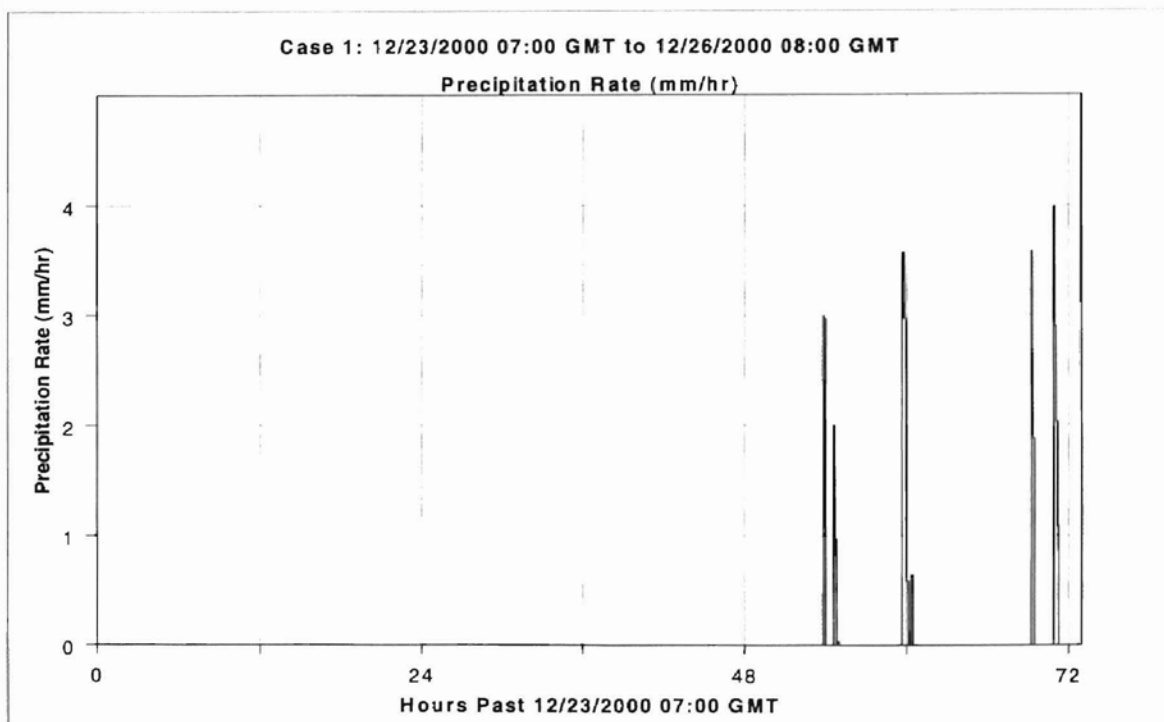


Figure 6- 4: Case 1 precipitation rate.

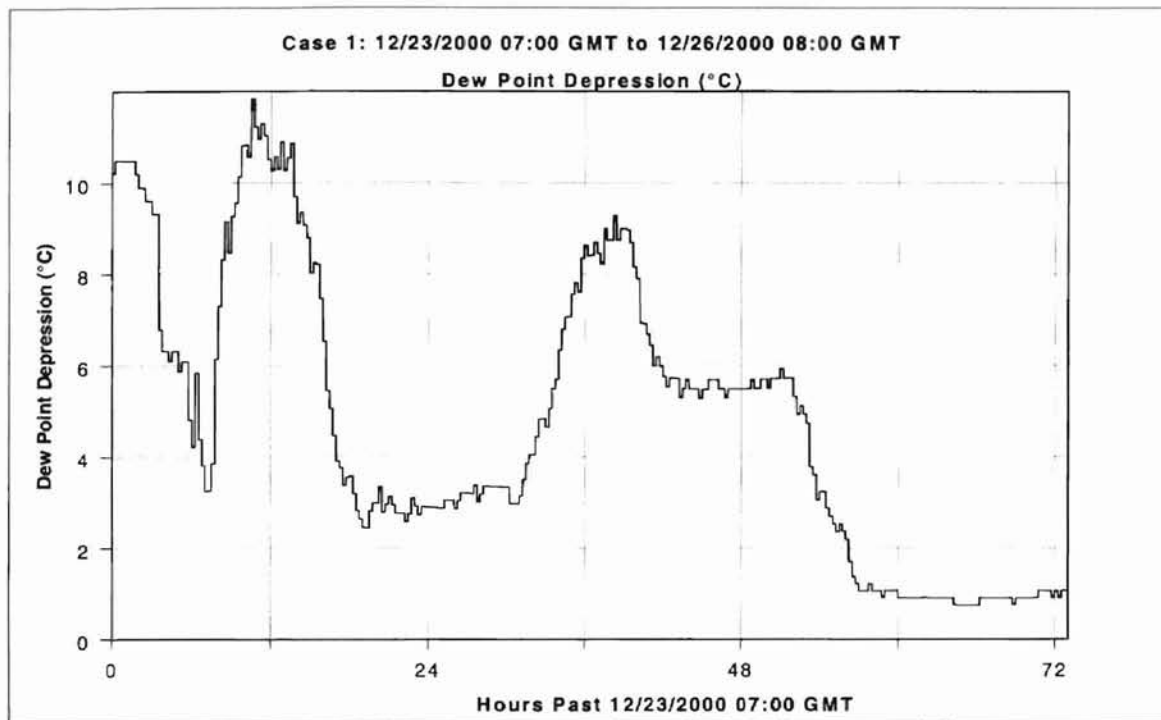


Figure 6- 5: Case 1 dew point depression (Dew point depression = Air temperature – Dew point temperature)

6.3.2 Case 1 - Performance for 2°C Dew Point Depression Rule

Figures 6-6 through 6-9 give performance results for Case 1. The dew point depression rule utilized a 2°C dew point depression threshold. Figure 6-6 shows the average bridge deck surface temperature for Case 1. The 1°C line in Figure 6-6 indicates periods when the potential for preferential icing was detected. As indicated in Figure 6-6, the Smart Bridge control system was able to maintain the average surface temperature within 1°C of the desired temperature. Approximately 12 hours were required after the heating system was first engaged to raise the average surface temperature to the desired value.

Figures 6-7 and 6-8 show the bridge loop supply temperature and flowrate, respectively. These figures indicate that the bridge deck heating system was not turned on until approximately 44 hours into the simulation. The bridge loop supply temperature profile shown in Figure 6-7 shows that the heating system was operating at maximum capacity (50°C bridge loop supply temperature) for most of the time that heating was required.

Although the control performance for this case was good, from a control engineering viewpoint operating the heating system at maximum capacity for an extended time is not desirable. Operating at maximum capacity essentially means that the system is not under control. Had the ambient conditions been slightly more severe on December 25, the controller would not have been able to increase the bridge loop supply temperature to compensate. This is especially apparent at 67 hours past the start time when the average surface temperature was just above 0°C and the bridge loop supply temperature was at maximum capacity. Therefore Case 1 suggests that the bridge deck heating system for the Smart Bridge located on the OSU campus is slightly undersized.

6.4 Case 2 - December 12-17, 2000

This section presents the results of a second simulated case study. Conditions recorded at the Stillwater, OK Mesonet station from December 12, 2000, 00:07 GMT to December 17, 2000, 00:07 GMT were used as weather inputs. Section 6.4.1 describes the weather conditions for this time period. Section 6.4.2 presents the Smart Bridge

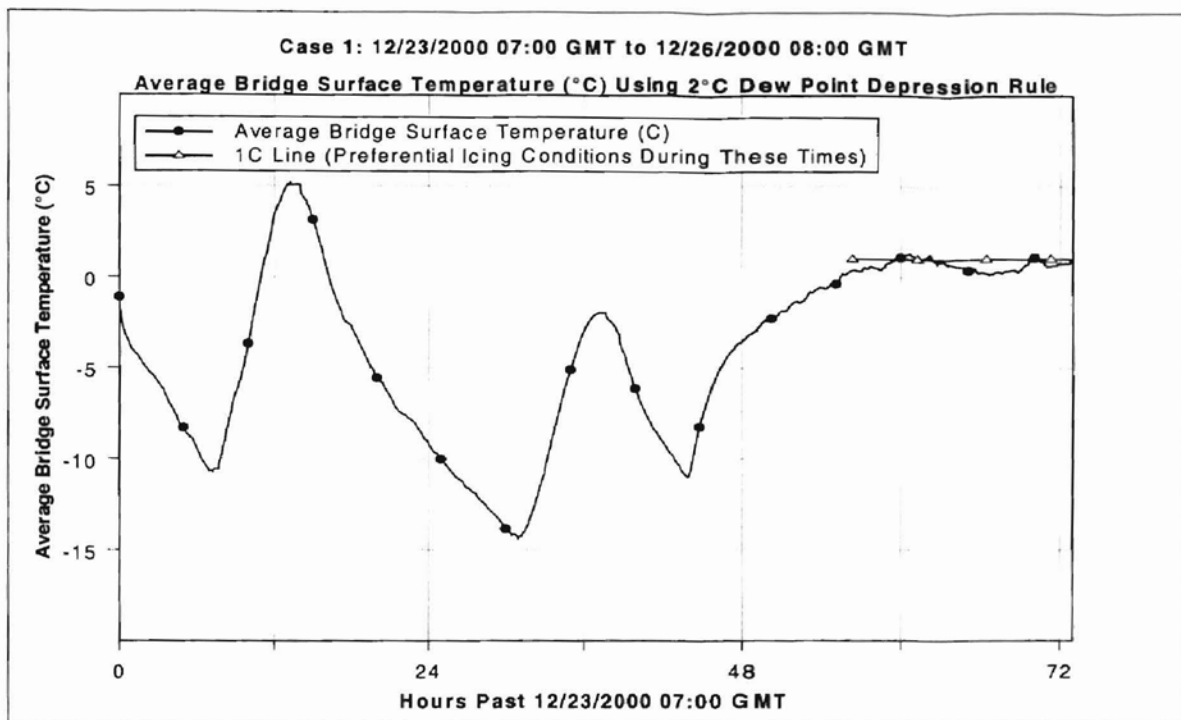


Figure 6- 6: Case 1 average bridge surface temperature.

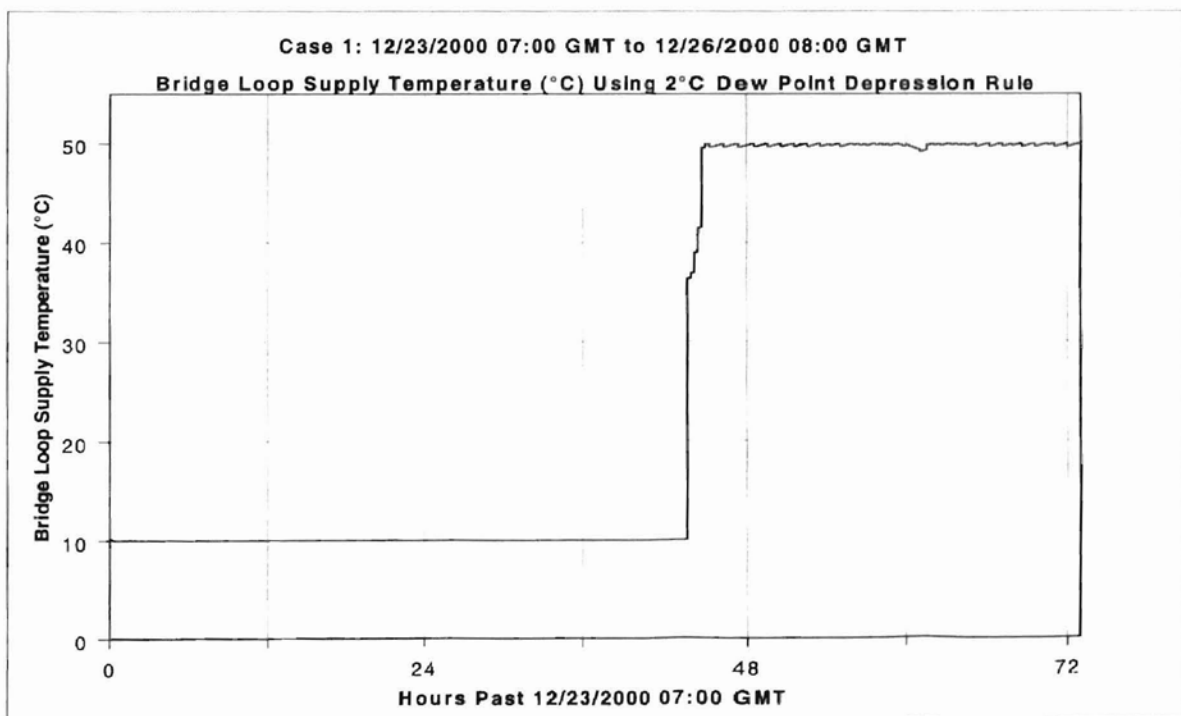


Figure 6- 7: Case 1 bridge loop supply temperature.

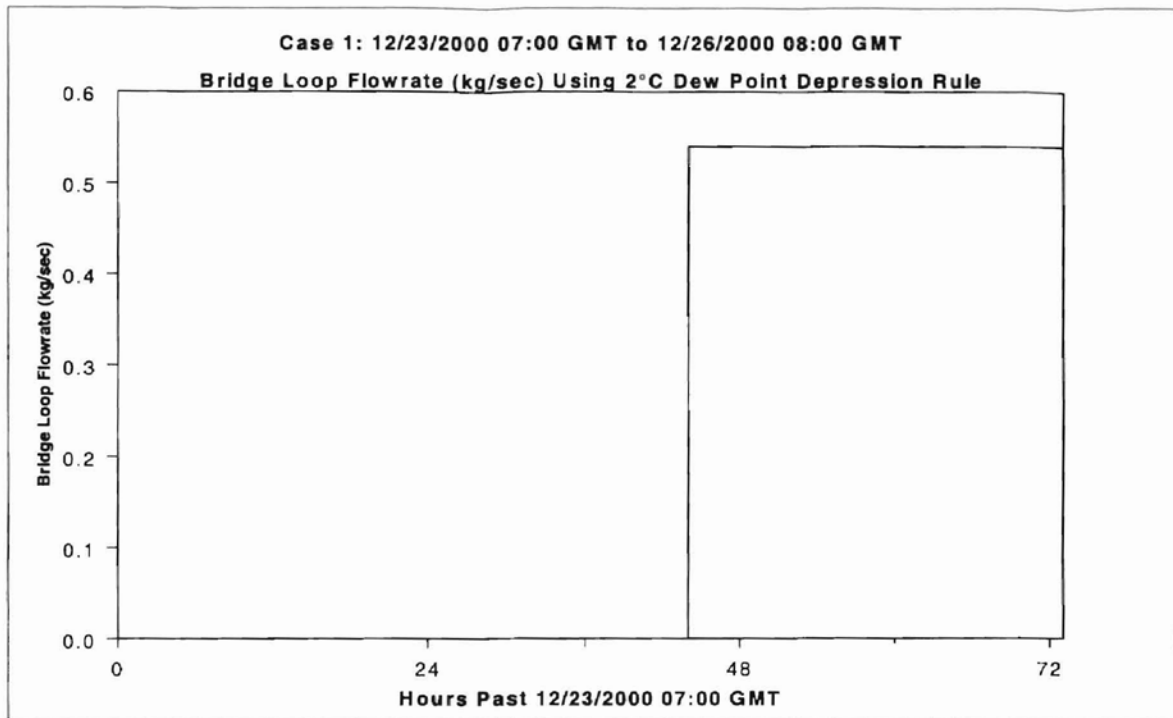


Figure 6- 8: Case 1 bridge loop flowrate.

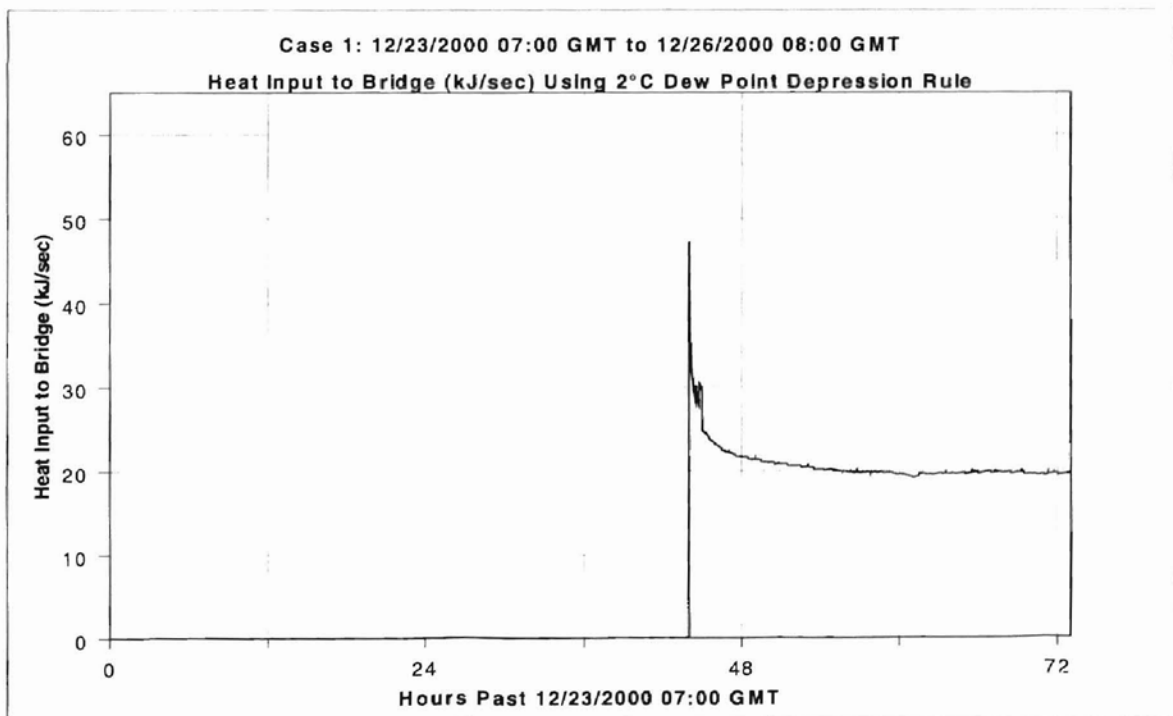


Figure 6- 9: Case 1 heat input to bridge.

control system performance results using a 4°C dew point depression rule. Section 6.4.3 presents results using a 2°C dew point depression rule. The main point for this case study is to illustrate the effect of different values of the dew point depression threshold on control performance.

6.4.1 Case 2 - Weather Conditions

Ambient conditions for this case are shown in Figures 6-10 through 6-13. Figure 6-10 indicates that the air temperature was below 0 °C for approximately 80% of the 120-hour study period. The nights of December 12 and 14 were particularly cold, with temperatures falling to -12.8 and -16.5 °C, respectively. Figure 6-11 is a plot of the

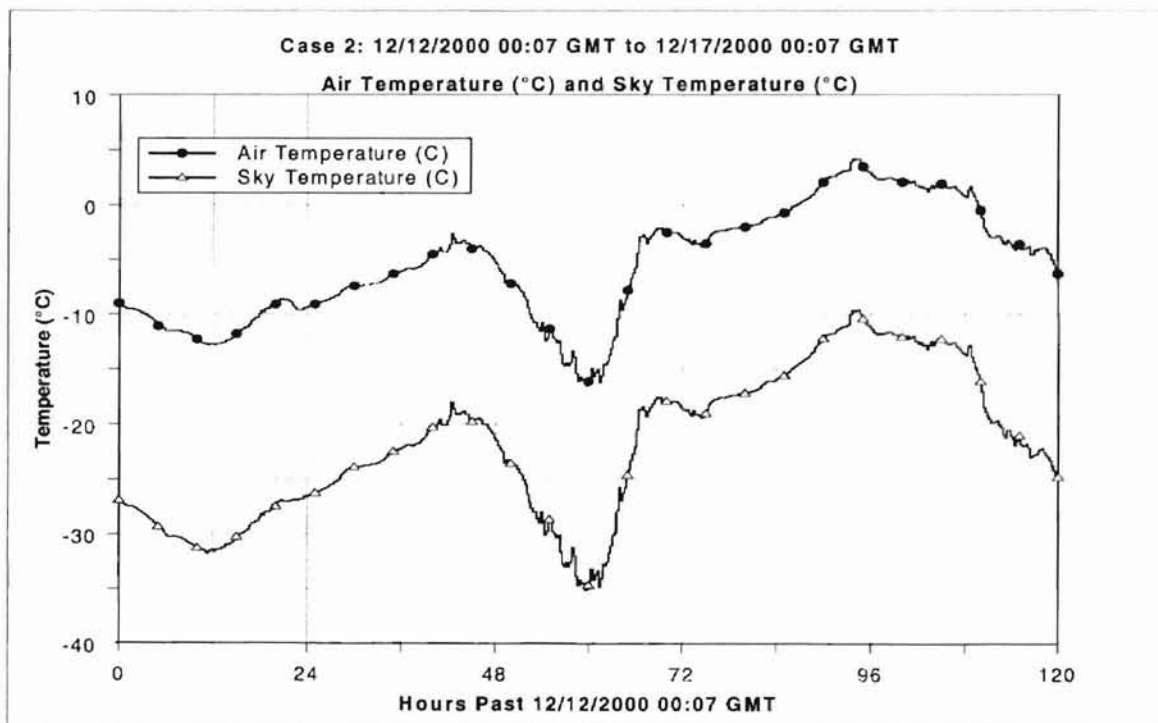


Figure 6- 10: Case 2 air temperature and sky temperature.

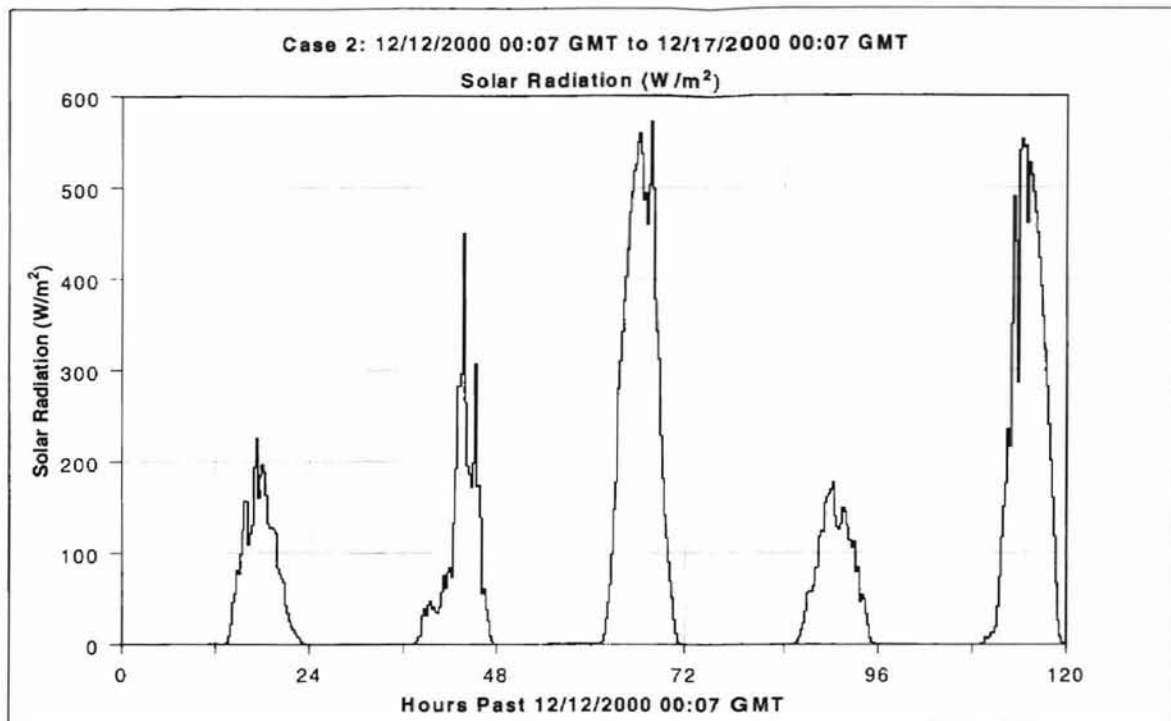


Figure 6- 11: Case 2 solar radiation.

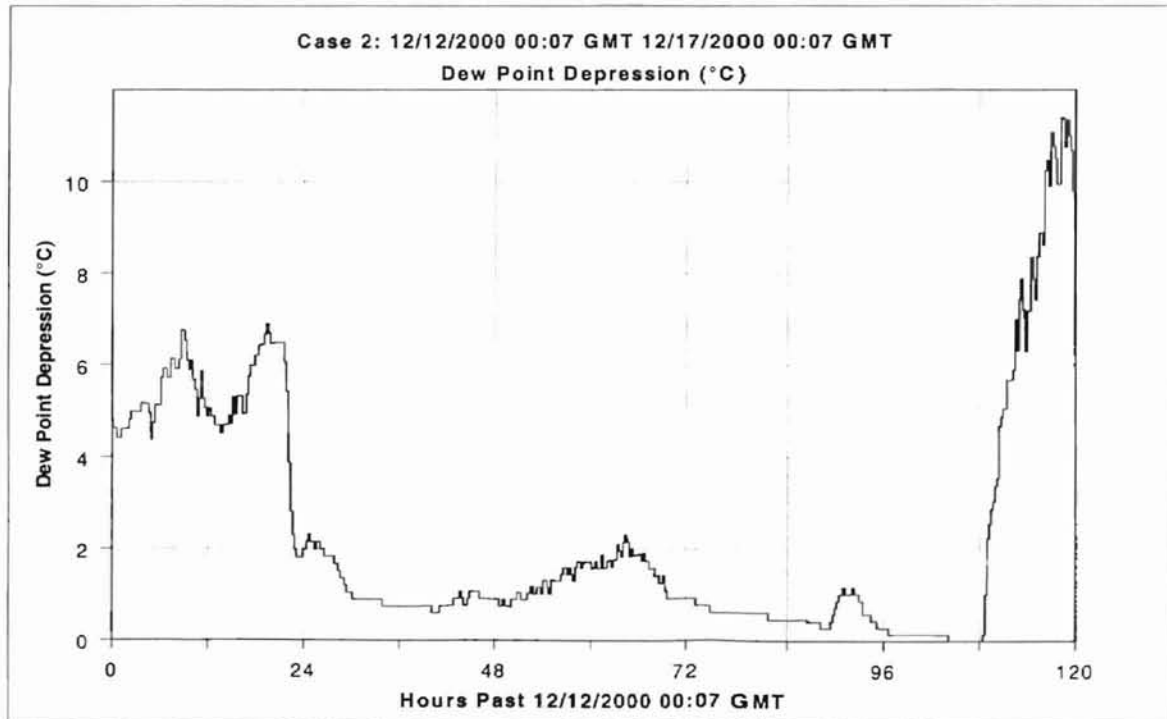


Figure 6- 12: Case 2 dew point depression (Dew point depression = Air temperature – Dew point temperature).

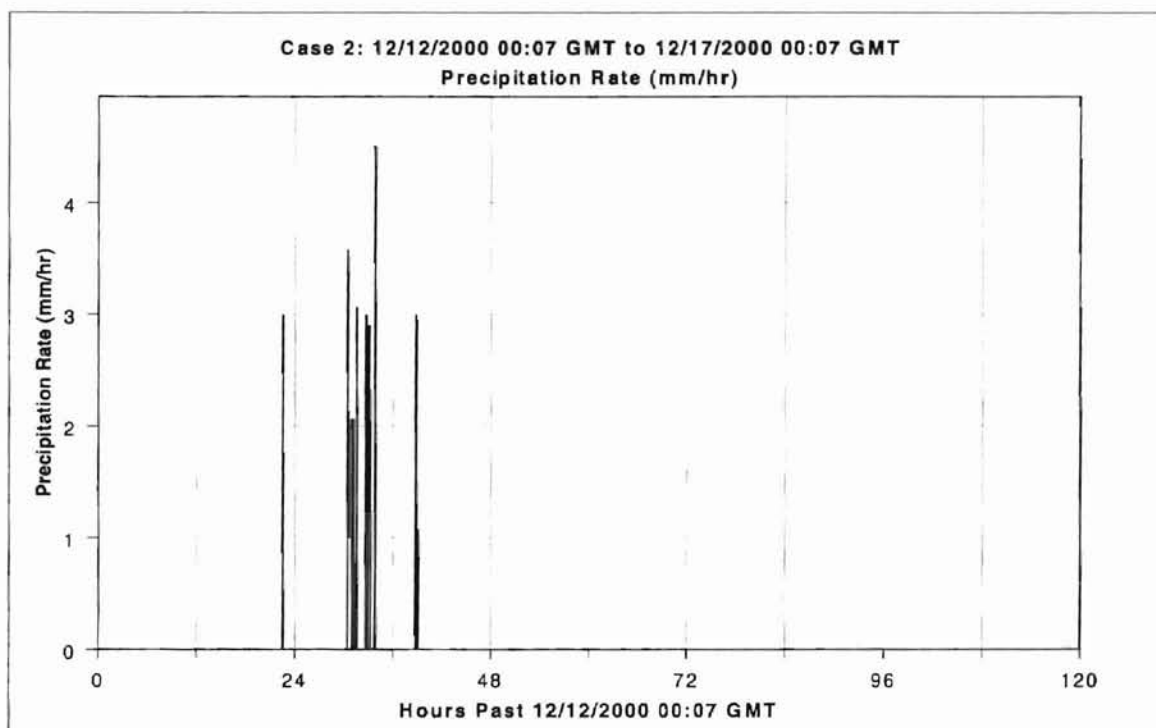


Figure 6- 13: Case 2 precipitation rate.

solar radiation for Case 1. December 14 and 16 were sunny days, with a peak solar radiation of about 550 W/m^2 . December 12 and 15 were cloudy days, with solar radiation readings peaking at 226 and 177 W/m^2 , respectively.

Figure 6-12 shows the actual dew point depression for the study period. Figure 6-12 indicates that for the first 24 hours the dew point depression varied from 4.5°C to 6.9°C . After the initial 24 hours the dew point depression dropped sharply to approximately 2°C and stayed below 2.3°C for the next 84 hours.

Figure 6-13 shows the precipitation rate for Case 2 as calculated from NEXRAD DPA data. Precipitation was briefly detected near the end of December 12. A longer precipitation event was detected on December 13. DPA data for December 14-16 was unavailable and precipitation is assumed to be zero for these dates. Mesonet precipitation

data was unavailable for the entire study period since Mesonet is unable to detect frozen precipitation.

6.4.2 Case 2A - Performance for 4°C Dew Point Depression Rule

Figures 6-14 through 6-17 give performance results using a 4°C dew point depression threshold. Figure 6-14 is a plot of the CV, average bridge deck surface temperature. Figure 6-15 is a plot of the MV, bridge loop supply temperature. Figure 6-16 shows the bridge loop flowrate. Figure 6-17 displays the heat input to the bridge during case 2A.

Figures 6-14 shows that the 4 °C dew point depression rule and the precipitation rule should cause the control system to drive the average bridge deck temperature to 1 °C or greater on the interval 22-110 hours after the start of Case 1A. Performance during this 88-hour interval was relatively good. The average bridge surface temperature was maintained above 0°C for 85% of the time when preferential icing was likely.

Figure 6-14 shows that the average bridge deck temperature did not reach 1 °C until 37.5 hours even though the desired bridge deck temperature was 1°C starting at 22 hours after the start of Case 1A. This 15.5-hour period when the bridge deck temperature is less than 1 °C is explained by variations in the RUC forecast. Figures 6-18 and 6-19 respectively show RUC dew point depression and precipitation forecasts for Case 2.

Figure 6-15 shows that the heating system is engaged from time 0 hours to time 5 hours, which indicates the RUC predicted either precipitation or the dew point depression threshold would be violated during the prediction horizon. Figure 6-18 confirms that in

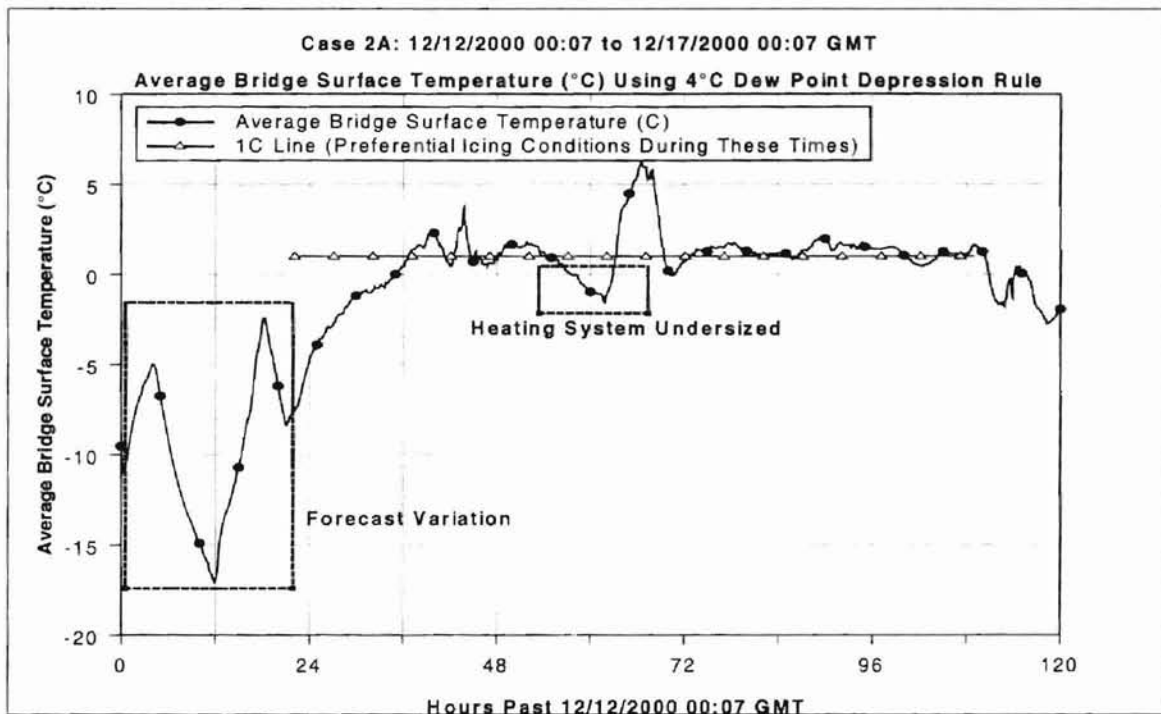


Figure 6- 14: Case 2A average surface temperature.

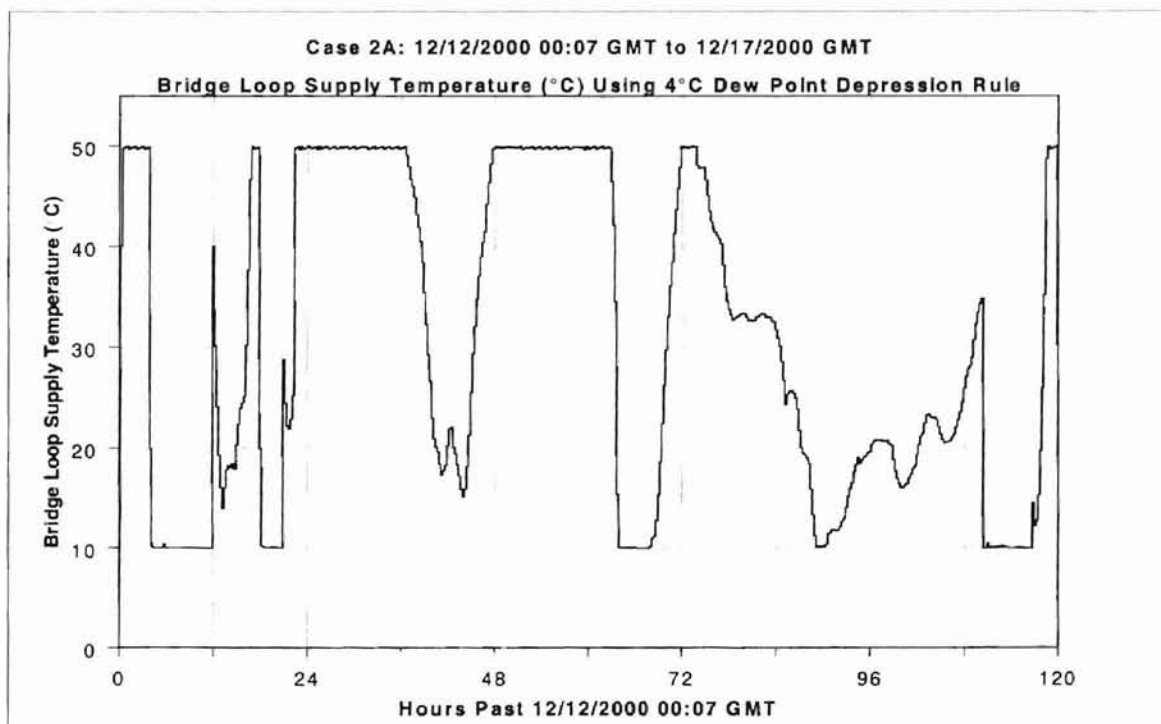


Figure 6- 15: Case 2A bridge loop supply temperature.

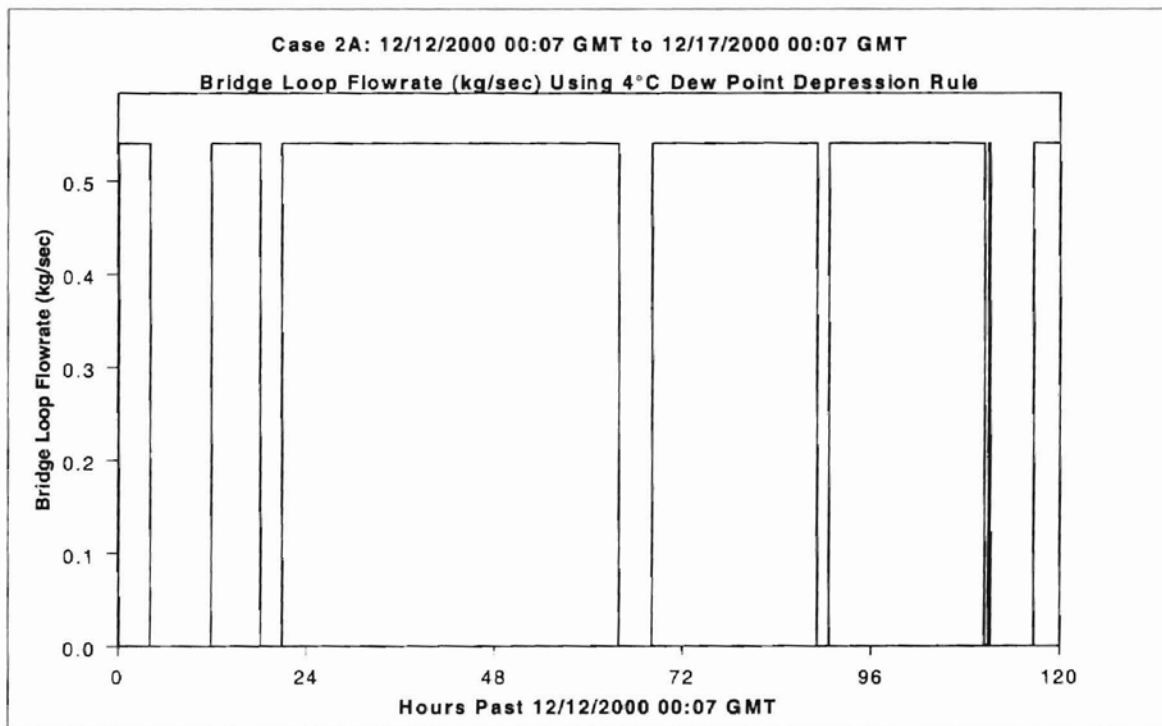


Figure 6- 16: Case 2A bridge loop flowrate.

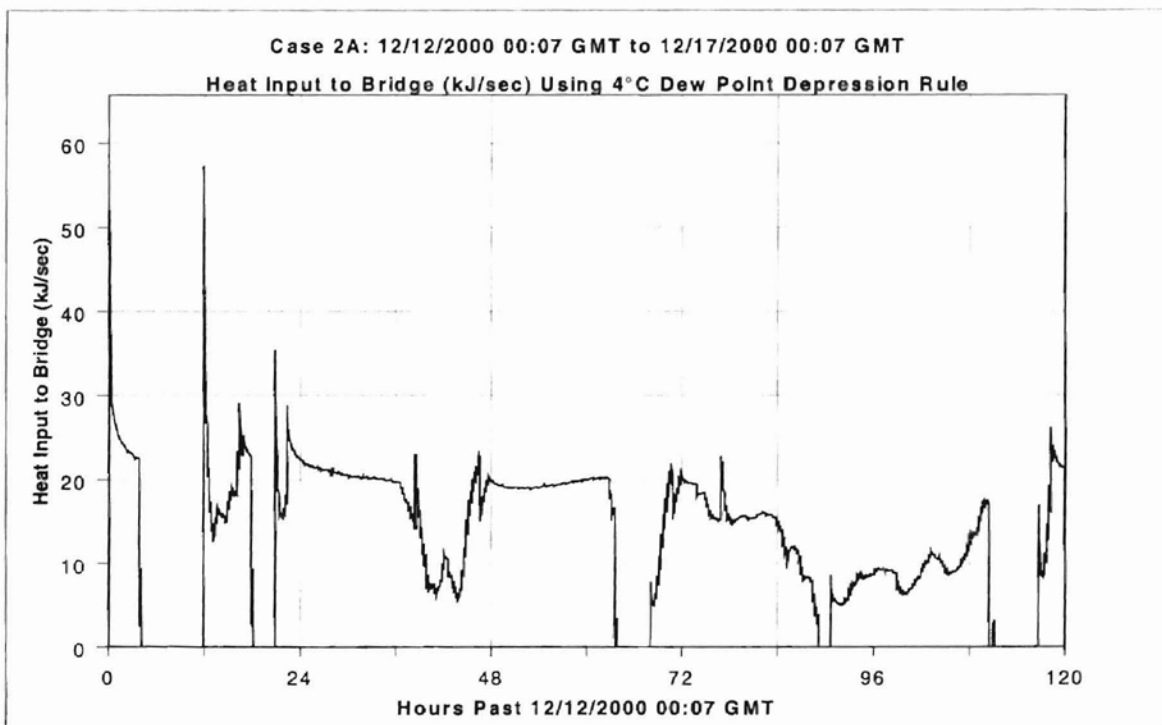


Figure 6- 17: Case 2A heating rate.

the initial 5 hours of the simulation RUC anticipated the dew point depression would slip below the 4°C dew point depression threshold. These forecasts caused the heating system to turn on even though Figure 6-18 indicates that actual the dew point depression did not go below 4°C during this time.

From time 5 hours to 12 hours past the start of Case 2A the heating system is turned off. Figure 6-18 shows that during this time period RUC predicted dew point depressions above the 4°C dew point depression threshold. In addition, Figure 6-19 indicates that RUC did not predict any precipitation during this time period.

This on/off cycle is repeated from times 12 hours to 21 hours. During this period the heating system turns on in response to dew point depression and precipitation forecasts. Later (at 18 hours into the simulation) the heating system is turned off when the updated forecast indicates no risk for preferential icing. At 21 hours the heating system is forced to turn on because the measured dew point depression dropped below the 4°C threshold.

Figure 6-14 also shows that the average bridge deck temperature dropped below 0°C over the interval 58-63 hours after the start of the simulation. During this interval the average bridge deck temperature dropped as low as -1.2 °C. Figure 6-15 shows that during this time period the controller set the bridge loop supply temperature at the upper limit, 50 °C. Although the bridge deck heating system was operating at maximum capacity for an extended period of time, enough heat could not be supplied to the bridge to compensate for the heat lost to the atmosphere. This implies that the bridge deck heating system is undersized.

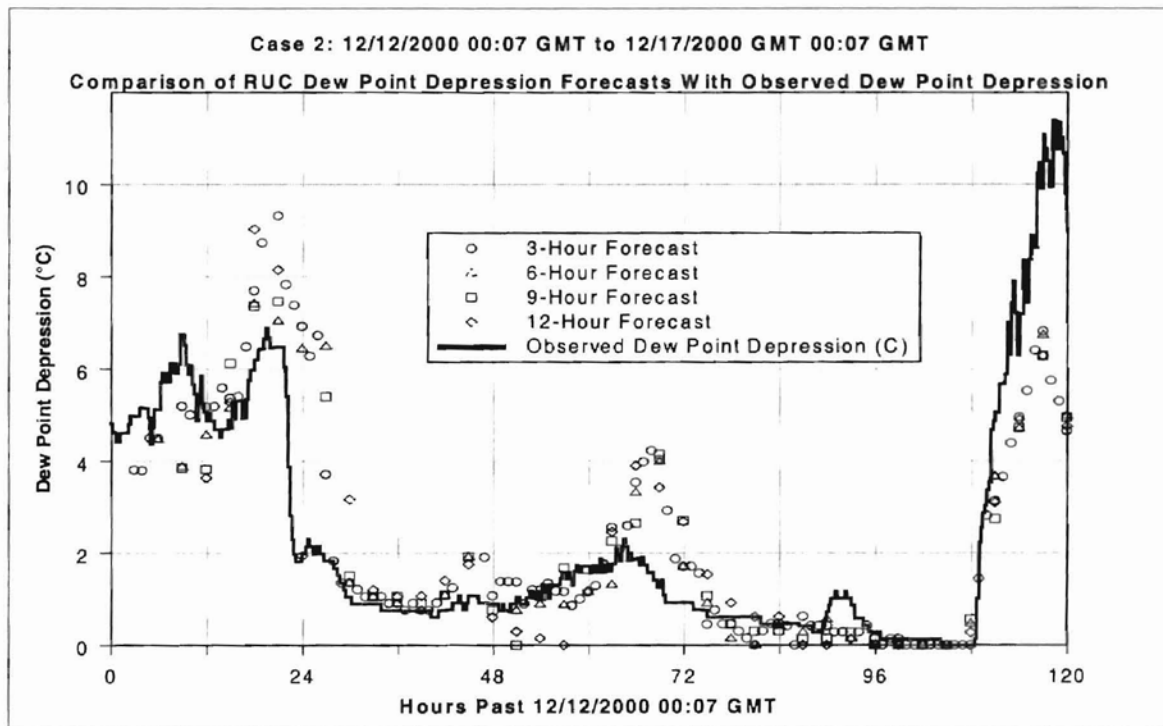


Figure 6- 18: Comparison of RUC dew point depression forecasts to observed values.

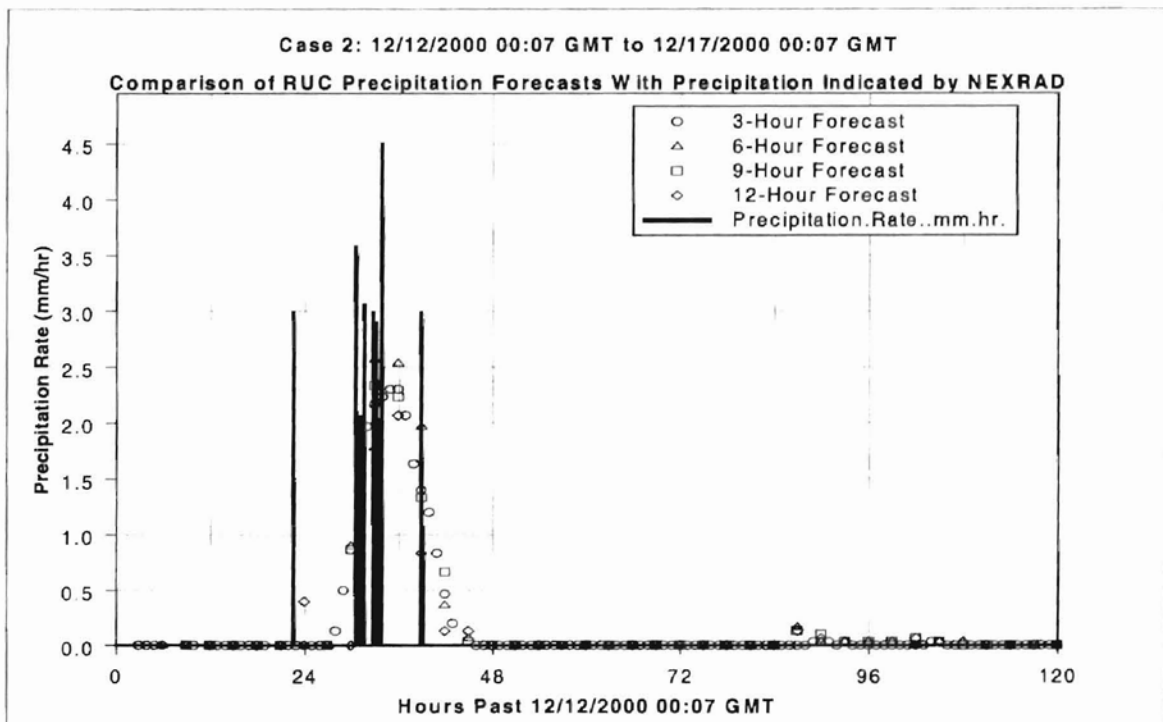


Figure 6- 19: Comparison of RUC precipitation forecast to observed values.

Another example of the controller operating against a constraint is during the interval 64-70 hours after the start of Case 2A. During this time the controller is against the lower bridge loop supply temperature constraint, 10°C. Here the weather conditions cause the bridge deck temperature to warm up. The control system reacts by setting the bridge loop supply temperature at the lower limit and eventually sets the bridge loop flowrate to zero. From the control system's perspective it is doing all it can to reduce the bridge deck surface temperature to 1°C, but the weather conditions force the surface temperature above the desired value. However, this situation is not a problem as there is no safety concern or unnecessary operating expense.

6.4.3 Case 2B - Performance for 2°C Dew Point Depression Rule

Figures 6-20 through 6-23 present performance results for Case 2B, where the dew point depression threshold is set at 2 °C. The average bridge deck temperature profile shown in Figure 6-20 is nearly identical for Case 2A after 12 hours past the simulation start time. However, Figures 6-20 and 6-13 are noticeably different on the interval 0-12 hours. With the 4 °C dew point depression threshold the controller engaged the heating system at time zero. With a dew point depression threshold of 2 °C the controller did not engage the heating system until 12 hours after the start of the simulation. This indicates that during the first 12 hours of Case 2, RUC predicted that the dew point depression would drop below 4 °C but not below 2 °C. This statement is confirmed by the dew point depression forecasts shown in Figure 6-18.

By using a 2 °C dew point depression rule the control system encounters similar problems as the 4 °C dew point depression rule. As in Case 2A, forecast variations during Case 2B cause the control system to cycle on and off, and eventually get into a situation it can't immediately recover from (i.e. between 22 hours and 37 hours in Figure 6-20). Also, Figure 6-20, like Figure 6-14, shows that the desired average bridge deck temperature cannot be achieved when the heating system is undersized (based on time 58-63 hours).

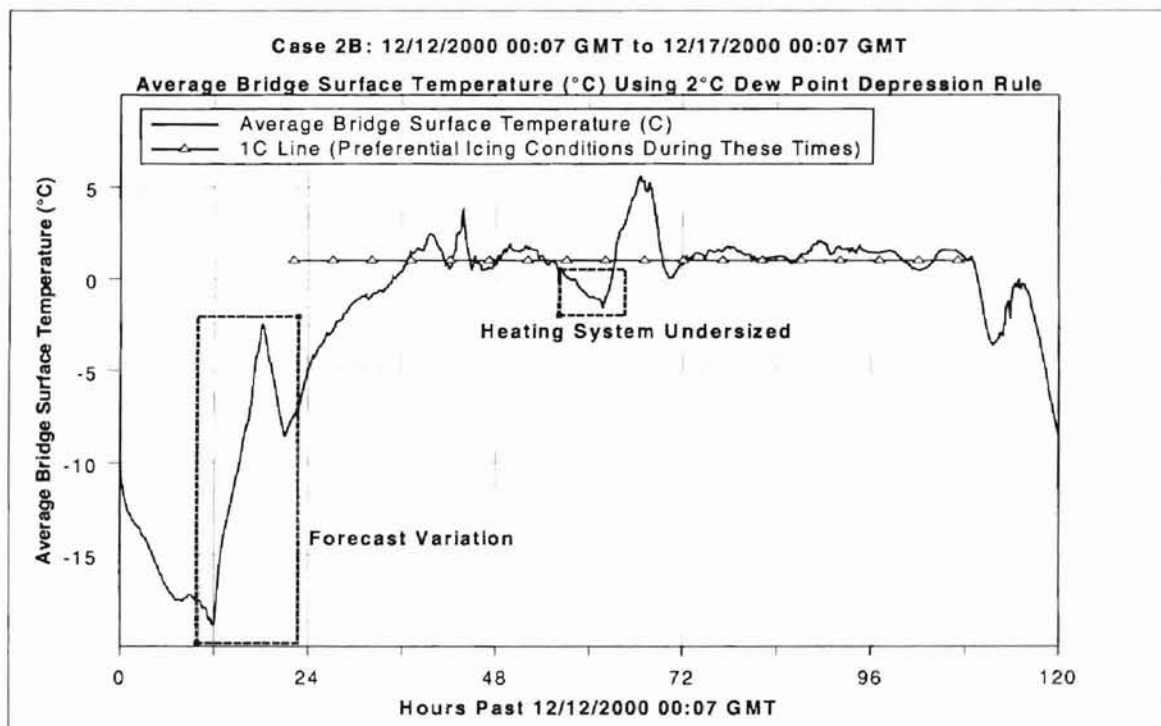


Figure 6- 20: Case 2B average surface temperature.

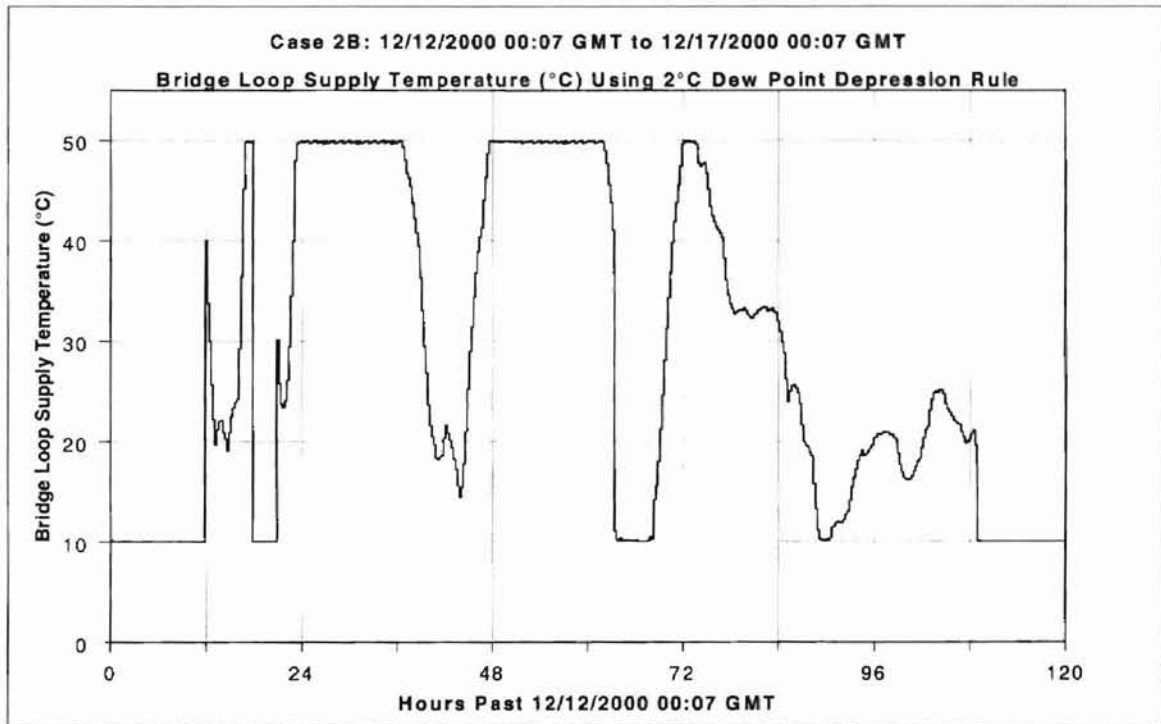


Figure 6- 21: Case 2B bridge loop supply temperature.

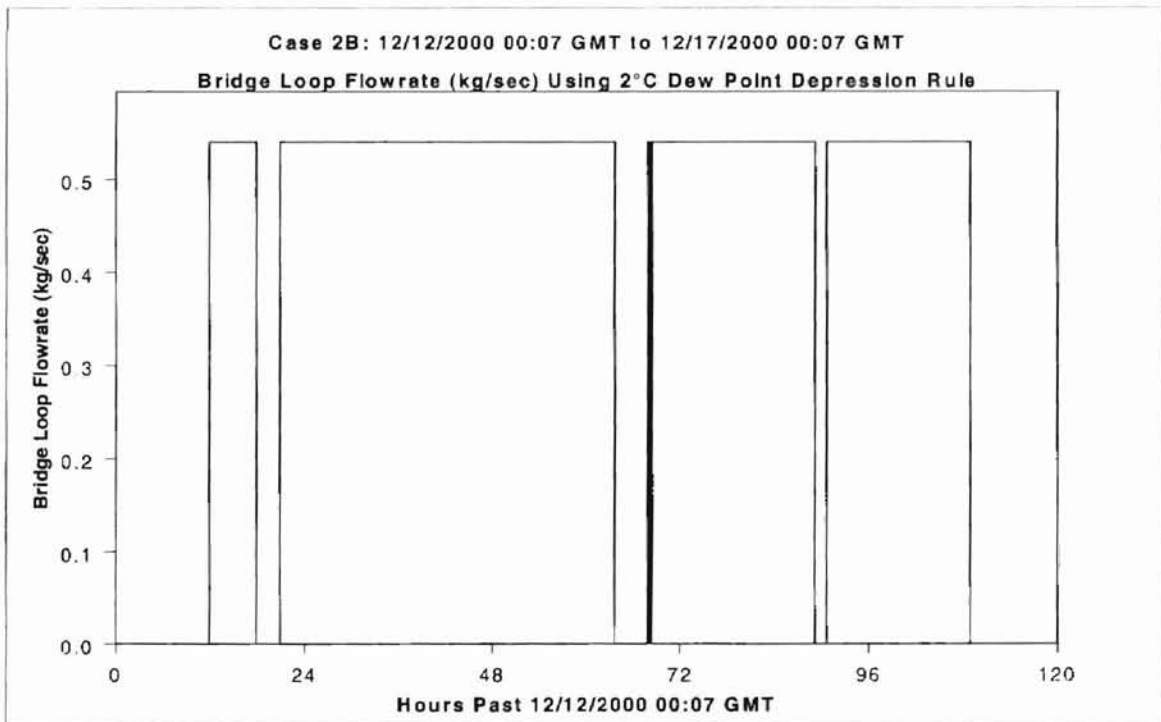


Figure 6- 22: Case 2B bridge loop flowrate.

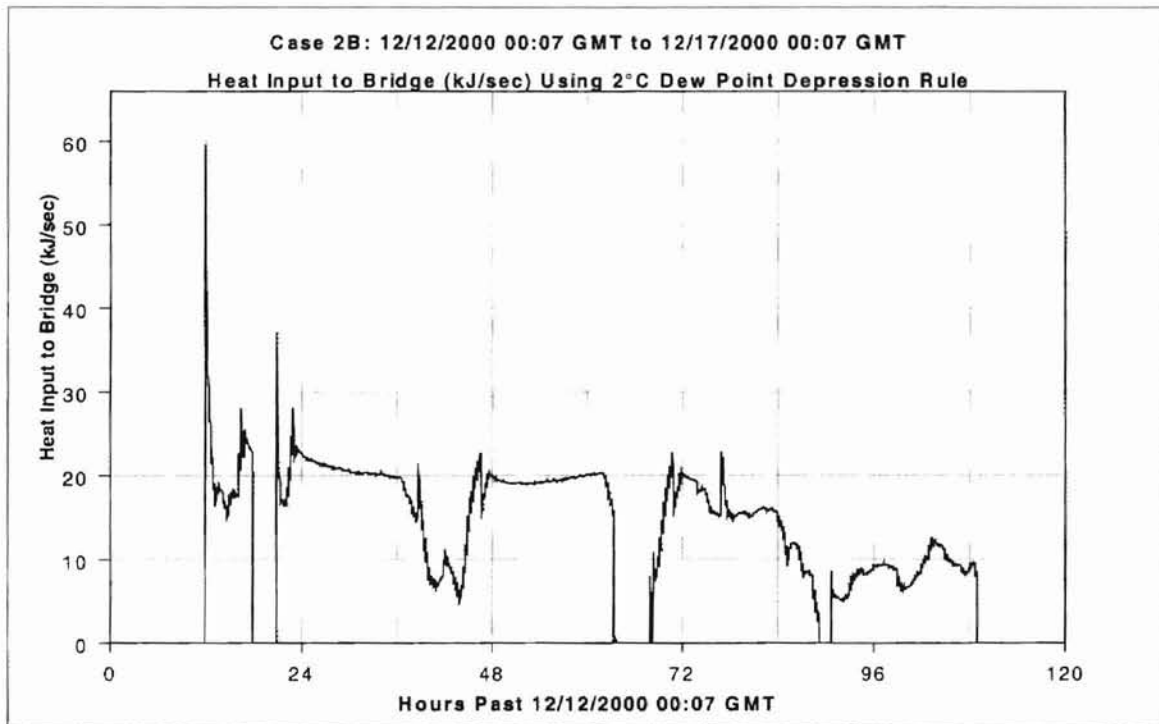


Figure 6- 23: Case 2B heat input to bridge.

6.5 Summary

This chapter presents case studies that demonstrate the performance of the Smart Bridge control system. The cases presented show that the Smart Bridge control system takes the proactive measures necessary to prevent preferential icing. Case 1 is a prime example, as the heating system was activated 12 hours before weather conditions indicated preferential icing was likely. Furthermore, once the average bridge surface temperature reached 1°C the control system was able to maintain a surface temperature within $\pm 1^\circ\text{C}$ of the target.

Case 2 also demonstrates that the control algorithm functions correctly. Note that when the control system did not keep the average bridge surface temperature very close

to the desired value, the control algorithm still functioned correctly. In Case 2A and 2B, although the control system did not initially increase the average bridge surface temperature to 1°C in time, it was adjusting the bridge loop supply temperature appropriately. This is to say that the control algorithm made the best control decisions based on the forecast information it was using. Also, note that at times when the controller operated the heating system at full capacity and the average surface temperature was below the target value, the controller still set the bridge loop supply temperature correctly. This is to say that the control algorithm made the best control decisions within the operating constraints of the heating system.

Poor control has been observed at times when predicted values of the dew point depression oscillate on either side of the threshold value. This problem could be fixed by employing a fuzzy threshold rather than a hard threshold in the dew point depression rule. Poor control has also been observed when the bridge deck heating system is undersized. This problem can be addressed by manipulating the reference trajectory to store heat in the bridge or by increasing the capacity of the heating system.

In summary, the Smart Bridge control algorithm functions correctly. The best course of action (in terms of the objective function presented in Chapter IV) is always taken. Performance is best when the dew point depression forecast does not oscillate around the threshold value and the bridge deck heating system is adequately sized.

CHAPTER VII

CONCLUSIONS AND RECOMMENDATIONS

7.1 Contribution of Reported Work

The work reported in this thesis represents a major advance in heated bridge technology. Existing heated bridge control systems use feedback techniques, capable of removing ice once it has been detected. The Smart Bridge control system developed for this thesis utilizes model predictive control, a much more sophisticated control technique. The advantage of using an MPC strategy is that the heating system is engaged before icing conditions reach the bridge deck, thus preventing preferential icing. As a result, the Smart Bridge control system significantly safer driving conditions than control systems employed by existing heated bridge decks.

7.2 Satisfaction of Project Deliverables

Task 4.3.1.3 of the OSU Geothermal Smart Bridge Project outlines specific deliverables that the Smart Bridge control system should address. This section summarizes how the current version of the Smart Bridge control system addresses these deliverables.

- The control system prevents bridge deck icing with minimal operating and capital costs. Simulation results presented in Chapter VI show that as long as forecast variation and insufficient heating capacity do not come into play, the control system is capable of preventing preferential icing. Operating costs are kept at a minimum

because the heating system is only used at times required to prevent preferential icing. Finally, capital costs are reduced because efficient control prevents the need to oversize the heating system.

- Bridge temperature measurements and other local conditions have been utilized to provide feedback control and guarantee avoidance of icing conditions. Local measurements from Oklahoma Mesonet and NEXRAD radar data are used to initialize forecast input vectors (as described in Section 5.5). This is a straightforward method to make forecasts consistent with actual measurements.
- As indicated in Chapter V, the RUC weather forecasting model plays an important role in the current version of the Smart Bridge control system. Weather forecasts provided by RUC are the foundation of this MPC strategy. RUC allows the control system to identify the onset of preferential icing conditions. Incorporation of this feedforward control capability is a major accomplishment of the work reported in this thesis.
- In addition to the RUC forecast model, the Smart Bridge control system utilizes a first-principles bridge deck model. This model plays an important role in the MPC strategy, facilitating calculation of the predicted bridge deck response to forecasted weather conditions.
- The control system has been developed in a modular fashion to ensure flexibility, reliability, and ease of maintenance. All code used to implement the Smart Bridge control system was written in Visual Basic, an inherently modular programming language.

- The final Smart Bridge control system should have the ability to learn with experience how to optimize bridge deck heating. This deliverable is outside the scope of the reported work. However, several parameters that could be used in the adaption module (to be completed by future investigators) have been identified in Chapter IV.

7.3 Conclusions

All of the deliverables within the scope of this work have been completed. Most importantly, simulations indicate the control system presented in this thesis can successfully prevent preferential icing. This performance is primarily the result of two key factors. First, real-time weather forecasts have been integrated into the control system, facilitating reliable predictions of future bridge deck behavior. Secondly, MPC techniques are designed to be proactive, which is especially important for controlling relatively slow processes like the Smart Bridge.

In general, the control system performs very well. Although some problems with control performance have been identified (forecast variation and lack of heating capacity), straightforward methods are available for resolving these issues.

Finally, the current version of the control system is well suited for incorporation of an adaption module by future investigators.

7.4 Recommendations for Future Work

The next phase of development of the Smart Bridge control involves the development of adaptive techniques for improving control performance with time. Several parameters have been identified in Section 4.6 that might be used in the adaption module. Adapting parameters that effect the reference trajectory, \mathbf{r} , the predicted bridge response, $\hat{\mathbf{y}}$, and tuning parameters ($\mathbf{\Gamma}$ and $\mathbf{\Lambda}$) in the objective function, will have an effect on controller performance.

The method for generating forecast vectors for RUC output should incorporate an additional linear interpolation to eliminate discontinuities in the forecast vector.

Additional sources of weather forecast data could be incorporated into the Smart Bridge control system to refine the solar radiation forecast. Currently, the assumption is made that the current degree of cloudiness will persist for the remainder of the day.

Simulation results suggest that a fuzzy, rather than crisp, dew point depression threshold might result in fewer problems associated with forecast variations. Therefore future investigators should run simulation cases were a fuzzy dew point depression threshold is employed.

Additional modules will be required to retrofit the current version of the software (suited for simulation only) for application to a real-world bridge deck. Specifically, code should be written to handle I/O from instruments and to properly initialize $\hat{\mathbf{y}}$.

LIST OF REFERENCES

1. Spitler, J.D., *Oklahoma State University Geothermal Smart Bridge*, . 1999, Oklahoma State University: Stillwater.
2. Gillham, O., *A Bridge Not Too Far Into the Future*, in *Tulsa World*. 2001: Tulsa, OK.
3. Callihan, B.K., *A Control System Framework For A Bridge Deck Heated By A Geothermal Heat Pump System*, in *Chemical Engineering*. 2000, Oklahoma State University: Stillwater, OK. p. 99.
4. Minsk, L.D., *Heated Bridge Technology*, . 1999, U.S. Department of Transportation, Federal Highway Administration, Office of Bridge Technology.
5. *Along the Road - FHWA Funds Foretell*. Public Roads, 1998. **61**(4).
6. www.ota.fhwa.dot.gov/roadsvr/CS036.htm, . 1996, Federal Highway Administration.
7. Sass, B.H., *A Numerical Model for Prediction of Road Temperature and Ice*. *Journal of Applied Meteorology*, 1992. **31**: p. 1499-1506.
8. Rawlings. *Model Predictive Control Technology, Theory and Applications. Short Course Notes*. 1997.
9. Qin, S.J. *An Overview of Industrial Model Predictive Control Technology*. in *5th International Conference on Chemical Process Control*. 1996. Tahoe City.
10. Chiasson, A., *Advances in Modeling of Ground-Source Heat Pump Systems*, in *Mechanical and Aerospace Engineering*. 1999, Oklahoma State University: Stillwater, OK.
11. Ramamoorthy, M., *Applications of Hybrid Ground Source Heat Pump Systems to Buildings and Bridge Decks*, in *Mechanical and Aerospace Engineering*. 2001, Oklahoma State University: Stillwater, OK.
12. Jenks, S., *User's Manual and Source Code Flow Diagrams for Smart Bridge Control Software*, . 2001, Oklahoma State University: Stillwater.
13. Marlin, T.E., *Process Control*. 1995: McGraw Hill.
14. High, D.K., *Optimization Applications Course Notes - Chemical Engineering 5703 - Oklahoma State University*, . 2001.

15. *The Oklahoma Mesonet - General Overview*, . 2000, Oklahoma Mesonet.
16. www.ncdc.noaa.gov/ol/radar/radarresources.html, , NCDC.
17. www.djburnette.com/projects/hexrad.html, , Dorian J. Burnette.
18. www.srh.noaa.gov/radar/radinfo/p19-r, , Dennis R. Cain.
19. *National Climatic Data Center Data Documentation for TD7000 - TD7599 NEXRAD Level III*, . 1998, National Climatic Data Center.
20. Mizzell, H.P., *Comparison of WSR-88D Derived Rainfall Estimates With Gauge Data In Lexington County, South Carolina*, in *Geography*. 1999, University of South Carolina.
21. maps.fsl.noaa.gov/, , Stan Benjamin.
22. maps.fsl.noaa.gov/ruc2.tpb.html, , Stanley Benjamin.
23. maps.fsl.noaa.gov/CWSU/ruc_feb00_CWSU_files/v3_document.htm, , Stan Benjamin.

VITA

Stephen Christopher Jenks

Candidate for the Degree of

Master of Science

Thesis: A MODEL PREDICTIVE CONTROL STRATEGY FOR A BRIDGE DECK
HEATED BY A GEOTHERMAL HEAT PUMP SYSTEM

Major Field: Chemical Engineering

Biographical:

Personal Data: Born in Saint Louis, Missouri, February 18, 1977, the son of
Ronald R. Jenks and Jessica R. Jenks

Education: Graduated from Rock Bridge Senior High School, Columbia,
Missouri, in June 1994; Received Bachelor of Science Degree in Chemical
Engineering from the University of Missouri – Rolla in December 1999;
Completed the requirements for Master of Science degree in Chemical
Engineering at Oklahoma State University in December, 2001.

Professional Experience: Process Engineering Co-Op at International Specialty
Products, in Calvert City, Kentucky from May 1996 to December 1996,
and from May 1997 to August 1997; Summer Intern at The Dow Chemical
Company, in Freeport, Texas from May 1998 to August 1998; Summer
Intern at Conoco Incorporated, in Ponca City, Oklahoma from May 2000
to August 2000; Process Control Engineer at Conoco Incorporated, in
Ponca City, Oklahoma, from October 2001 to the present.